



Scientific Excellence • Resource Protection & Conservation • Benefits for Canadians
Excellence scientifique • Protection et conservation des ressources • Bénéfices aux Canadiens

13565

Rup

Validation of Airborne Sea Ice Thickness Measurement using Electromagnetic Induction during Limex '89

J.R. Rossiter, J.S. Holladay, and L.A. Lalumiere

Published by:

Physical and Chemical Sciences Branch
Scotia-Fundy Region
Department of Fisheries and Oceans

Bedford Institute of Oceanography
P.O. Box 1006
Dartmouth, Nova Scotia
Canada B2Y 4A2

1992

**Canadian Contractor Report of
Hydrography and Ocean Sciences
No. 41**



Fisheries
and Oceans

Pêches
et Océans

Canada

Canadian Contractor Report of Hydrography and Ocean Sciences

Contractor reports are unedited final reports from scientific and technical projects contracted by the Ocean Science and Surveys (OSS) sector of the Department of Fisheries and Oceans.

The contents of the reports are the responsibility of the contractor and do not necessarily reflect the official policies of the Department of Fisheries and Oceans.

If warranted, contractor reports may be rewritten for other publications of the Department, or for publication outside the government.

Contractor reports are abstracted in *Aquatic Sciences and Fisheries Abstracts* and indexed in the Department's annual index to scientific and technical publications.

Contractor reports are produced regionally but are numbered nationally. Requests for individual reports will be filled by the issuing establishment listed on the front cover and title page. Out of stock reports will be supplied for a fee by commercial agents.

Regional and headquarters establishments of Ocean Science and Surveys ceased publication of their various report series as of December 1981. A complete listing of these publications is published in the *Canadian Journal of Fisheries and Aquatic Sciences*, Volume 39: Index to Publications 1982. The current series, which begins with report number 1, was initiated in January 1982.

Rapport canadien des entrepreneurs sur l'hydrographie et les sciences océaniques

Cette série se compose des rapports finals non révisés préparés dans le cadre des projets scientifiques et techniques réalisés par des entrepreneurs travaillant pour le service des Sciences et levés océaniques (SLO) du ministère des Pêches et des Océans.

Le contenu des rapports traduit les opinions de l'entrepreneur et ne reflète pas nécessairement la politique officielle du ministère des Pêches et des Océans.

Le cas échéant, certains rapports peuvent être rédigés à nouveau de façon à être publiés dans une autre série du Ministère, ou à l'extérieur du gouvernement.

Les rapports des entrepreneurs sont résumés dans la publication *Résumés des sciences halieutiques et aquatiques* et ils sont classés dans l'index annuel des publications scientifiques et techniques du Ministère.

Les rapports des entrepreneurs sont produits à l'échelon régional, mais numérotés à l'échelon national. Les demandes de rapports seront satisfaites par l'établissement auteur dont le nom figure sur la couverture et la page du titre. Les rapports épuisés seront fournis contre rétribution par des agents commerciaux.

Les établissements des Sciences et levés océaniques dans les régions et à l'administration centrale ont cessé de publier leurs diverses séries de rapports en décembre 1981. Une liste complète de ces publications figure dans le volume 39, Index des publications 1982 du *Journal canadien des sciences halieutiques et aquatiques*. La série actuelle a commencé avec la publication du rapport numéro 1 en janvier 1982.

Canadian Contractor Report of
Hydrography and Ocean Sciences No. 41

1992

VALIDATION OF AIRBORNE SEA ICE THICKNESS MEASUREMENT
USING
ELECTROMAGNETIC INDUCTION DURING LIMEX'89 (UP-CV8-028)*

by

James R. Rossiter¹, J. Scott Holladay², and Louis A. Lalumiere¹

Physical and Chemical Sciences
Scotia-Fundy Region
Department of Fisheries and Oceans

Bedford Institute of Oceanography
P.O. Box 1006
Dartmouth, Nova Scotia
Canada B2Y 4A2

¹Canpolar Inc., 265 Rimrock Road, Unit 4, Toronto, Ont., Canada, M3J

²Aerodat Ltd., 3883 Nashua Drive, Mississauga, Ontario, Canada, L4V 1R3

*Prepared under contract to DSS Unsolicited Proposal Program through DSS Contract No. FP953-8-0848/01-OSC. Published by the Department of Fisheries and Oceans for the sea-ice program at the Bedford Institute of Oceanography through funds of the Federal Panel of Energy Research and Development.

© Minister of Supply and Services Canada, 1992
Cat. No. FS 97-17/41E ISSN 0711-6748

Correct citation for this publication:

Rossiter, J.R., J.S. Holladay and L.A. Lalumiere. 1992. Validation of airborne sea ice thickness measurement using Electromagnetic Induction during LIMEX'89 (UP-C8-028). Can. Contractor Rep. of Hydrogr. and Ocean Sci. 41: x + 86 pp.

ABSTRACT

Rossiter, J.R., J.S. Holladay and L.A. Lalumiere. 1992. Validation of airborne sea ice thickness measurement using Electromagnetic Induction during LIMEX'89 (UP-C8-028). Can. Contractor Rep. of Hydrogr. and Ocean Sci. 41: x + 86 pp.

During LIMEX'89 ice thickness measurements were obtained by an airborne Electromagnetic Induction technique. Measurements were made using one of Aerodat's four-frequency EM systems mounted in a bird along with a laser profilometer. The bird was towed about 30m below a helicopter which flew at 50 to 80m elevation. EM, laser and navigation data were recorded digitally on tape in the helicopter and processed off-line.

Measurements were made both over shore fast first year ice and over first year pack ice. The ice was near the freezing point and offshore had a salinity of about 5 ppt and a thickness averaging about 0.5m. Agreement with auger thickness measurements was within ± 0.1 m over relatively level ice and 0.2m in the worst-case comparison. Ice conductivity was at the point of resolution for the instrument used.

Simultaneous video-camera imagery was also collected. This imagery was processed to estimate ice concentration and floe size at selected points. In addition, an overlay of the EM ice thickness data onto the video imagery was produced. These products are expected to be useful in assessing ice cover as part of climatological investigations.

RESUME

Rossiter, J.R., J.S. Holladay and L.A. Lalumiere. 1992. Validation of airborne sea ice thickness measurement using Electromagnetic Induction during LIMEX'89 (UP-C8-028). Can. Contractor Rep. of Hydrogr. and Ocean Sci. 41: x + 86 pp.

Pendant le LIMEX'89 des mesures de l'épaisseur de la glace ont été obtenues depuis un aéronef par la méthode de l'induction électromagnétique. Les mesures ont été effectuées au moyen de l'un des systèmes EM à quatre fréquences de la société Aerodat installé dans une torpille avec un profilomètre laser. La torpille était remorquée à 30 m sous un hélicoptère volant à une altitude de 50 à 80 m. Les données EM, laser et de navigation étaient enregistrées numériquement sur bande dans l'hélicoptère et traitées en différé.

Des mesures ont été effectuées sur la banquise côtière de première année et sur la banquise de première année. La glace était à une température voisine du point de congélation et présentait au large une salinité d'environ 5 ppt (parties par billion) et une épaisseur moyenne d'environ 0,5 m. Les mesures obtenues concordaient à $\pm 0,1$ m près avec les épaisseurs mesurées à la tarière sur la glace relativement unie et à 0,2 m près dans le cas de la pire comparaison. La conductivité de la glace se situait au seuil de résolution de l'instrument utilisé.

Une imagerie sur caméra vidéo a de plus été simultanément recueillie. Cette imagerie a été traitée de manière à estimer la concentration et la taille des floes en des points choisis. De plus, un calque de superposition des mesures EM de l'épaisseur de la glace sur l'imagerie vidéo a été produit. Ces produits devraient être utiles pour l'évaluation des couvertures glacielles dans le cadre d'études climatologiques.

Table of Contents

	Page
List of Figures	vi
List of Tables	vii
Acknowledgements	viii
Executive Summary	ix
1. Introduction	1
1.1 Background	1
1.2 Objectives	2
1.3 Scientific Basis	2
1.4 Report Outline	4
2. Data Collection	5
2.1 Introduction	5
2.2 Equipment Used	5
2.3 Measurements	5
2.3.1 Overview	5
2.3.2 Chronology	7
2.4 Problems encountered	10
3. Ice Thickness Data Processing	12
3.1 Introduction	12
3.2 EM Data Reduction	12
3.2.1 Calibration and drift removal	12
3.2.2 Inversion of survey data for ice thickness	13
3.2.3 Ice conductivity estimate	13
3.2.4 Flight path recovery	14
3.2.5 Data processing and accuracy	14
3.3 Results	18

3.4 Two-Dimensional EM Inversion	24
4. Processing of the Video Tape Imagery	27
4.1 Introduction	27
4.2 Ice Concentration	27
4.3 Ice Floe Size	29
4.4 Video Overlay	32
4.4.1 Producing the overlay	33
4.5 Automatic Image Processing	33
4.6 Comparison to Other Imagery	35
5. Conclusions and Recommendations	38
5.1 Conclusions	38
5.2 Recommendations	38
References	40
Appendix A EM Ice Thickness Data	
Appendix B Statistics of Ice Thickness Distribution	
Appendix C Histograms of Floe Size	
Appendix D OMAE Conference Paper	

List of Figures

1.1	Sketch of EM system and ice sounding concept.	3
2.1	Airborne ice thickness measurements, March 1989 - Field Site Map.	6
2.2	Depth - conductivity profile at two sites in Bay of Exploits.	9
3.1	Sensitivity of EM sensor to ice conductivity as a function of frequency.	15
3.2	Flight path and survey points in Bay of Exploits.	16
3.3	Flight path in the vicinity of the <u>M/V Terra Nordica</u> .	17
3.4	EM and auger ice thickness measurements for shorefast ice in the Bay of Exploits.	20
3.5	EM and auger ice thickness measurements in the vicinity of the <u>Terra Nordica</u> .	21
3.6	Histograms of ice thickness measured in the vicinity of the <u>Terra Nordica</u> by auger and for different segments of the airborne EM survey.	22
3.7	Plot of ice thickness and conductivity in vicinity of <u>Terra Nordica</u> .	25
4.1	Example of a digitized video image.	28
4.2	Histograms of the brightness of water, ice, and water and ice together.	28
4.3	Image (a) before and (b) after thresholding to determine ice concentration.	29
4.4	Image with ice floes outlined to measure floe size.	31
4.5	Histogram of floe size for image 15:33:46.	31
4.6	Example of overlay graphics.	32

4.7	Block diagram of equipment used to make overlay video.	34
4.8	Photograph of overlay and original video image.	34
4.9	Data from the NOAA-10 satellite at 8:59 NST on March 24, 1989.	36
4.10	Ice concentrations as calculated from SSM/I overpass at approximately 18:45 NST on March 24, 1989.	37

List of Tables

1.	Surface Measurements made March 20/90 along Line 3, Bay of Exploits	8
2.	Extremal Ice Thickness for Offshore Survey Lines	23
3.	Summary of Digitized Images, Line 2100	30
A1.	Raw and Processed EM System Data for Line 2050, 32 kHz	43

Acknowledgements

This work was funded under the DSS Unsolicited Proposal Program through DSS Contract No. FP953-8-0848/01-OSC. Departmental sponsors were Fisheries and Oceans (Simon Prinsenberg), Atmospheric Environment Service (Don Champ), Transportation Development Centre (Maurice Audette), and National Defence (Rob Cross).

Dr. Simon Prinsenberg, of the Bedford Institute of Oceanography, Dartmouth, N.S. was the Scientific Authority. Dr. Clive Mason of BIO was very helpful in planning this project.

We express our thanks to other LIMEX'89 investigators who provided surface information and assistance; including W. Winsor and G. Crocker of C-CORE; B. Eid and S. Melrose of MacLaren Plansearch; L. McNutt and S. Argus from the Radarsat Office; and K. Asmus of AES. We also thank C. Livingstone of CCRS, R. Rämseier of AES/York University, S. Paterson of Intera and S. Prinsenberg of BIO for access to imagery. Field work was conducted with the able assistance of C. Bassani and B. Simon from Aerodat. C. Coram of Canpolar assisted with data processing.

Executive Summary

Remote measurement of ice thickness is important both for practical operations and for a variety of scientific applications. Over the past few years electromagnetic (EM) induction has been shown to be a useful method for measuring ice thickness from a low-flying helicopter. In this report, results from measurements made off the coast of Newfoundland as part of the LIMEX'89 project in March 1989 are presented.

Measurements were made using one of Aerodat's four-frequency EM systems mounted in bird along with a laser profilometer. The bird was towed about 30 m below a helicopter which flew at 50 to 80 m elevation. EM, laser and navigation data were recorded digitally on tape in the helicopter and processed off-line.

Measurements were made both over shorefast first year ice and over first year pack ice. The ice was near the freezing point and offshore had a salinity of about 5 ppt and a thickness averaging about 0.5 m. Agreement with auger thickness measurements was within ± 0.1 m over relatively level ice and 0.2 m in the worst-case comparison. Ice conductivity was at the point of resolution for the instrument used.

Simultaneous video-camera imagery was also collected. This imagery was processed to estimate ice concentration and floe size at selected points. In addition, an overlay of the EM ice thickness data onto the video imagery was produced. These products are expected to be useful in assessing ice cover as part of climatological investigations.

These results confirm that EM induction can be used to collect ice thickness data reliably over long traverses. Work is underway to design systems for operational use.

1. Introduction

1.1 Background

There are a variety of reasons for requiring knowledge of ice thickness, including route selection for ships, scientific ice dynamics and climatology studies, design of offshore structures, and defence applications. To date, ice thickness has been measured directly at specific locations, inferred from other observations, or measured using impulse radar. All these approaches have strong limitations, particularly for saline and deformed ice (Canpolar Consultants Ltd., 1985).

The first airborne electromagnetic (EM) survey designed for sea ice measurement was carried out near Prudhoe Bay in 1985 by Geotech Ltd. of Markham, Ontario for the U.S. Army Corps of Engineers Cold Regions Research and Engineering Laboratory (CRREL) over cold Arctic ice (Kovacs and Valleau, 1987, Kovacs *et al.*, 1987a). This initial survey utilized a modified mineral prospecting bird operating at four frequencies ranging from 530 to 30,000 Hz. It was quite successful, although instrument drift caused some problems for the interpretation and insufficient surface information was obtained to permit thorough validation.

Two years later, a second survey was performed at Prudhoe Bay (Kovacs *et al.*, 1987b; Kovacs and Holladay, 1989). A prototype 3-frequency bird operating at 800, 4500 and 50,000 Hz, specifically developed for CRREL, was flown over a variety of ice types and features which were rigorously surface-verified by a CRREL team. The system used included a 3.5 m bird weighing 150 kg, a 0.01 m laser profilometer and a global satellite positioning system. Good agreement with surface data was achieved over relatively level ice.

The same year Canpolar and Geotech conducted a comparative survey in the Canadian Arctic over first-year and multi-year ice (Rossiter and Lalumiere, 1988). Agreement with auger and radar results was within ± 50 cm or better and further development of the technology was recommended.

In April, 1988 Canpolar and Aerodat performed an EM ice measurement survey off Cape Breton Island using a modified mineral prospecting system (MacLaren Plansearch, 1988). The results were very encouraging: drift problems were essentially negligible, noise levels were lower than expected, and calibration was obtained in flight from an area of open water. The accuracy of the results appears to have been constrained primarily by the ± 20 cm accuracy of the laser altimeter available at the time. Unfortunately, it was not possible to obtain one-to-one surface comparisons, but statistical agreement was achieved with surface measurements.

A practical technique for the measurement of sea ice thickness from an airborne platform based on electromagnetic induction is now reaching the end of its validation stage (although the more difficult problem of detailing the thickness of ice ridges is still the subject of research). The current study was planned to take advantage of the multi-disciplinary LIMEX'89 ice and ocean dynamics experiment being undertaken off Newfoundland in March 1989 (Raney and Argus, 1988). The objective was to evaluate the EM technique for relatively warm, saline ice. In particular, the evaluation of the technique as a tool for rapid collection of ice thickness data over long traverses and melting ice conditions was contemplated.

1.2 Objectives

The project had three major objectives:

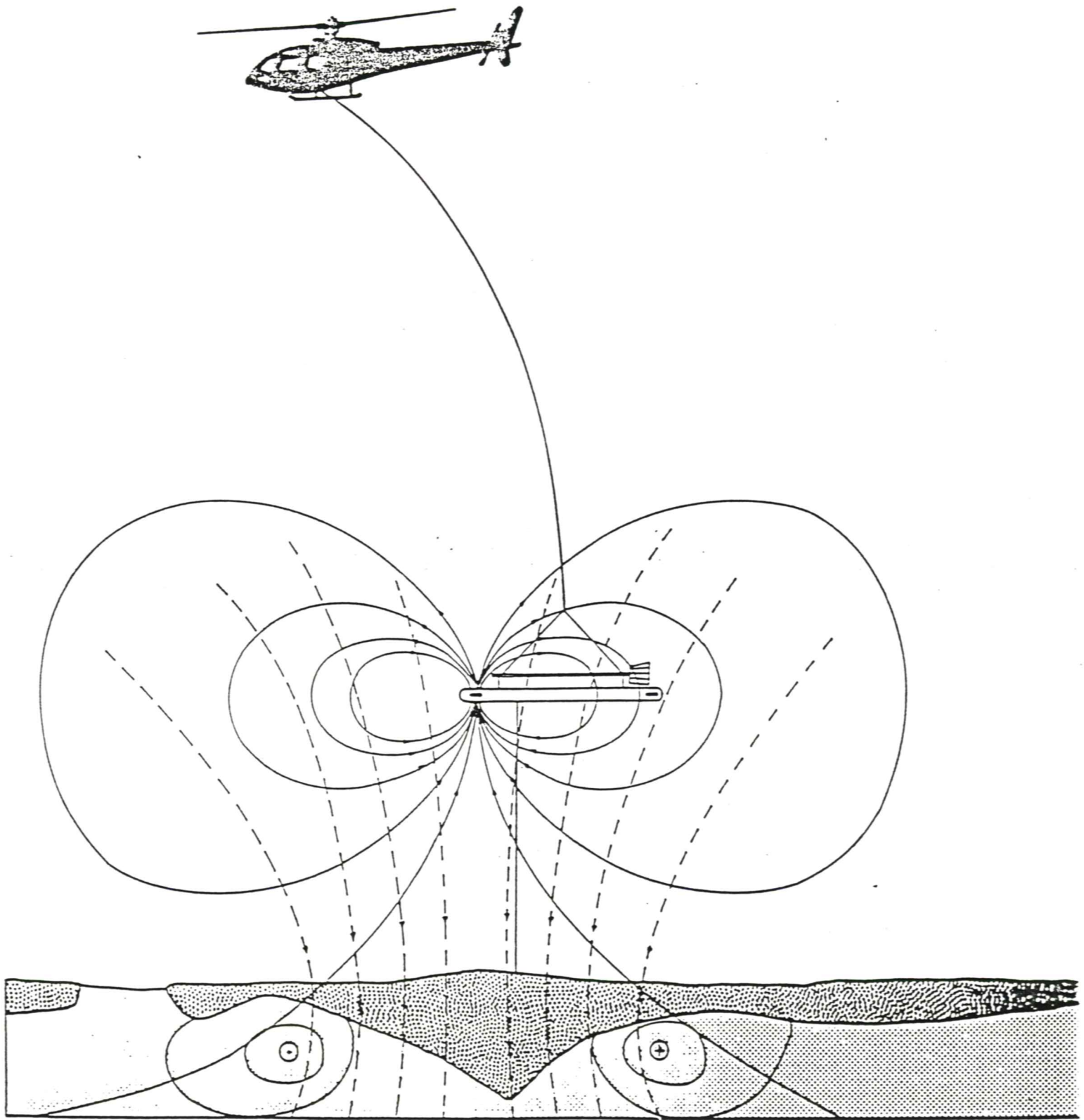
1. To evaluate airborne EM induction as a tool for measuring sea ice thickness off Canada's East Coast during LIMEX'89 by taking advantage of the available on-site information.
2. To prepare the software required in order to reduce the data collected into appropriate statistics of ice thickness, ice concentration and floe size, for inclusion as part of the LIMEX'89 data set, and to prepare and overlay of the ice thickness data with ice imagery on videotape.
3. To recommend further development activities for this technology based on the results of this study, particularly toward an operational capability.

1.3 Scientific Basis

The EM induction method uses frequencies in the 50 Hz to 100,000 Hz range. A set of transmitter and receiver coils are towed in a bird about 15 to 50 m above the ice, as shown in Figure 1.1. The transmitted primary field induces eddy currents in nearby conductors which in turn generate secondary EM fields. These secondary fields are detected at the receiver.

For ice thickness measurement, the sea water is the dominant conductor, since it is typically several orders of magnitude more conductive than the ice. By measuring the amplitude and phase of the secondary field (in parts per million of the primary field) at the receiver coil location, the distance from the bird to the water can be estimated. A laser profilometer is used to measure the distance from the bird to the top of the snow and/or ice. The difference between the two measurements gives the thickness of the snow plus ice layer. Areas of open water provide calibration points for the system.

Figure 1.1 Sketch of EM system and ice sounding concept.



The approximate "footprint" of the EM system is about the same as the bird height (the laser spot size is much smaller). When lateral changes in ice thickness are rapid compared to the flying height, such as are observed near ridges, the peak ice thickness tends to be underestimated.

1.4 Report Outline

The report will describe the equipment used and the data collection activities in chapter 2; the inversion of the EM data in chapter 3; the video processing in chapter 4; and conclusions and recommendation in chapter 5. Plots of the data collected will be given in the appendices.

2. Data Collection

2.1 Introduction

In this chapter, the equipment used will be described, the survey methods and chronology will be detailed, and ancillary data will be described.

2.2 Equipment Used

The sensor package used during this work included three principal elements: an Aerodat 4-frequency helicopter EM system in a towed bird; an Optech G-150 laser profilometer mounted in the bird; and a Sony DXC-101 video camera mounted in the helicopter. The EM system operated with 935 and 4,600 Hz co-axial, 4,175 and 32,000 Hz co-planar coils, and included an electromagnetic signal processor unit and a data acquisition/logging system mounted inside the helicopter. A set of attitude sensors was located inside the bird to measure pitch and roll. All data were sampled at 0.1 s intervals before digital recording on magnetic tape.

The video imaging system mounted on the helicopter monitored ice conditions below the bird. The image was annotated with time, flight and survey line identifiers before being recorded on video tape using a Panasonic AG-2400 VHS video cassette recorder. The camera had a 4.8 mm auto-iris lens.

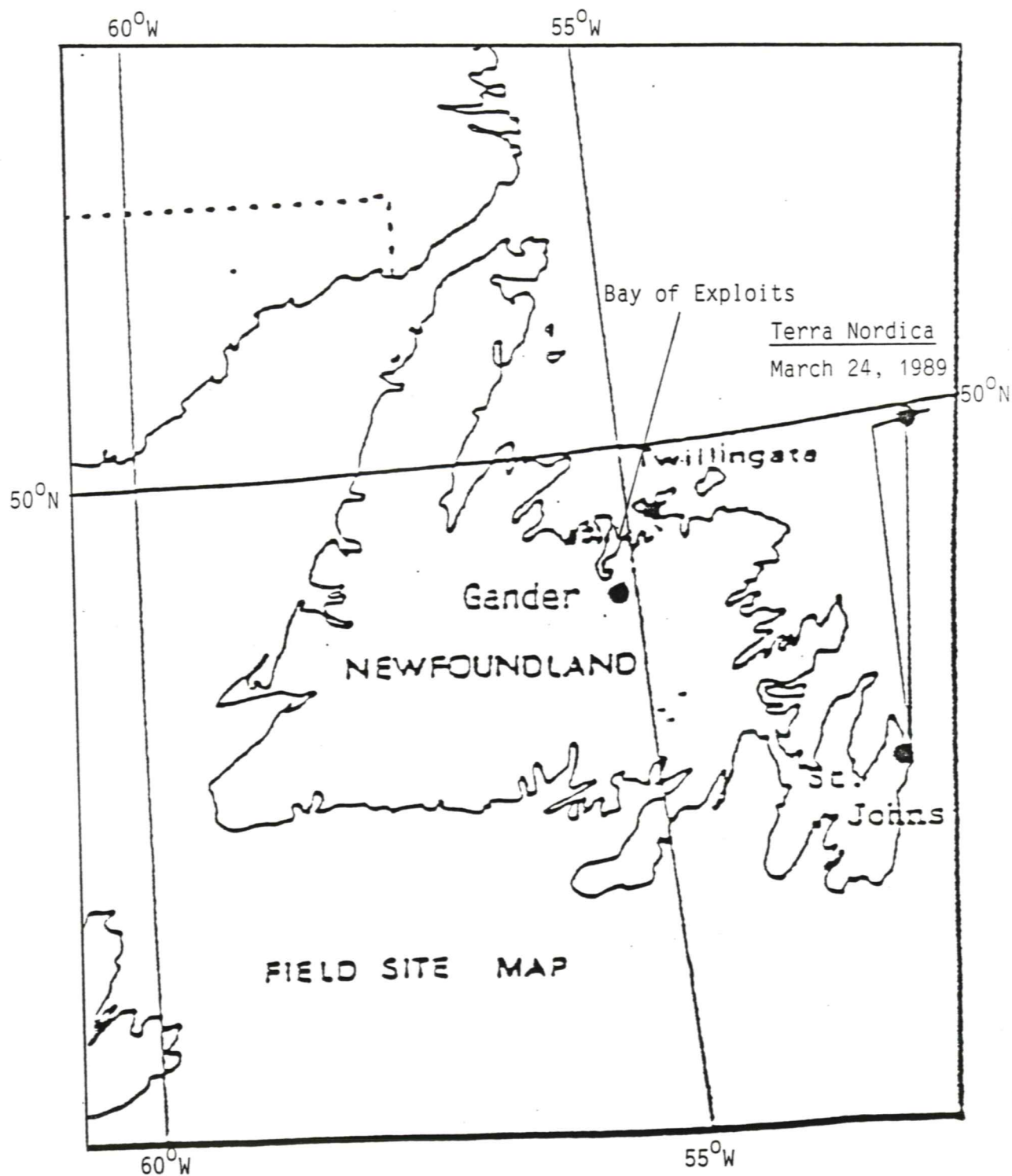
A LORAN-C navigation system was used to obtain approximate positions, which were also logged on tape. A Global Positioning System (GPS) system was available and would have been preferable in terms of accuracy, but satellite viewing conditions were not favourable for reliable positioning during the survey.

2.3 Measurements

2.3.1 Overview

The survey actually consisted of two distinct efforts (see Figure 2.1 for a location map). The first concentrated on shorefast ice in the Bay of Exploits, and provided a check on system performance and further validation of the method using relatively detailed surface truth measurements conducted by Canpolar and Aerodat personnel. The second consisted of a 500 km run from St. John's out to the M/V Terra Nordica and back. Surface truth for this survey was provided mainly by C-CORE personnel. At the time of the flight, two marked sites (the C-CORE Ice Motion Sensor and the MacLaren Plansearch ARGOS beacon S/N 4458) had been set up for other purposes, and auger estimates of ice

Figure 2.1 Airborne ice thickness measurements, March 1989



thickness were available there. A number of other sites were also augered, but either were not marked and therefore could not be located using the video record, or were too near the ship.

2.3.2 Chronology

Equipment and personnel from Canpolar and Aerodat were mobilized on schedule at Gander on March 16. It became clear that the Franklin and the Terra Nordica would be available for surface truth the next day before returning to port. Therefore, a flight was planned for as soon as possible on March 17.

Due to minor difficulties with the laser and a requirement to refuel in Twillingate, the nearest point of land to the ships, the flight did not commence until 14:00 local. Weather was clear and perfectly calm. The lack of wind precluded take-off with the bird and full fuel; therefore, the helicopter had a maximum range of 2 hours (about 120 nmi towing the bird), putting the ships (at about 51°05'N, 52°35'W) just out of range. The helicopter flew with the sensors on toward the ship for 1 hour and returned to Twillingate. Almost no ice was encountered en route and the helicopter returned in near white-out conditions due to a snow storm.

The extreme range of open water around the shore caused the helicopter company to revise their operating requirements for the single-engine Aerospatiale AS-350D A-Star, restricting it to a maximum 30 km range from shore. We had specifically taken up this issue with them in January and February and had been assured that there would be no problem carrying out our program of flying 100+ nmi from shore to refuel at the ship. On inquiry in March, no small twin helicopters were available. The only option available was to use a large Aerospatiale AS-332C Super Puma helicopter designed for heavy offshore work.

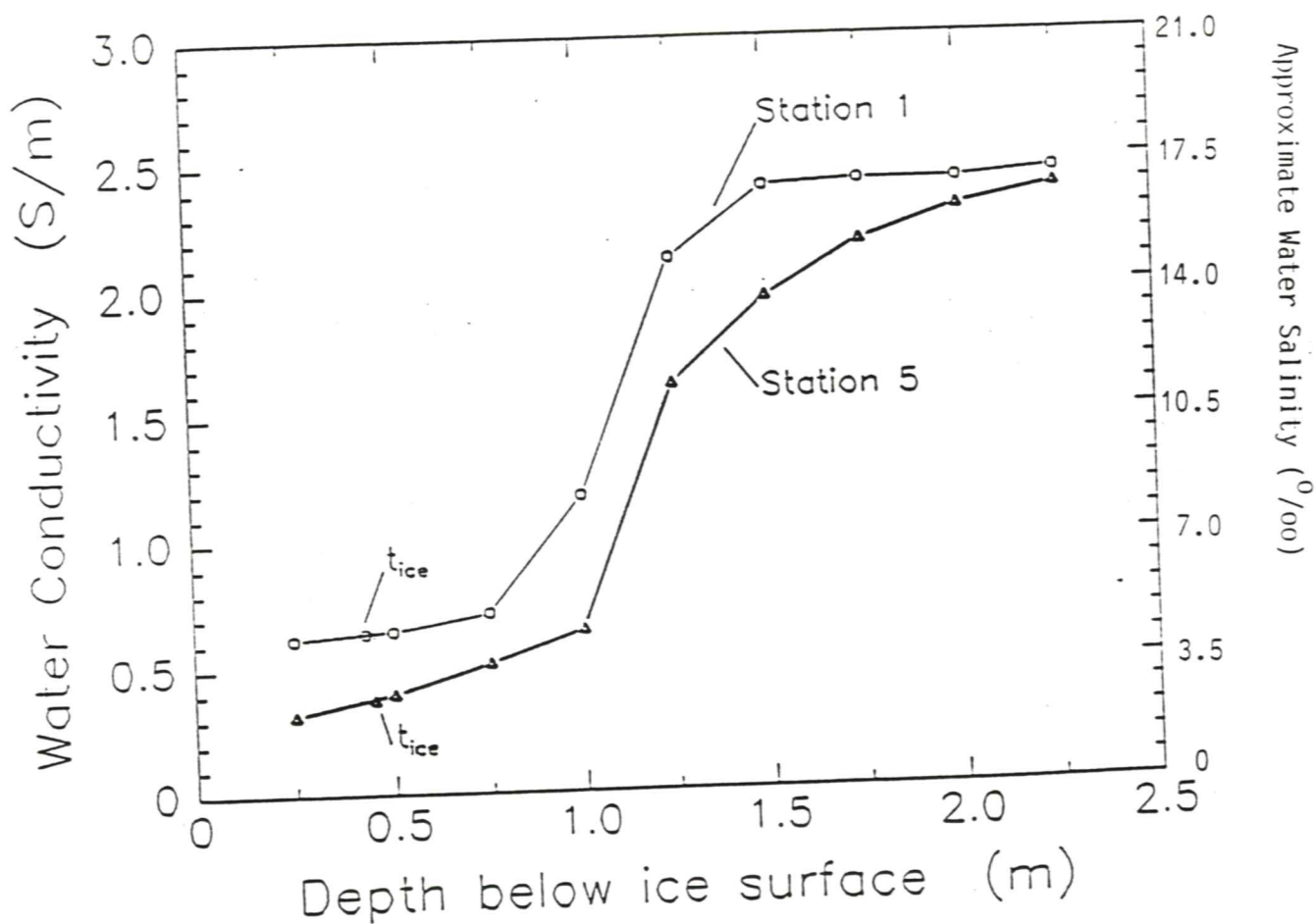
In the interim, measurements were made over fast ice at the approaches to Botwood in the Bay of Exploits. A total of 16 augered holes were measured, along with ice, water, and CDT profiles to 2.25 m depth (see Table 1 and Figure 2.2). Ice varied from 38 to 59 cm in thickness; snow cover, from 0 to 21 cm in thickness; the water under the ice had a conductivity of about 0.5 S/m, increasing sharply to 2.5 S/m at a depth of about 1.0 m. The ice had a salinity of less than 1 ppt.

The EM system was re-installed in the Super Puma while the Terra Nordica sailed from St. John's. A second flight, of about 5 hours duration, took place on March 24, from St. John's to the ship at 49°45'N, 52°00'W, toward Gander to the ice edge, and back to St. John's. Weather was excellent with clear sky, moderate wind and (except in local snow showers) 15+ miles visibility. There were waves and swell visible in the ice until well into the pack.

Table 1. Surface Measurements made March 20/89 along Line 3, Bay of Exploits.

Station No.	Ice thick (m)	>-----Water conductivity (S/m) at depth of (m)----->								
		.25	.5	.75	1.00	1.25	1.50	1.75	2.00	2.25
1	0.45	0.32	0.40	0.52	0.65	1.62	1.96	2.18	2.31	2.39
2	0.44	0.50	0.52	0.80	0.95	2.30	2.42	2.48	2.50	2.50
3	0.52	0.15	0.32	0.40	0.55	1.70	1.95	2.08	2.12	2.14
4	0.42	0.58	0.55	0.82	1.05	2.20	2.45	2.48	2.48	2.48
5	0.43	0.62	0.65	0.72	1.18	2.12	2.40	2.42	2.42	2.45
6	0.45	0.68	0.70	0.70	1.65	2.10	2.28	2.35	2.38	2.40
7	0.38	0.65	0.66	0.72	1.05	2.05	2.15	2.20	2.35	2.35

Figure 2.2 Depth-conductivity profiles at two sites (see Figure 3.2) in Bay of Exploits, March 20, 1989. Note increase in salinity at about 1.0-1.5 m depth. Ice thickness (t_{ice}) is also shown.



Measurements were made over most of the flight, i.e. about 175 nmi. Ice encountered varied from strips and patches of brash ice, to small cakes of first year ice, to small floes of first year ice around the ship. Although most of the ice was not rafted, there were some rafted pieces. Subsequent to the flight the equipment was removed for other work.

2.4 Problems Encountered

The single most critical problem encountered during this work was the position of the ice pack relative to the shore: during the survey time window, the ice vessel was always at least 100 km from the nearest point of land. The difficulty in reaching the ice pack from land lead, after some consideration, to a shift from the relatively economical A-Star 350D to the much more expensive Super Puma 332C. This twin-engine helicopter had sufficient range to make the round trip to the Terra Nordica easily. In future, a small twin-engine helicopter, such as a Twinstar AS-355, a Bell 212 or an MBB BO-105 (planned for use by the Canadian Coast Guard) should be used. Any of these would have the required safety factors and would have capacity to carry the equipment and crew. However, they would have to be re-fuelled for runs of more than a few hours duration.

The performance of the EM hardware on the survey flights was, for the most part, highly satisfactory. Small amounts of drift were observed during the early portions of the Bay of Exploits flights, but did not affect the passes over the main lines. A slightly longer warm-up period (about 1 hour) would have prevented most of this drift.

One of the two Optech G-150 altimeters purchased by Aerodat before this survey failed to operate properly and was sent back for repair. The backup unit performed well over snow and ice, but was inconsistent over open water. The explanation offered for the latter by the manufacturer was that the automatic exposure control firmware built into the unit to handle variable-reflectance targets was confused by occasional specular reflections of the laser beam from the water surface; diffuse reflectors such as snow and ice did not trigger this problem. A modification of the hardware and firmware of the profilometer is being considered.

The video system performed well during the Exploits flights: the images were sharp and contrast, good. The installation of the camera in the Super Puma was nearly ideal, as it was mounted in a "bubble" window at the rear of the aircraft. Unfortunately, it appears that dirt or oxide accumulations on the video recording heads, coupled with the characteristics of the camera's auto-iris and the partially cloudy weather, lead to a recorded video image with reduced contrast, visible scan lines and fluctuating brightness. These problems complicated the video tape analysis considerably. Disabling the auto-iris and cleaning the video heads before flight should prevent such problems in future.

The LORAN-C positions were not particularly reliable during the offshore run. This may be a result of weak signal strength, the location of the LORAN antenna on the Super Puma, or magnetic storm activity which was unusually severe at the time. GPS navigation is the obvious solution to this problem, but it is not yet available around the clock. It is anticipated that enough GPS satellites will be in orbit by 1991 to permit use of GPS positioning at almost any time of the day, which will dramatically improve the accuracy of flight path recovery. In addition, most offshore-capable helicopters are equipped with OMEGA navigation, which can provide approximate positions to the data acquisition system in RS-232 format.

Lack of communication with the surface team on the Terra Nordica resulted in survey auger holes being made too near the ship to be used as reference comparisons. The paucity of marked auger hole positions in the offshore ice meant that little point-to-point validation could be performed, and also meant that the two sites which were measured and marked assumed an unrealistic importance: statistics are hard to formulate on the basis of two data points.

3. Ice Thickness Data Processing

3.1 Introduction

This section summarizes the acquisition, reduction, interpretation and assessment of the data.

3.2 EM Data Reduction

3.2.1 Calibration and drift removal

There are three stages in the data reduction: transcription of the field data tape to a computer disk (data volumes range up to 4 Mbytes per hour at present); removal of baseline drift; and calibration of the data. The data transcription operation is relatively straightforward, and leaves the data in a format in which it can be manipulated easily in later stages of reduction.

The removal of drift presently requires that the sensor package be flown to high altitude (above about 400 metres) approximately every 30 minutes during the flight to remove the sensor package from the vicinity of the highly conductive seawater. Variations in these high-altitude measurements provide a reliable way to correct for small amounts of drift in the system, based on the assumption of linear drift between these baseline measurements. As EM system drift becomes smaller and more predictable with improved equipment, the permissible baseline interval will become progressively longer, increasing survey efficiency.

When the data have been drift-corrected, they are calibrated. At present, the most reliable way to estimate the sensitivity of the system is to fly over deep, open water of known conductivity: an accurate prediction of the response is then compared with the measured response, and correction factors applied to bring the measured response into line with the expected response. This technique has become known as "ground-truth recalibration", and has proven quite satisfactory under a variety of conditions. Instrumentation advances are expected to provide a stable, accurate internal calibration method during the next year, at which point the surface-truth comparison will become a verification tool rather than a calibration tool.

Another operation which is sometimes performed on EM data is called spheric removal, and involves removal of noise pulses in the EM data caused by distant lightning strokes. The algorithm used for this operation is useful for removing spikes from other relatively smooth data as well; the laser profilometer data was filtered in this way to remove errors caused by inconsistent performance of the profilometer over open water.

3.2.2 Inversion of survey data for ice thickness

The drift-corrected, calibrated data, which consist of the secondary field response in phase with and out-of-phase with the transmitted, or primary, field, vary according to the altitude of the bird (and, to a small extent, upon its attitude) above the surface of the seawater underlying the ice. The response is not a particularly simple function of altitude, and is also affected by the conductivity of the seawater (at low frequencies) and of the ice (at high frequencies), but forward computer models which can predict the EM response over a given ice/water model have been written (Holladay, 1980). Inverse models which directly calculate bird height from measured data do not yet exist.

For this reason, a number of relatively complex methods have been developed to invert the data approximately. The most robust of these methods, in the sense of providing good results even in the presence of data error, is the Generalized Inverse method, which uses a forward model to generate model responses and a matrix of derivatives of those responses with respect to the desired parameters, such as ice thickness and seawater conductivity. An initial forward model response is compared to the observed response, and the differences between them are used, along with the generalized inverse of the derivative matrix, to estimate the changes in the model parameters required to make the model response resemble more closely the measured response.

After a few iterations this algorithm usually provides estimates of the ice thickness that are accurate to within the range of accuracy of the laser altimeter (about 5 cm), at least for relatively level ice. Ice that has large thickness variations over short horizontal distances tends to have its thickness underestimated by this method; more suitable approaches are being developed to deal with these situations as described in Section 3.4.

3.2.3 Ice conductivity estimate

The Generalized Inverse method discussed above should, under suitable conditions, obtain stable and accurate estimates of average ice conductivity from survey data. However, the accuracy of such estimates is critically dependent on the quality of the data and of the calibration. Numerical experiments have been conducted to define the frequencies at which measurements should be obtained for ice conductivity estimation and field data have been analyzed to validate the numerical experiments.

The sensitivity, as a function of frequency, of an EM system to the conductivity of an ice layer 1 m thick overlying seawater varies by about an order of magnitude (see Figure 3.1), but is almost constant at a given frequency with respect to ice conductivity in the 0.05 to 0.001 S/m range anticipated for most sea ice. The plot in Figure 3.1 thus defines the minimum conductivity that can be resolved at a given frequency, provided that system

noise is about 1 ppm in a system with a 6.45 metre coil separation. Therefore, a system operated at a frequency of 4,175 Hz should resolve down to about 0.013 S/m; 33,000 Hz, to about 0.008 S/m; and, 100,000 Hz, to about 0.005 S/m.

In order to make practical measurements of ice conductivity, it may be necessary to calibrate the system over ice of known properties, although there is no fundamental reason why this step would be required. It should be noted that flying the system at altitudes lower than the nominal 30 m should increase the resolution of ice conductivity. Ice conductivity estimates for ice thicker than 1 m should have a proportionately higher resolution and vice versa. For the 0.5 m thick ice encountered during LIMEX'89, the 32 kHz data should be able to resolve ice conductivity to about 0.02 S/m.

3.2.4 Flight path recovery

Precise positioning of the system is essential in some ice measurement applications, particularly if gridded data is being sought, e.g., for contour mapping. For the LIMEX'89 survey, and indeed for most such surveys where long lines over mobile ice are being flown, positioning becomes less critical. Surface measurement sites used as tie-ins or for validation of system performance must be marked on the ice and correlated with system outputs visually or with video imagery, since their absolute and even relative positions can change rapidly in the course of a few days. With these considerations in mind, and knowing that suitable GPS windows were not available, LORAN-C was selected to provide approximate positional control. The LORAN-C outputs were recorded as latitude and longitude on tape, and were converted to appropriate UTM coordinates during post-processing.

The quality of the LORAN-C data was quite good during the work in the Bay of Exploits, permitting surprisingly good flight path recovery there (see Figure 3.2). Positioning was not nearly as good for the flight from St. John's to the Terra Nordica (Figure 3.3), particularly in the E-W direction, in which unexpected variations of about 1 km were observed. These errors appear to be the result of low signal strength from one of the LORAN slave transmitters, although it is possible that magnetic storms occurring at the time may have altered radio propagation conditions sufficiently to generate the spurious fixes. It was therefore necessary to correct the positions manually using smoothing and visual or flight log information; an example of the latter is shown in the repeated passes over the Ice Motion Sensor.

3.2.5 Data processing and accuracy

An example of the detailed steps taken to produce ice thickness and conductivity estimates is given in Appendix A. For the data collected during this study, the inversion was

Figure 3.1

Sensitivity of EM sensor to ice conductivity
as a function of frequency.

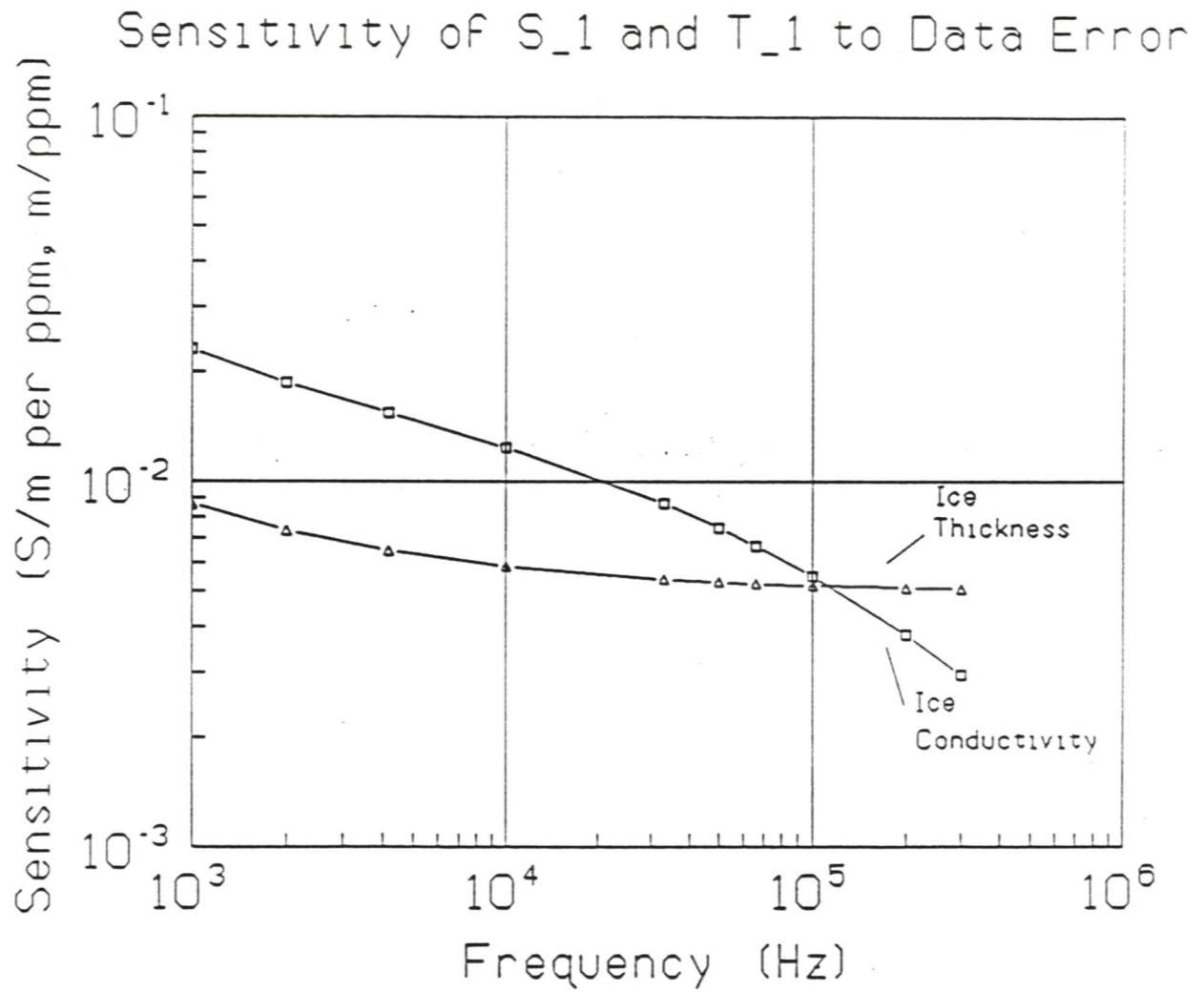
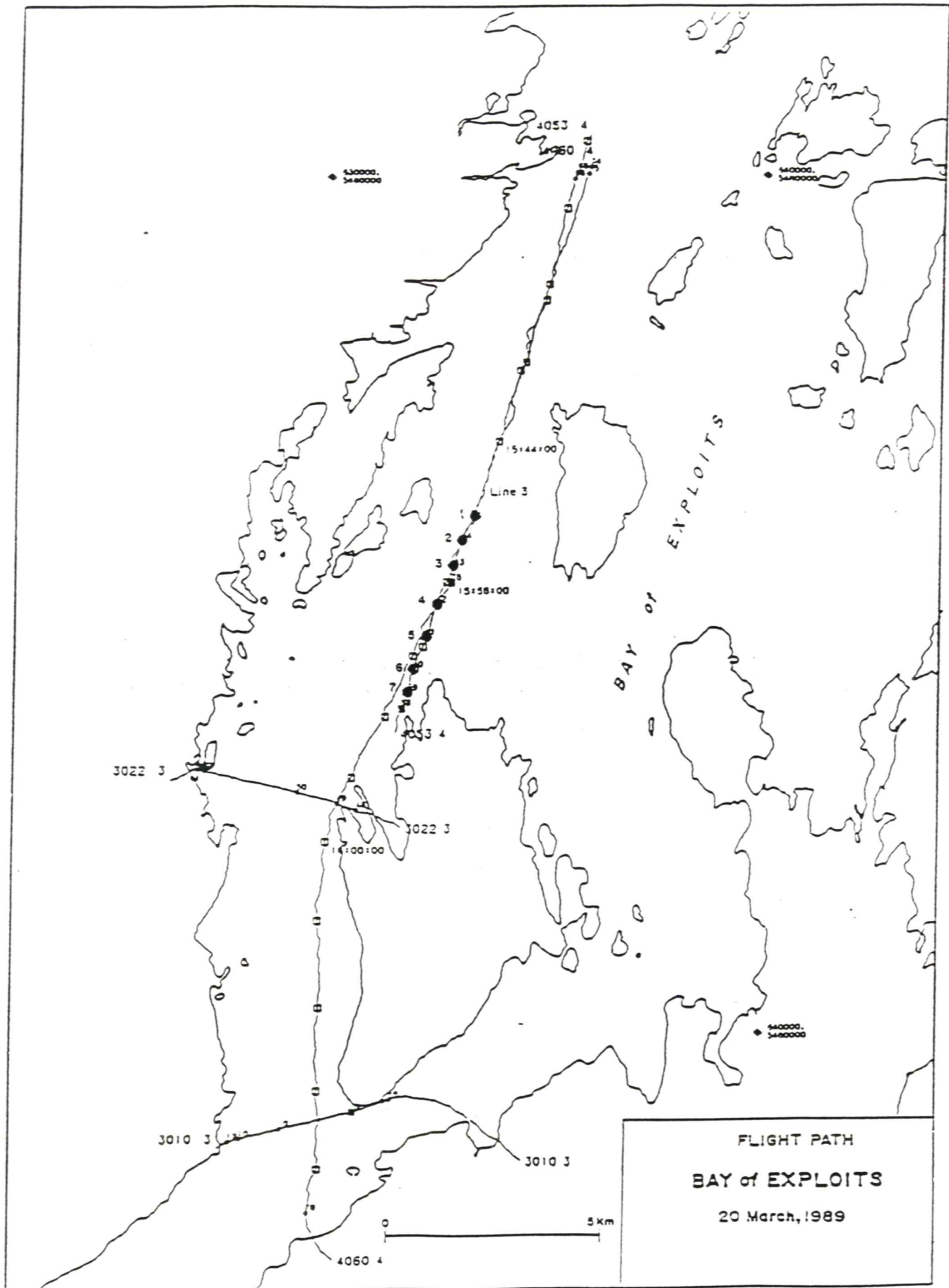


Figure 3.2



17



performed on each frequency independently, and the results were usually very similar. A complete set of plots is given in Appendix A based on the 4,175 Hz, co-planar coils, which generally had the lowest noise levels in this data set.

Accuracy of the system is limited by several factors (see Holladay *et al.*, 1986). The intrinsic precision of the instruments provide a vertical accuracy limit. The EM system has an maximum sensitivity of several ppm of the primary field, which would give an ice thickness estimation error of about ± 1 cm at a height of 30 m for typical sea water conductivity. The laser altimeter used has an accuracy of ± 5 cm, for a total possible error of ± 6 cm. Laser altimeters with accuracy of ± 1 cm or better are available.

The above analysis assumes relatively smooth ice; i.e. that the vertical changes are small over the EM footprint, which is approximately equal to the bird flying height for co-axial coils and equal to about four times the bird height for co-planar coils (Liu and Becker, 1990). For two and three dimensional structures errors in the one dimensional inversion process will soon overwhelm any other sources of error and can be detected by examining the error of fit in the inversion using several frequencies.

Horizontal resolution is governed both by the footprint and by the sampling rate. The sampling rate used here of 0.1 s, which was then averaged to 0.2 s, provides a sample every 5 m at a speed of 50 knots (25 m/s), so that there were typically 5 to 25 samples per footprint. Higher flying speed will therefor not greatly diminish the horizontal resolution, but will start to induce vibration-related noise into the system, reducing the EM sensitivity.

In areas where the footprint covers both ice floes and open water, the EM estimate of ice thickness will underestimate the average thickness of the floes. It is expected from physical principles that the underestimate will be approximately proportional to the open water area fraction within the EM footprint. The maximum ice thickness that can be measured is more closely related to total distance from the bird to the water, and is likely in excess of 30 m. Although melt water on the ice surface could induce errors if it were highly saline, a thin layer would not likely give much response. Use of several frequencies would alleviate this ambiguity.

3.3 Results

Data were collected over two main traverses off the East coast of Newfoundland during March 1989: over shorefast ice in the Bay of Exploits (Figure 3.2) and a 500 km long run over pack ice from St. John's to the *Terra Nordica*, stationed at $49^{\circ} 45' \text{ N}$, $52^{\circ} 00' \text{ W}$, and back (Figure 3.3). Surface data included ice thickness measurements by auger and conductivity-depth profiles in the ocean.

At the Bay of Exploits site the shorefast ice was relatively level and auger-sampled ice thicknesses ranged from 0.38 to 0.59 m. Snow cover was 0 to 0.21 m thickness. The ice salinity was less than 1 ppt. Underlying the ice was a 1.0 m thick layer of relatively fresh water with a conductivity of 0.5 S/m, overlaying water with a conductivity of 2.5 S/m (Figure 2.2). The fresh water is presumed to have come from local rivers, but this situation is also likely to occur during ice melt conditions. Interpretation of the EM response was based on a two-layer model for the water. Results of the inversion are given in Figure 3.4. The agreement with auger measurements is within ± 0.1 m. The EM results suggest a gradual thickening of ice from 1.2 m to 0 m as the line progresses offshore. Water depth was typically greater than 75 m so that bias in the ice thickness measurement due to finite water depths should be negligible.

A selected portion of data near the ship is given in Figure 3.5. The first year pack ice was made up of many pans, typically 10 m in diameter and varying from 0.3 to over 1.6 m in thickness. Ice salinity was typically 5 ppt and temperature around -2°C . Although there were few comparative points, data from two auger holes are shown. The EM results agree with the surface data within 0.05 m at one site (the Ice Motion Sensor) and within 0.2 m at another (the ARGOS beacon). The larger disparity at the latter location is probably due to local rafting. A complete set of the EM ice thickness data plots is given in Appendix A.

A histogram of ice thickness based on 125 "random" measurements made by auger by investigators in the same area is shown in Figure 3.6, along with 11 histograms taken from sections of the airborne survey made near the Terra Nordica. Extremal ice thicknesses are given in Table 2. Although some of the histograms (e.g. Line 2060) are very similar to that of the surface data, others (e.g. Line 2030) are quite different. The differences point out local variability in the ice.

However, they also underline the difficulty in comparing airborne and auger results: a) the surface measurements are only taken at specific points whereas the EM system averages over an area of approximately $10^2 - 10^3 \text{ m}^2$; and b) surface measurements are inevitably biased against thin ice (too thin to stand on) and/or thick ice (beyond the auger stem). These differences represent one of the important advantages of remote ice thickness measurement for scientific applications.

There are also important statistical factors to consider when comparing surface and aerial data. Some of these have been outlined by Dr. C. Dalzell in a letter given in Appendix B, and include the implicit spatial averaging by the EM measurement over a finite footprint, smoothing over the footprint, non-stationary and non-independent measurements, etc. A more thorough evaluation of some of these factors is probably warranted before the two sets of measurements are compared statistically.

Comparison of the surface measurements and the EM results indicates that the typical accuracy of the method was within ± 0.05 m in ice that was typically 0.5 m thick. It

Figure 3.4 EM sounding and auger ice thickness measurements (circled points) for shorefast ice in the Bay of Exploits.

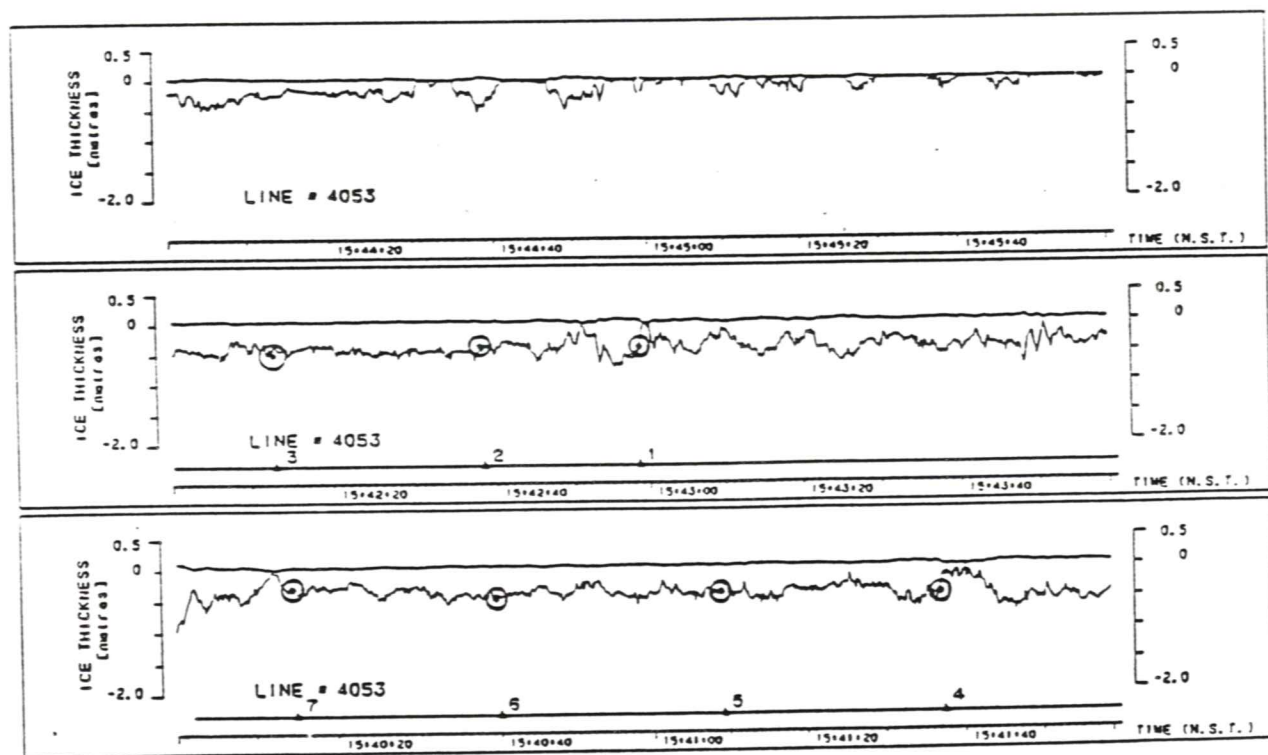
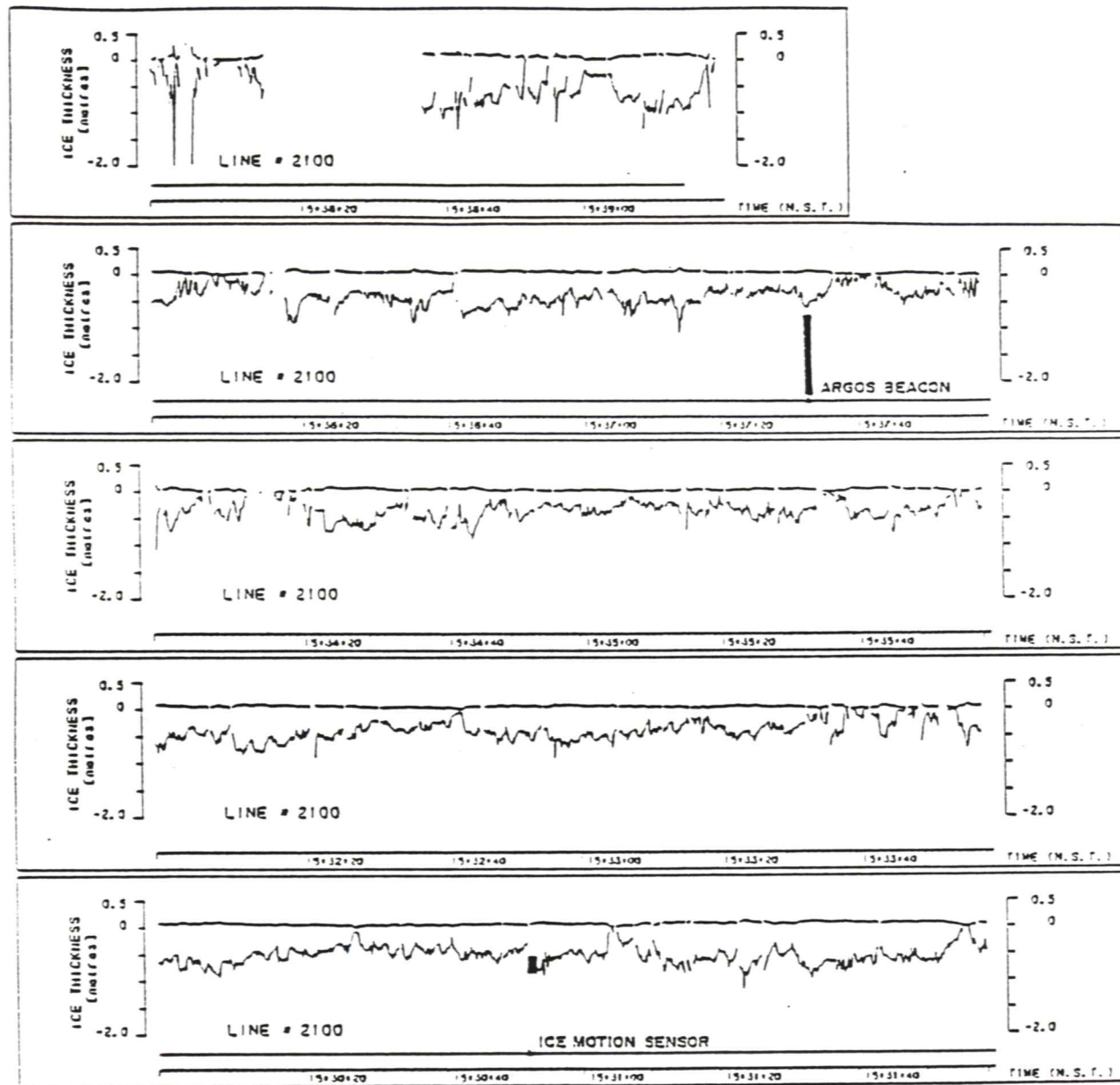


Figure 3.5 EM and auger ice thickness measurements (range of auger estimates shown as bar) near the Terra Nordica.



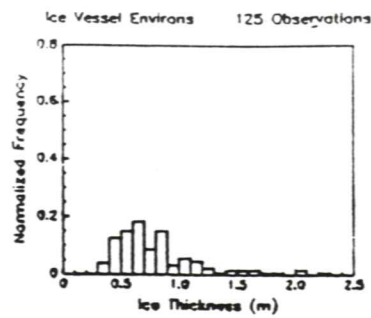


Figure 3.6 Histograms of ice thickness measured in the vicinity of the Terra Nordica by auge and for different segments of the airborne EM survey

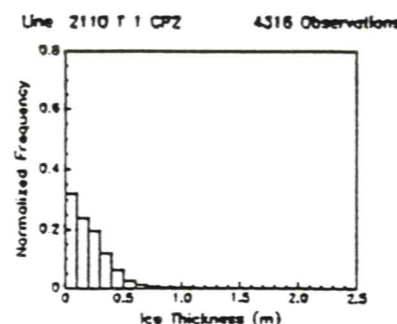
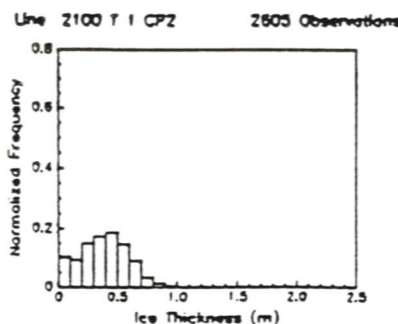
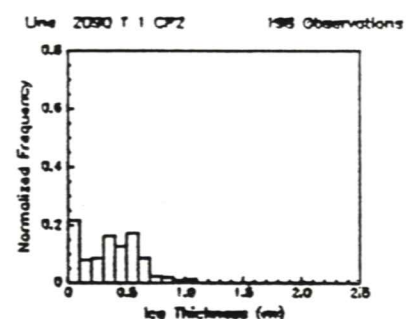
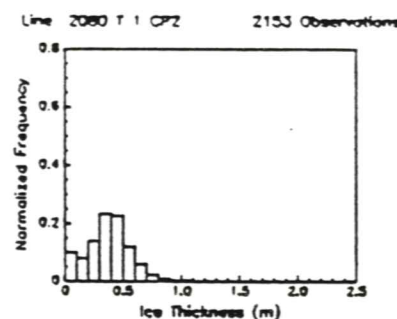
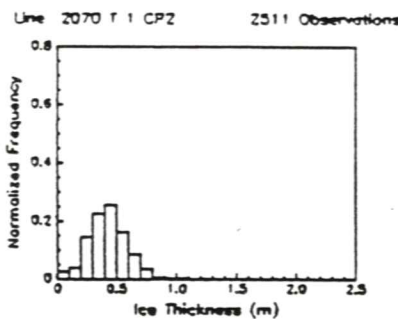
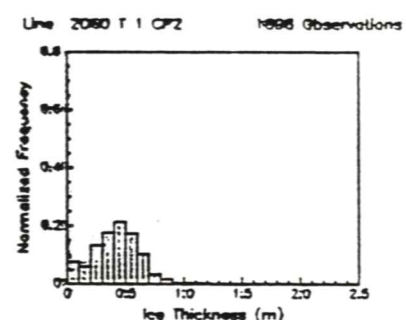
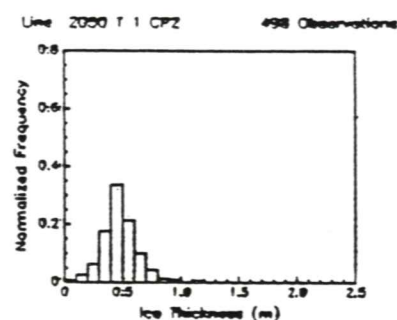
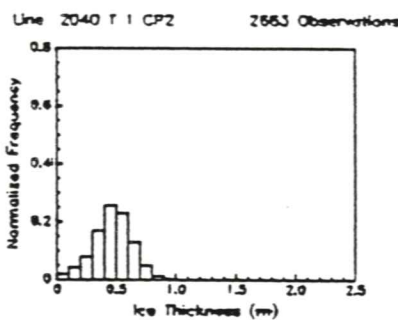
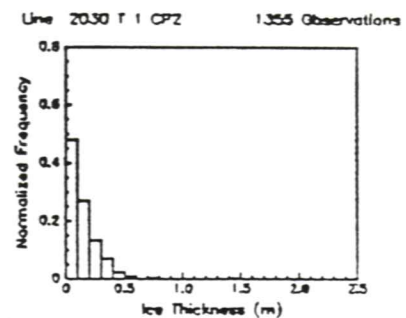
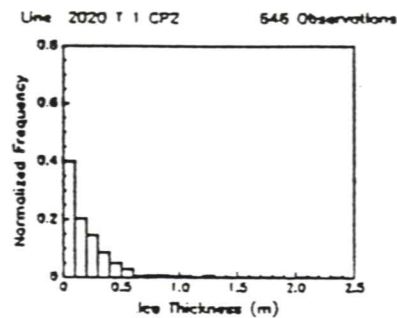
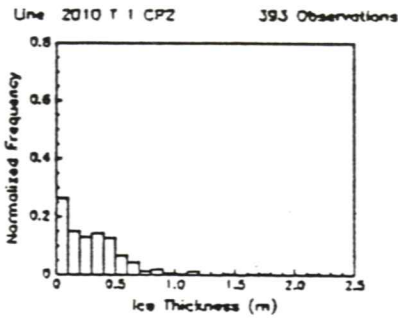


Table 2. Extremal Ice Thicknesses for Offshore Survey Lines

Line Number	Minimum (m)	Maximum (m)	Spike Max* (m)
2010	0.00	0.45	2.5
2020	0.00	0.47	2.5
2030	0.00	0.58	2.5
2040	0.00	1.20	---
2050	0.20	1.27	---
2060	0.00	1.15	2.3
2070	0.00	1.33	---
2080	0.00	1.30	2.5
2090	0.00	1.15	---
2100	0.00	1.40	2.3
2110	0.00	1.45	2.5

* For this table, "spikes" are defined as apparently unreliable single-point thickness estimates. However, in some cases, single-point thicknesses have been accepted as reliable where the surrounding ice is thick as well.

should be noted that the 0.05 m accuracy appears to have been mainly the result of laser profilometer errors, which would be constant for ice of any thickness. There was one significant exception to this observed accuracy: in the one survey line that passed over the ARGOS beacon, the EM-measured ice thickness was 0.2 m less than the smallest of the three auger measurements. The two most likely reasons for this disparity are local rafting in the floe (three auger holes all encountered water-filled zones, the first at 0.5 metres depth) and the effects of lateral thickness variation (the floe was less than one system footprint wide and about one footprint long, and was largely surrounded by slush and seawater).

In the Bay of Exploits the ice was relatively low salinity (1 ppt) and would therefore be expected to have a conductivity in the order of 10^{-2} S/m at this frequency (Morey *et al.*, 1984), which is just at the edge of our resolution of ice conductivity at 32 kHz. The presence of the 1 m layer of brackish water between the ice and the sea water generated sufficient uncertainty in the interpretation that estimates of ice conductivity from EM results would be problematic with the data collected.

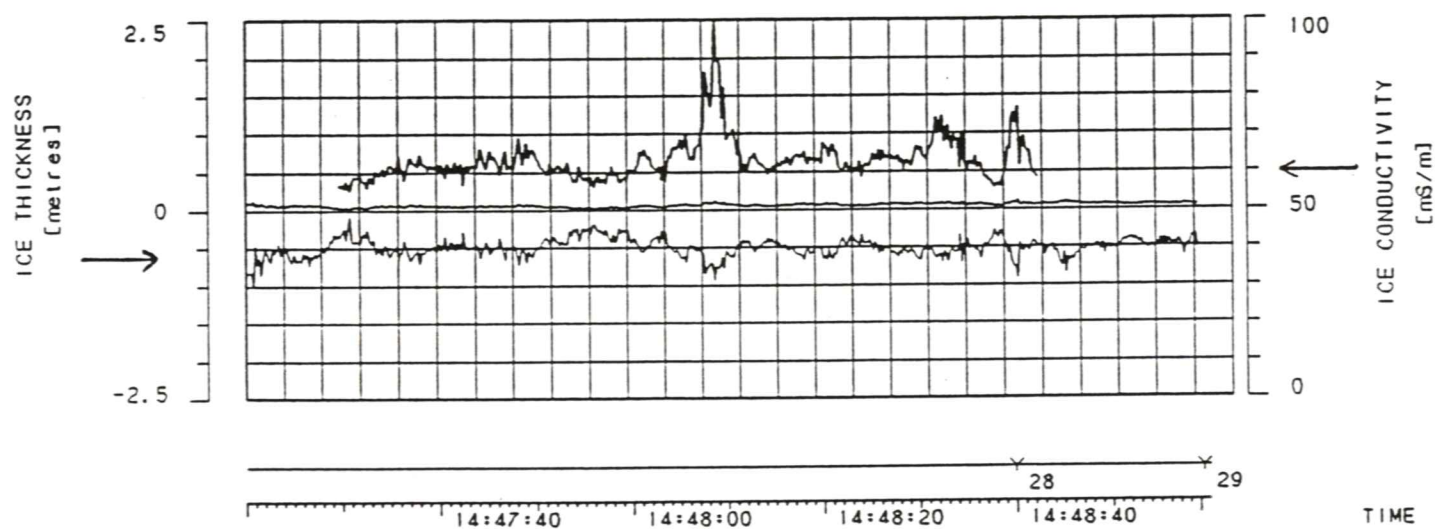
EM ice conductivity estimation was attempted on the survey lines near the Terra Nordica; the results for one short line very close to the ship are given in Figure 3.7. Although the values appear to be consistent with values expected for the ice, in the absence of ice samples from the marked surface-measurement sites it is difficult to comment further on the validity of the EM ice conductivity estimates. It should be noted that the conductivity estimates were not stable for bird heights above 26 m. Since most of the survey was flown between 30 and 40 m elevation, relatively few conductivity estimates were obtained overall.

3.4 Two-Dimensional EM Inversion

The traditional inversion method for EM induction data uses a one dimensional (1-D) model of the ice-sea water interface; i.e., assuming that the interface changes only in distance from the bird. Therefore, the interface must have relatively gentle topography for correct results. When non-uniform ice is encountered the 1-D inversion underestimates ice thickness and more complex two or three dimensional models are required (Becker *et al.*, 1987; Liu and Becker, 1988; Liu and Becker, 1990).

Guimin Liu's Ph.D. thesis (Liu, 1989) was on the development of a computationally rapid technique for inversion of two dimensional structures typical of sea ice ridges; i.e. assuming that the strike length is much greater than height of the bird above the ice. The modelling program assumes that the ice is transparent at the frequency used and that the sea water is infinitely conductive. These are not strong constraints for the ice thickness problem and ease the computation since inductive limit values of the EM field can be used instead of both in-phase and quadrature components.

Figure 3.7 Plot of ice thickness and conductivity in vicinity of Terra Nordica.



The two dimensional inversion program requires an array of inductive limit EM data points crossing an ice keel as input. The output of the inversion program is a solution for the smoothest keel shape that fits the input data. As a result, the thickness of sharp keels will still be underestimated slightly.

Liu has developed several other programs for modelling and processing EM induction data:

- * a 2-D inductive limit forward model program takes the shape of a discretely sampled curved metal surface as an array input and outputs an array of inductive limit data corresponding to positions above the surface.
- * a general 2-D forward model program uses a discretely sampled curved surface with finite conductivity as input and outputs an array of in-phase and quadrature components.
- * a 3-D inductive limit forward model calculates inductive limit data at any point above a three dimensional surface. The surface is created by gaussian curves in both x and y planes.
- * an altitude correction program removes the effect of varying flight height from raw in-phase and quadrature data and outputs corrected in-phase and quadrature data. The EM response from altitude variations can be much larger than the 2-D response from an ice keel. In raw EM data, an ice keel can be obscured by altitude variations. Once the response from altitude variations is removed from the raw EM data, the response from 2-D structures are clearly visible.

Although we did not collect any pertinent data relating to ridges during LIMEX'89, this aspect of ice thickness measurement will be important for both icebreaker and scientific applications. Based on Liu's work, appropriate data inversion procedures appear to be available.

4. Processing of the Video Tape Imagery

4.1 Introduction

A video camera was mounted looking down from inside the helicopter. Through a wide angle lens, the EM bird and the ice and water surface could be seen in the video image. The data acquisition system on board the helicopter added flight information and a time stamp to the video signal.

The video imagery was digitized so that measurements could be made of floe size and ice concentration. The ice concentration values can be used to supplement the EM interpretation since low values of ice concentration cause the EM system to underestimate ice thickness.

The data set used for this work was line 2100, which began at 15:29:46 (local) and ended at 15:39:22 on March 24/89. The line started near the Terra Nordica, overflowed the ice motion sensor at 15:30:52 and the ARGOS beacon at 15:37:34.

In addition a video sequence was made to overlay a set of EM ice thickness measurements with the original video imagery. Ice thickness, ice thickness histograms, ice concentrations and laser altimeter data from line 2100 were incorporated as a graphic plane for the overlay.

In this chapter the steps taken to produce this additional ice information and the overlay are described.

4.2 Ice Concentration

To measure ice concentration, the video imagery had to be digitized. The poor quality of the video recording required special processing of the tape at a professional video house to correct sync pulses and to remove the colour information, which caused noise when grabbing frames of imagery.

Using an Oculus 300 square pixel frame grabber, 40 images were captured from the video tape. The video tape was advanced through the flight and frames were captured every 15 seconds. The digital images were compressed from their original resolution of 512 x 484 x 8 bits to 256 x 242 x 8 bits before analysis. Figure 4.1 is an example of a digitized image.

Ice concentration was measured by thresholding the image between an average water brightness and an average ice brightness. Fluctuating image brightness caused by the camera problems made it necessary to make separate histograms for each image. Figure 4.2 shows histograms of areas containing open water, ice only and open water and ice. The histograms cover a 16 x 16 pixel area of the digitized image defined using the



Figure 4.1 Example of a digitized video image.

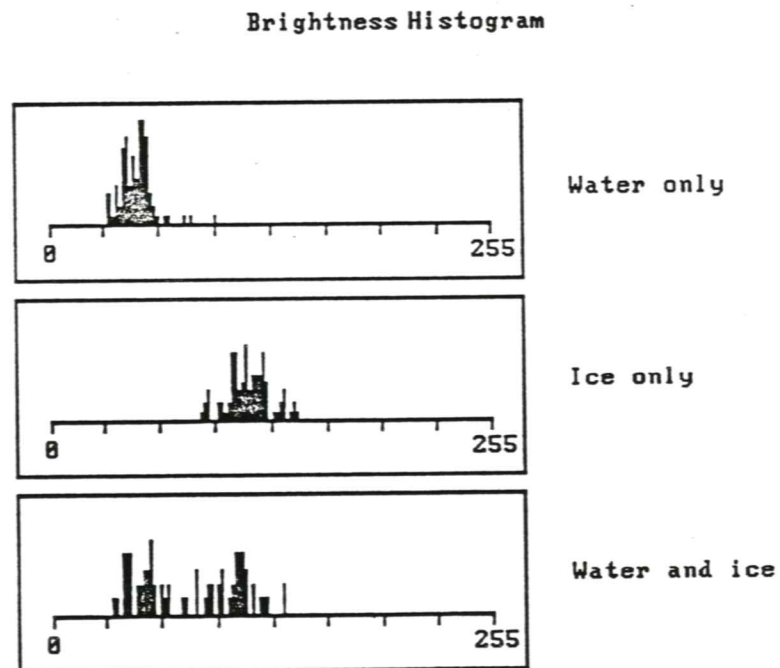


Figure 4.2 Histograms of the brightness of water, ice and water and ice together.

computer's mouse. Two distinct distributions could be seen between ice and water, the mid-point being the threshold for the calculation. The horizontal axis is pixel brightness and the vertical axis is number of counts.

All points below the threshold were counted as open water and all points above the threshold were counted as ice. Ice concentration was calculated as the number of ice pixels divided by the total number of pixels in the image. Figure 4.3 a) shows a section of the video image taken at time 15:33:46. Figure 4.3 b) shows the same image with all pixels below the threshold as black and all pixels above the threshold as white. The ice concentration measured for this image was 70%.

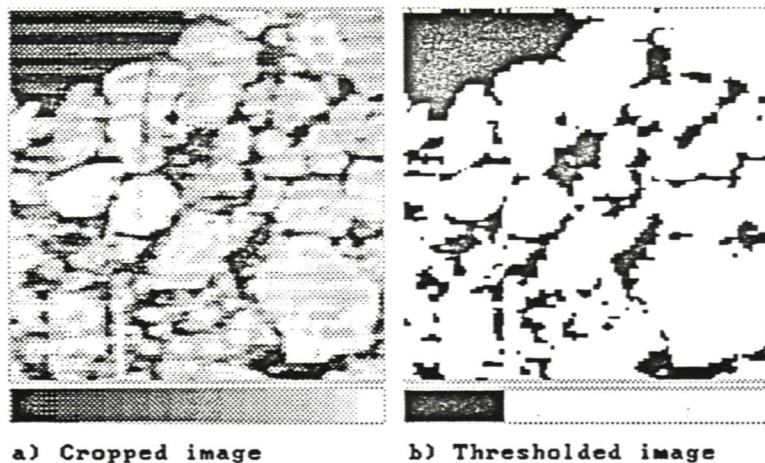


Figure 4.3 Image (a) before and (b) after thresholding to determine ice concentration.

Table 3 shows the time stamp for all 40 images along with the calculated threshold value and ice concentration for each image. The laser altimeter reading and the scale conversion factor to convert pixel counts to floe size in square metres is also shown.

4.3 Ice Floe Size

The same set of digitized images were used to measure the area of individual ice floes. Each image was displayed on the computer screen and ice floes were traced by hand using the computer's mouse. The area of each floe was measured first in pixels then converted to squared metres using the laser altimeter height reading at that point in time (see Table 3).

Table 3. Summary of Digitized Images, Line 2100

Image Time (local)	Ice Concentration Threshold (0-255)	Value (%)	No. of Floes in Histogram	Laser Altimeter Height (m)	Instantaneous Ice Thickness (m)
15:29:46	80	91	21	40	0.76
15:30:30	68	90	14	37	0.69
15:30:16	85	88	18	31	0.42
15:30:31	90	85	19	32	0.35
15:30:46	90	88	20	34	0.40
15:31:02	80	91	28	34	0.56
15:31:16	83	93	20	41	0.72
15:31:31	65	94	18	38	0.31
15:31:46	65	95	18	30	0.61
15:32:01	80	97	97	38	0.86
15:32:16	65	95	79	37	0.51
15:32:31	75	92	79	30.5	0.12
15:32:46	80	94	114	33	0.44
15:33:01	60	95	90	26	0.32
15:33:16	60	89	90	25	0.1
15:33:31	70	84	93	25.3	0.36
15:33:46	70	75	76	29.5	0.18
15:34:01	80	89	86	31	0.1
15:34:16	0	0	-	37	0.01
15:34:31	64	85	112	33.4	0.32
15:34:46	60	82	113	24.5	0.19
15:35:01	80	89	106	21.5	0.42
15:35:16	64	72	115	24	0.74
15:35:31	80	76	141	28	0.43
15:35:46	80	88	143	27.5	0.82
15:36:00	80	90	170	33.2	0.63
15:36:16	70	49	126	30	0.01
15:36:32	80	90	145	27	0.31
15:36:46	70	86	119	25	0.61
15:37:01	60	92	145	28.5	0.42
15:37:16	63	82	113	27.5	0.63
15:37:31	70	81	141	24.3	0.36
15:37:46	60	82	153	19.4	0.25
15:38:01	80	60	126	21	0.49
15:38:16	70	83	189	45	0.56
15:38:31	70	79	169	52	0.55
15:38:46	60	91	132	36	1.02
15:39:01	60	84	154	26.5	0.43
15:39:16	60	86	149	19	1.03
15:39:32	64	82	257	26	-

Figure 4.4 shows image 15:33:46 with the floe edges traced out. Figure 4.5 is a histogram of the floe sizes measured from the image. Appendix C contains plots of the measured histograms for 39 of the 40 digitized images; the other image (15:34:16) was over open water.

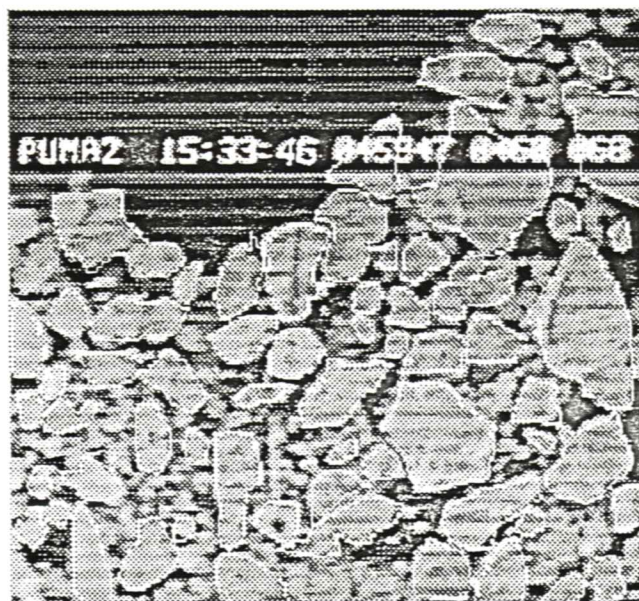


Figure 4.4 Image with ice floes outlined to measure floe size.

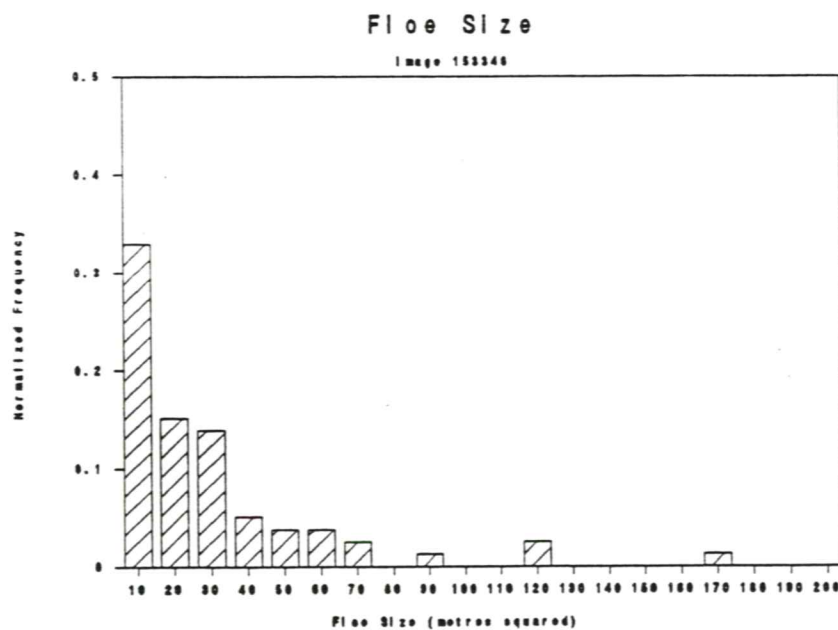


Figure 4.5 Histogram of floe size for image 15:33:46.

4.4 Video Overlay

A video overlay was produced which incorporated ice thickness, EM bird height and ice concentration as a graphics and text display mixed with the video imagery. Figure 4.6 shows an example of the overlay section of the produced video.

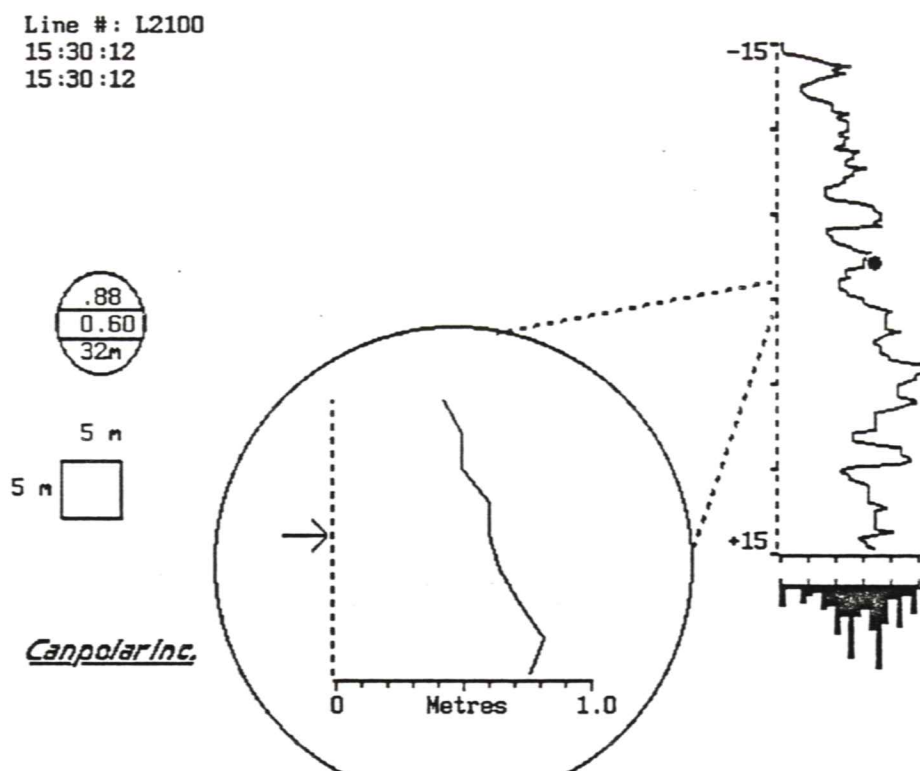


Figure 4.6 Example of overlay graphics.

The overlay contains a circle approximating the EM sensor footprint and, within the circle, a graph of ice thickness closely following ground position. On the right of the overlay is a graph of ice thickness over a 30 second interval with a histogram of that time period below it. At the left is a box indicating ground scale and an "egg" containing ice concentration in the top line, ice thickness in the middle line and bird height in the bottom position.

The ice thickness data from the EM sensor is on the screen in four forms. In the bottom centre of the TV screen (as shown in Figure 4.6) the ice thickness is plotted with the vertical axis scale closely matching the ice surface position and with ice thickness plotted on the horizontal axis from 0 to 1.0 m. The arrow to the left indicates the point

corresponding to the ice thickness value written in the middle of the "egg". On the far right of the screen, the ice thickness data is plotted over a 30 second time period, 15 seconds before and 15 seconds after the current point indicated by the arrow. Below this plot is a histogram of the ice thickness over the same time period. The horizontal axis is ice thickness from 0 to 1.0 m. The vertical axis of the histogram is the number of occurrences for each ice thickness.

Ice concentration is located in the top section of the "egg" and is updated every 15 seconds. Based on ice concentration, the EM interpretation of the ice thickness can be adjusted to a thicker value. A small dot moves down with the ice thickness at the point in time where the ice thickness was calculated. The laser altimeter data provides the height of the EM bird above the ice. The height of the bird (in metres) is written in the bottom section of the "egg". A square box at the left of the screen provides an accurate two dimensional distance-area scale. Each side of the box is 5 m for an area of 25 m².

4.4.1 Producing the overlay

The video overlay is a mixture of the original video imagery with computer-generated graphics. The computer graphics were generated on a VGA graphics adapter at a resolution of 640 x 480 pixels. All lines were drawn with double width so that flicker would not be noticeable when the overlay was shown on a conventional NTSC composite monitor. VGA Producer by Magni Systems was used to convert the VGA graphics to NTSC standard composite video format for genlocking with the video imagery played back from a VCR. A second VCR recorded the mixed output from the VGA Producer. Figure 4.7 shows a block diagram of the equipment used to make the overlay. Figure 4.8 is a photograph of a television screen showing the computer-generated graphics mixed with the original videotape image.

The program which generates the graphics follows the computer's clock closely to synchronize the graphs with the correct time. The overlay program is triggered to begin when the playback VCR is at the start time of the line. Every 0.2 seconds, the plots of the ice thickness data, the box indicating scale and ice thickness and bird height values in the "egg" are updated. Every 15 seconds the ice concentration value in the egg is updated. The dot on the 30 second plot of ice thickness data follows the data point corresponding to the ice concentration value in the egg.

4.5 Automatic Image Processing

In the future, some of the software developed during this project could be automated.

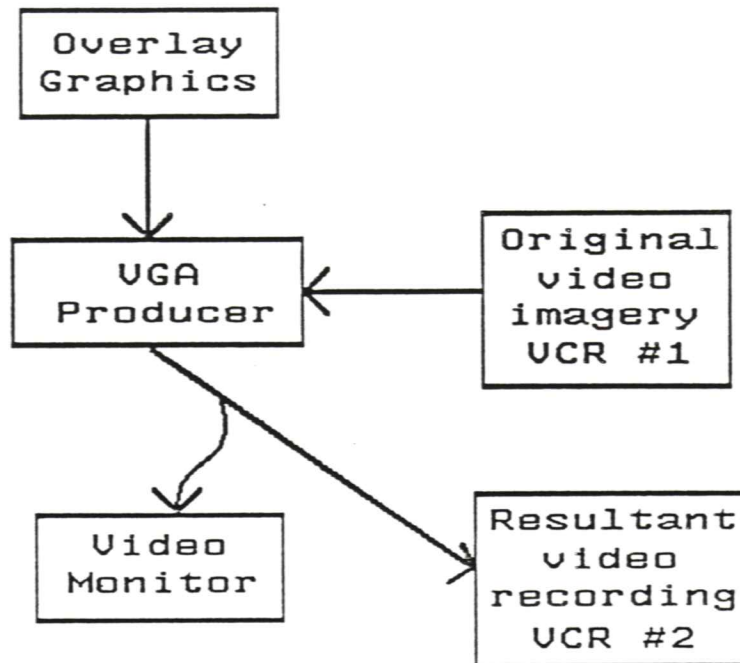


Figure 4.7 Block diagram of equipment used to make overlay video.

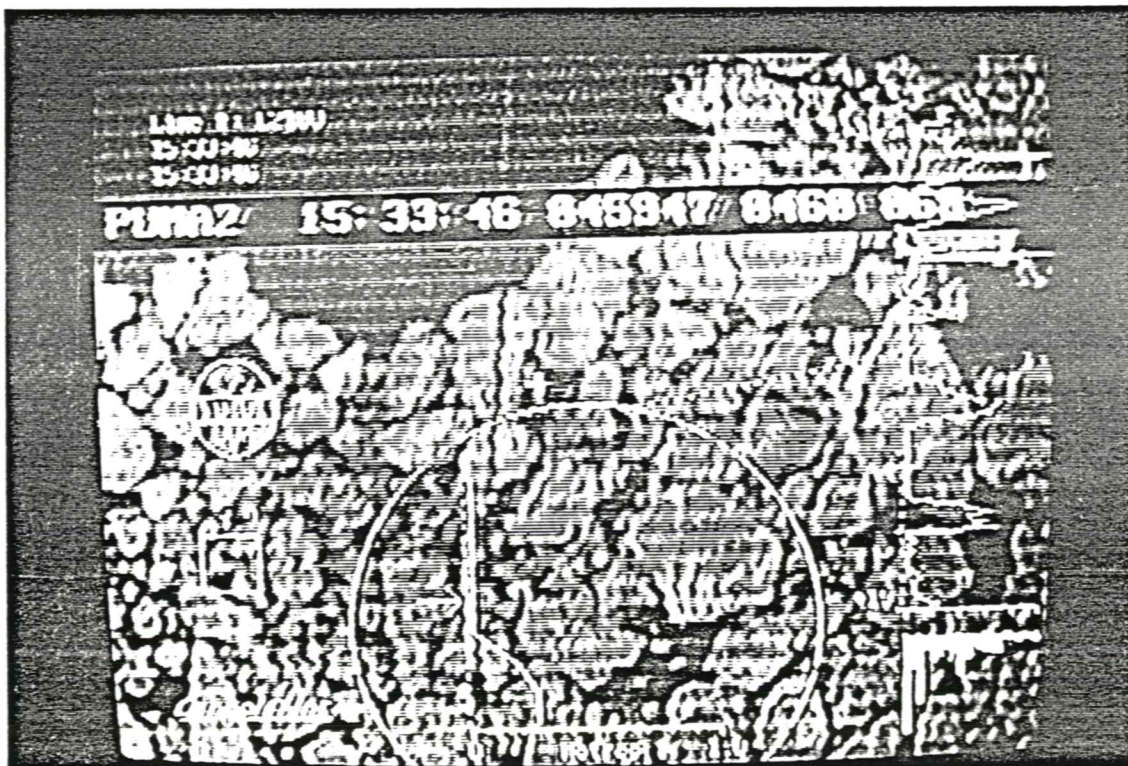


Figure 4.8 Photograph of overlay and original video image.

The frame grabber could be programmed to collect video images at preset intervals. Ice concentrations could be measured automatically, by first detecting the threshold between ice and water the in histograms, then counting pixels. This is currently done manually for each image.

Automating floe size measurement seems more difficult as there is often only a small contrast between individual floes. A literature search may identify a solution to a similar problem.

4.6 Comparison to Other Imagery

Four other types of imagery were collected during LIMEX'89 on the day of the flight to the Terra Nordica (March 24) or the day after: NOAA low resolution visual satellite imagery, SPOT high resolution visual satellite imagery, SSM/I passive microwave imagery, and high resolution airborne SAR imagery (March 25). Data from each of these sources was acquired and examined for comparison with the helicopter ice thickness/imagery data set.

An example of the NOAA imagery (black and white reproduction) is given in Figure 4.9. The position of the ship is indicated to be in a region of high ice concentration with strips of more open water on a scale of approximately 10 km. The scale of the image is so small that more detailed comparisons do not seem warranted.

An example of the processed SSM/I data processed, using the AES/York algorithm to extract ice concentration, is shown in Figure 4.10. The ship is shown in a region of ice concentration varying from about 56 to 80%. As seen in Table 3, the values of ice concentration over one line near the ship varied from 0 to 95%, with an average of 83% and a standard deviation over the 40 images of 4%. These results would tend to validate the SSM/I interpretation, especially since the EM line was over the most concentrated ice, not open water, whereas the SSM/I 25 km x 25 km footprint incorporates both.

Unfortunately, the SPOT data were just off to the west of the EM line for the day of the overflight. The SAR data were taken the next day, and although general ice conditions were similar, specific ice features could not be correlated between the two sets of data with any assurance.

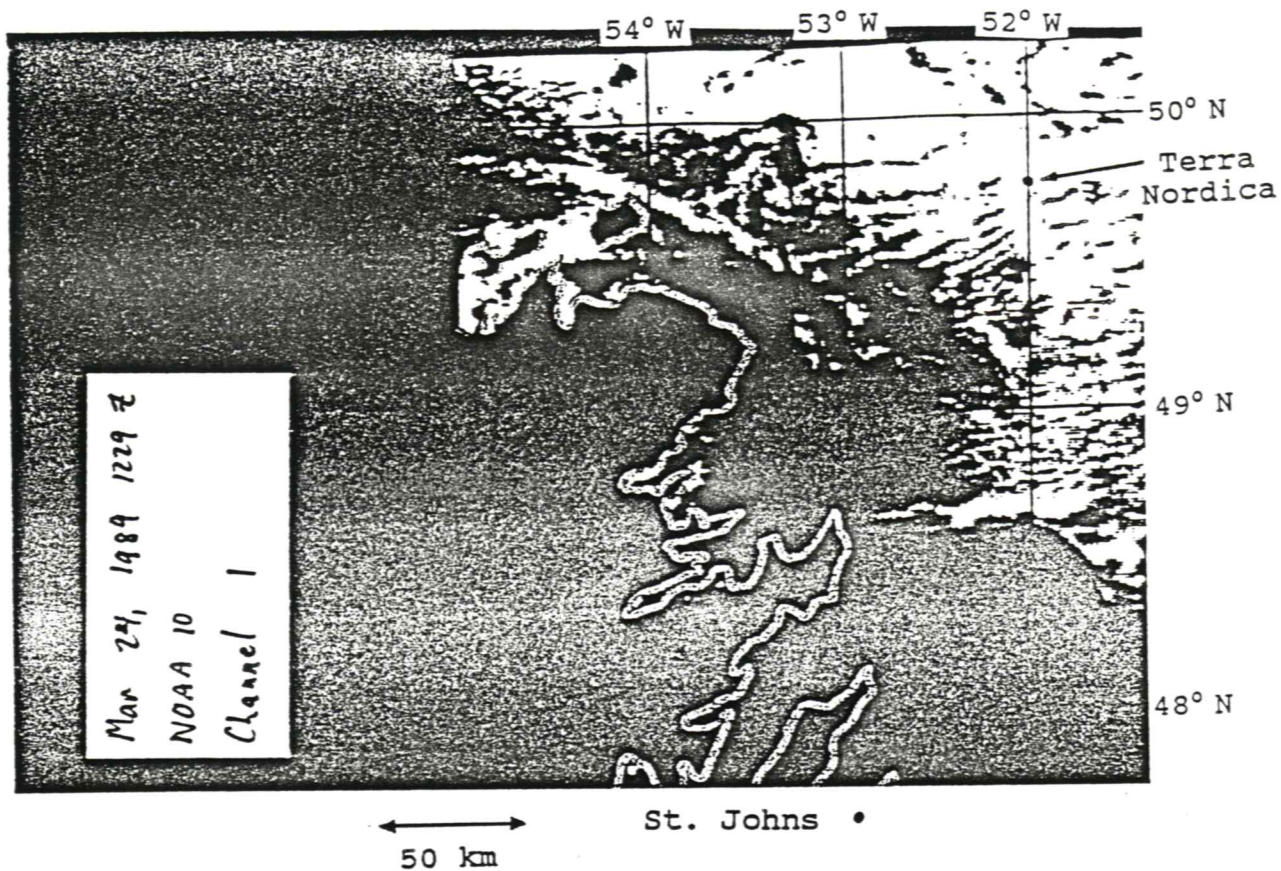
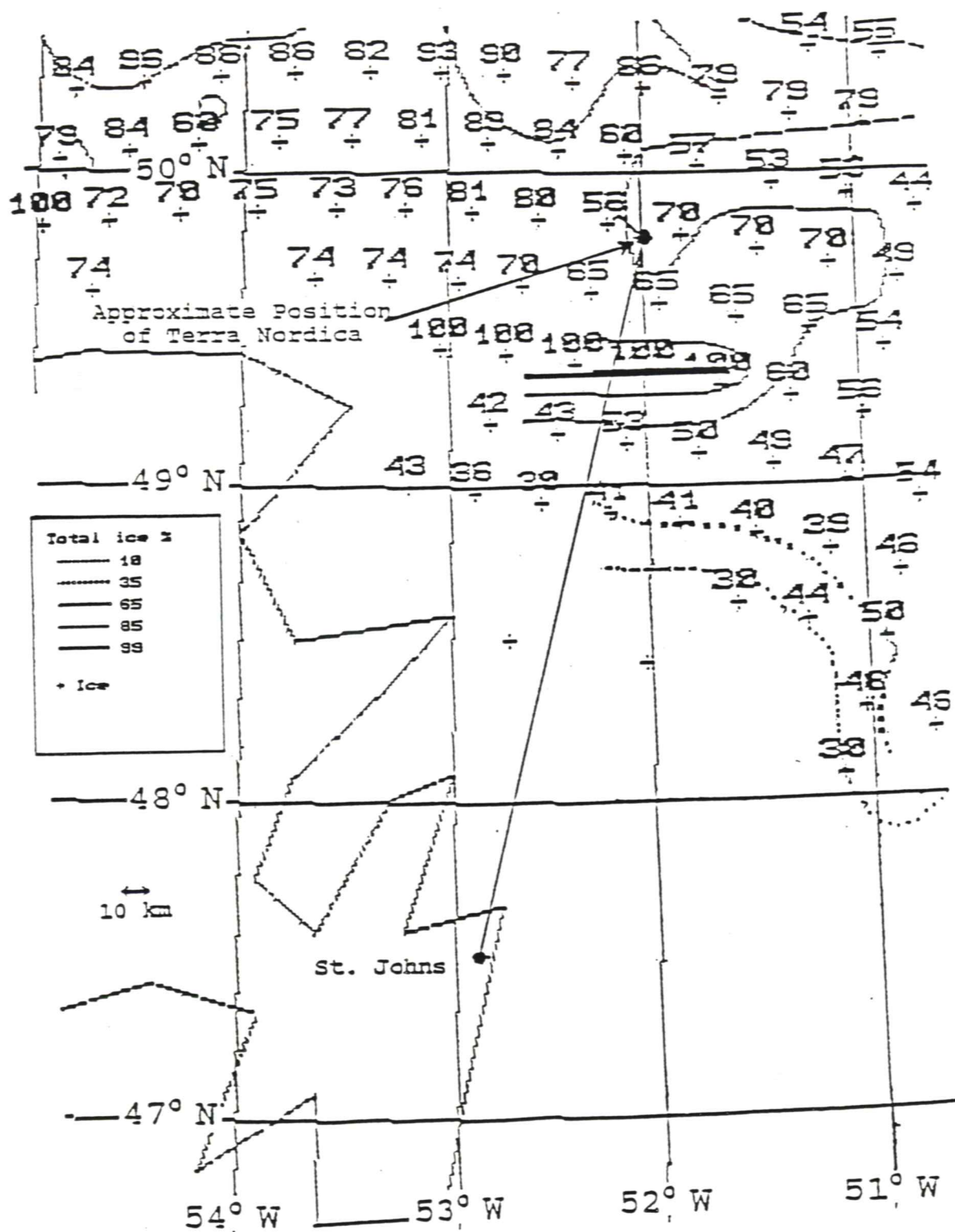


Figure 4.9 Data from the NOAA-10 satellite at 8:59 NST on March 24, 1989. Since the day was relatively clear, the white areas are ice-covered. The position of the Terra Nordica and St. John's are shown.

Figure 4.10 Ice concentrations as calculated from SSM/I overpass at approximately 18:45 NST on March 24, 1989. The concentrations were calculated by the Institute for Space and Terrestrial Science using the AES/York Algorithm. The outbound path of the helicopter is shown, as is the path (NW of the ship) over which ice concentration data were collected.



5. Conclusions and Recommendations

5.1 Conclusions

The major objectives of the study appear to have been met. Even more than on previous studies, the airborne EM technique was capable of being used for routine ice thickness measurement. In this study, relatively warm, saline ice was sounded from a helicopter over a traverse several hundred kilometres long. The data were processed into an video overlay of EM and ice image data and semi-automated procedures for measuring ice concentration and floe size have been developed.

Although the EM induction technology is relatively mature in terms of geophysical measurements, there is still room for optimization for ice sounding applications. In particular, the use of higher frequencies to estimate ice conductivity would be particularly useful, since this parameter is closely coupled to ice strength.

Several presentations of the results were made to professional groups over the project (for example, see Appendix D). This process will need to continue in order to potential users of this technology to become familiar with its capabilities and limitations.

5.2 Recommendations

1. The technique can be used as an scientific data collection tool when used by specialists. It can be used on long traverses over which it would be impossible to collect ice thickness data manually. Use of a smaller, twin-engine helicopter should provide a practical compromise between over-ocean safety requirements and cost.

2. Further validation of the technique, particularly over ridges and during melting conditions, is required. The processing techniques developed at the University of California at Berkeley should be incorporated into data inversion procedures.

3. The development of a operational prototype should proceed, to include:

- (1) reducing the size and weight of the bird from approximately 7 m length and 250 kg to 4 m length and 100 kg;
- (2) developing a system that can be used by non-specialist personnel;
- (3) providing real-time output;
- (4) including processing capability for two- and three-dimensional structures;
- (5) including provision for measurement of ice conductivity;
- (6) including capability of estimation of snow thickness.

This recommendation is being pursued under a separate contract and a prototype system is expected to be ready for testing in winter 1990-91.

4. Further understanding of the statistics of ice thickness measurement would be useful in making comparisons with auger measurements and should be pursued.

References

- Becker, A., Liu, G., and Morrison, H.F., "Airborne Electromagnetic Sensing of Sea Ice Thickness," Final Report prepared for CRREL under U.C.B. contract DACA89-85-K-0008, U.C. Berkeley, 1987, 77 pp.
- Canpolar Consultants Ltd., "Review of Floating Ice Thickness Measurement Capability, Technologies and Opportunities," report to Department of Fisheries and Oceans, Contract No. 01SE.FP921-3-0624, 1985, 76 pp.
- Holladay, J.S., "Interpretation of Electromagnetic Sounding Data for a Stratified Earth by means of Non-linear Regression," Research in Applied Geophysics, No. 16, Department of Physics, U. of Toronto, 1980.
- Holladay, J.S., Valleau, N.C., and Morrison, E., "Application of Multi-frequency Helicopter Electromagnetic Surveys to Mapping of Sea-ice Thickness and Shallow-water Bathymetry," in Airborne Resistivity Mapping, ed., G.J. Palacky, Geological Survey of Canada Paper 86-22, 1986, pp. 91-98.
- Kovacs, A. and Holladay, J.S., "Airborne Sea Ice Thickness Sounding," **Proc. 10th International Conference on Port and Ocean Engineering under Arctic Conditions**, Lulea University of Technology, 12-16 June 1989, pp. 1042-1052.
- Kovacs, A., Valleau, N.C., and Holladay, J.S., "Airborne Electromagnetic Sounding of Sea Ice Thickness and Sub-ice Bathymetry," **Cold Regions Science and Technology**, vol. 14, 1987a, pp. 289-311.
- Kovacs, A., Valleau, N.C., and Holladay, J.S., "Airborne Measurement of Sea Ice Thickness and Subice Bathymetry," in Proc. Developments and Applications of Modern Airborne Electromagnetic Surveys, U.S.G.S., Denver, CO, Oct. 7-9, 1987b, in press.
- Kovacs, A. and Valleau, N.C., "Airborne Measurement of Sea Ice Thickness and Subice Bathymetry," **Proc. 9th International Conference on Port and Ocean Engineering under Arctic Conditions**, University of Alaska-Fairbanks, 17-21 August 1987, in press.
- Liu, G., "Airborne Electromagnetic Sensing of Sea-Ice Thickness," Ph.D. thesis, Department of Materials Science and Mineral Engineering, U. of California at Berkeley, 1989, 143 pp.
- Liu, G. and Becker, A., "Two-dimensional mapping of sea-ice keels with airborne electromagnetics," **Geophysics**, vol. 55, 1990, pp. 239-248.

Liu, G. and Becker, A., "Inversion of Airborne Electromagnetic Data For Sea Ice Keel Geometry," report to Naval Ocean Research & Development Activity (NORDA) under contract no. N00014-87-K-6005, University of California, Berkeley, September, 1988, 20 pp.

MacLaren Plansearch Ltd., "Study the Sea Ice Climate of the Northumberland Strait," Report to Fisheries and Oceans, Bedford Institute of Oceanography, Contract No. FP950-7-0058/01-OSC, 1988.

Morey, R. M., Kovacs, A., and Cox, G.F.N., "Electromagnetic Properties of Sea Ice," CRREL Report 84-2, 1984, 38 pp.

Raney, R.K., and Argus, S., "Science Plan for LIMEX'89," RADARSAT Program Office, Ottawa, 1988, 34 pp.

Rossiter, J.R. and Lalumiere, L.A., "Evaluation of Sea Ice Thickness Sensors," report to Transportation Development Centre, Report No. TP9169E, 1988, 58 pp.

Appendix A. EM Ice Thickness Data

The plots in the appendix contain a complete set of the processed EM data collected during this experiment. The line numbers are included with the plots and refer to the line numbers shown on Figures 3.2 and 3.3.

Table A1 contains an example of data for line 2050 (Figure 3.7), 32,000 Hz co-planar coils during the various processing steps.

The first column contains the time stamp (local) along the line in hours, minutes, and seconds. Although data were collected every 0.1 s and then averaged to a 0.2 s sampling interval, only samples every second are shown.

The second and third columns contain the raw EM data, in-phase (I-P) and quadrature (Q) components, in bits.

The fourth and fifth columns contain the EM data after baseline corrections and reference height level have been removed, in arbitrary units.

The sixth and seventh columns contain the final EM secondary fields, in parts per million of the primary field, after calibration factors have been applied. The calibration factors are determined using an open water measurement as described in Section 3.2.

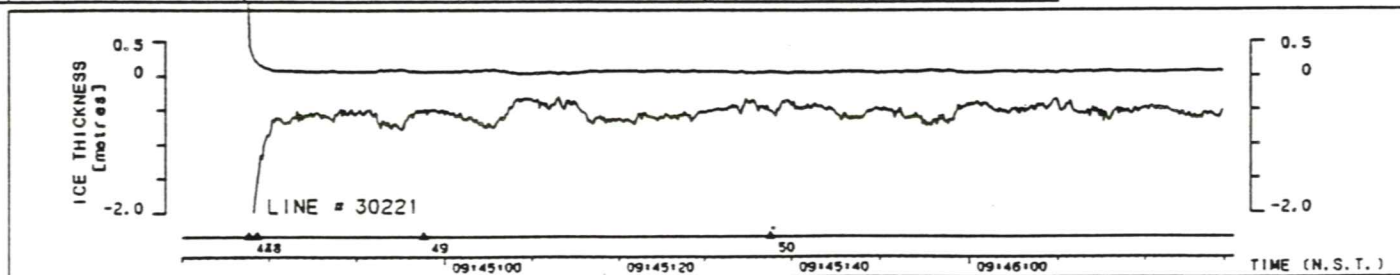
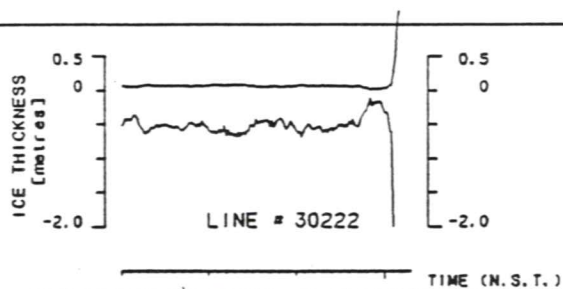
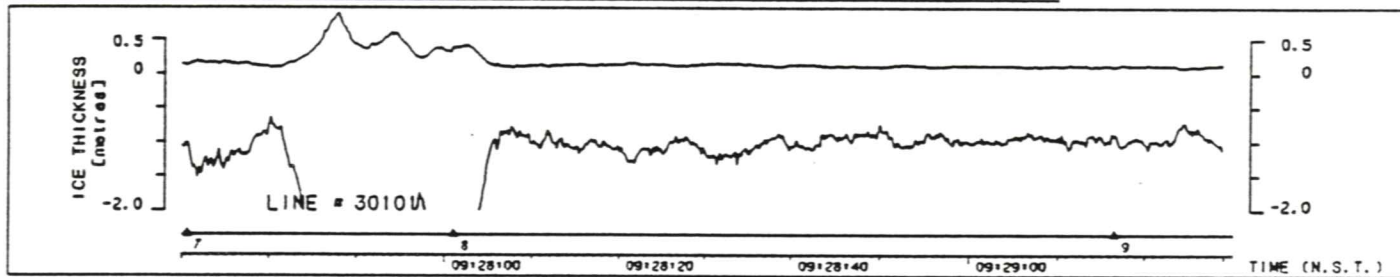
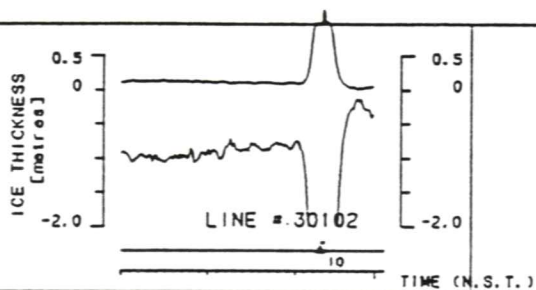
The eighth column contains the calculated ice thickness in metres from the inversion routine. The ninth column contains the calculated ice conductivity in S/m. A "0" value indicates that the conductivity estimate was unreliable.

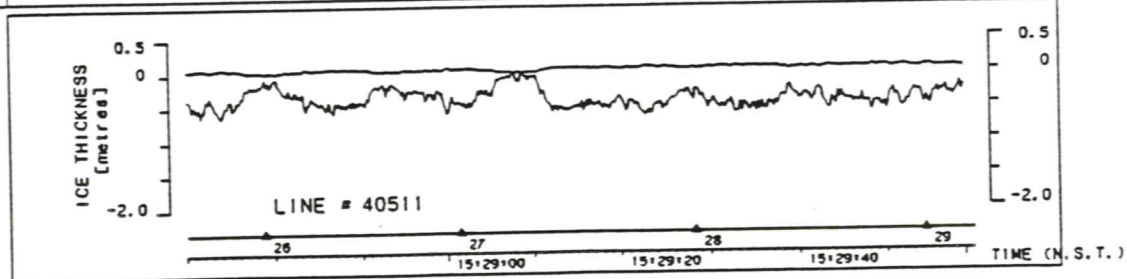
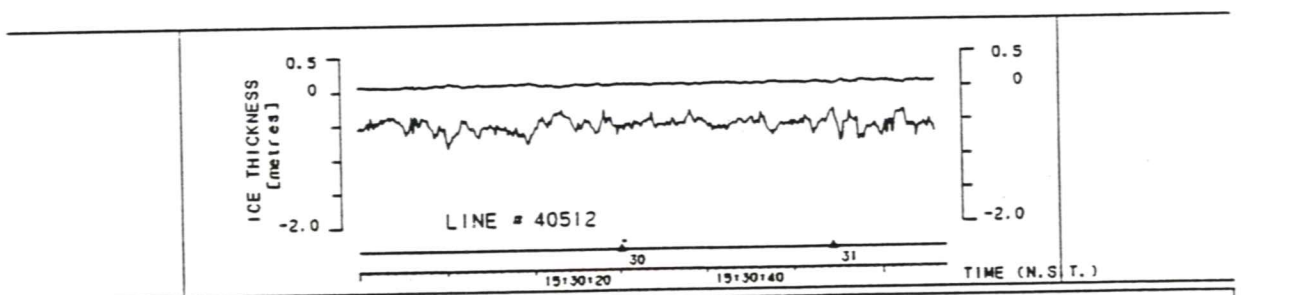
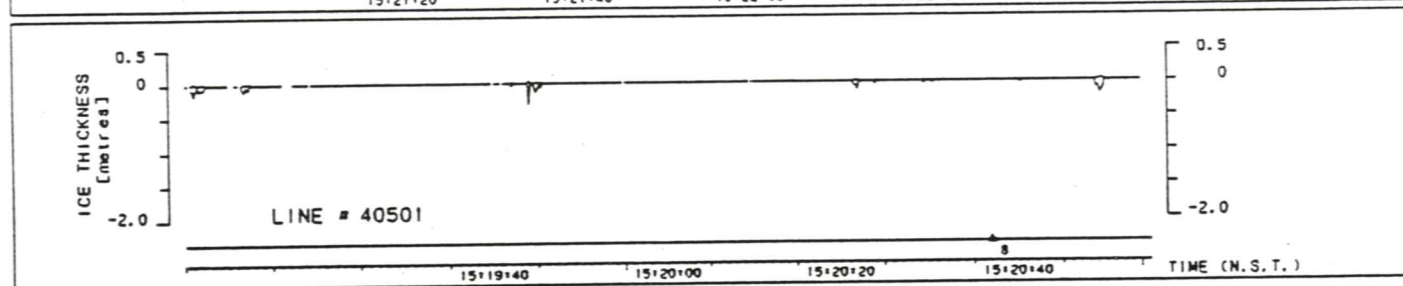
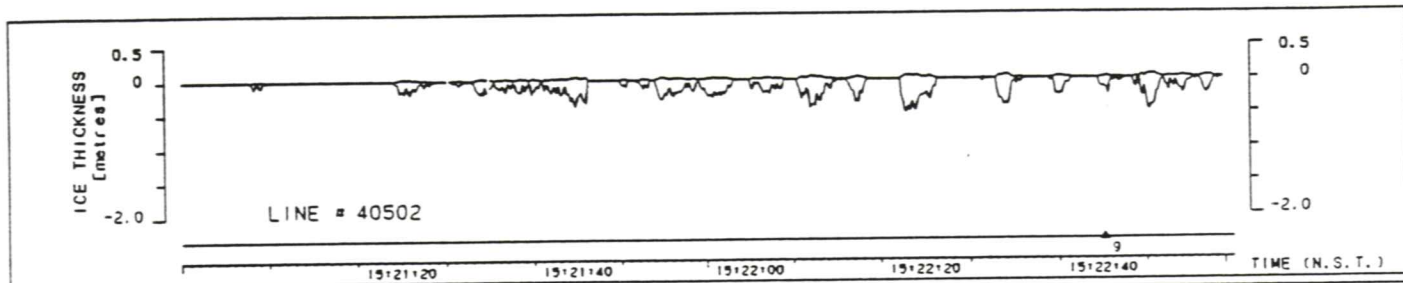
The tenth column contains the raw bird altitude from the laser altimeter in metres. The final column contains the laser measurement after passing through a de-spiking algorithm which is designed to remove laser glitches.

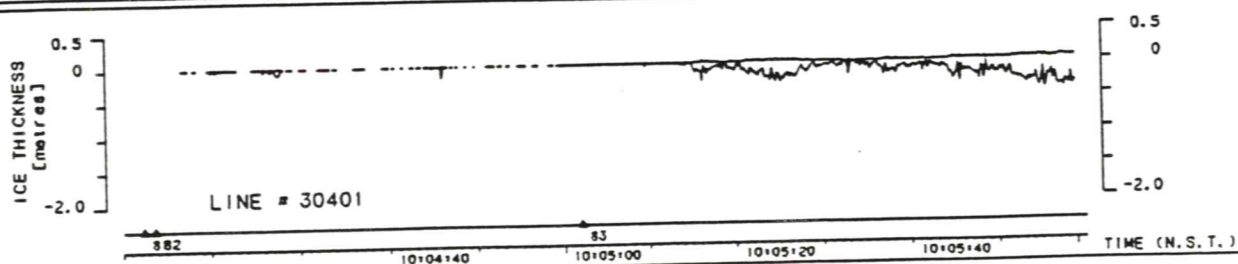
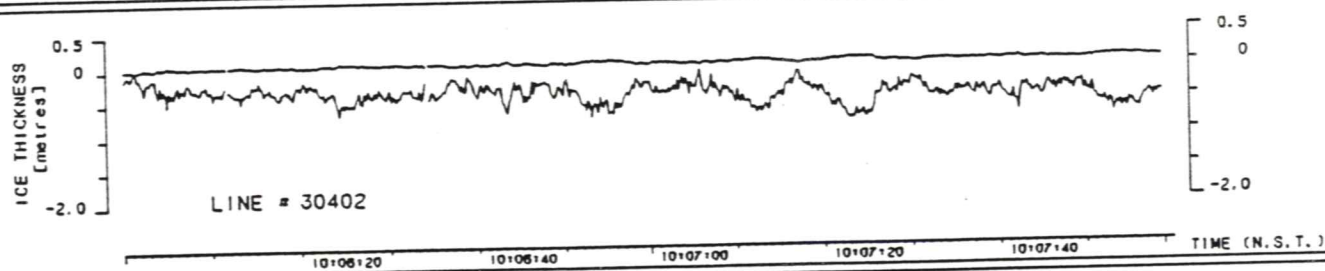
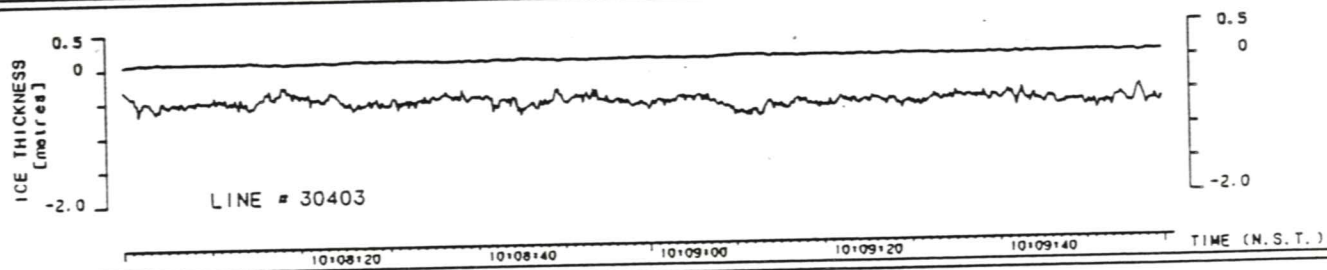
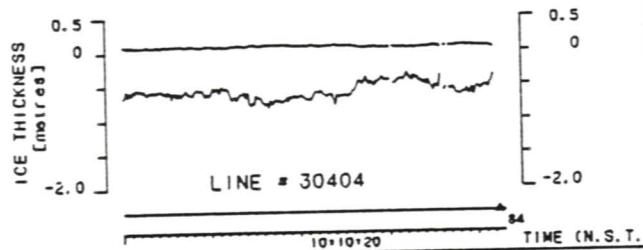
Table A1. Raw and processed EM system data for line 2050, 32 kHz (see Figure 3.7)

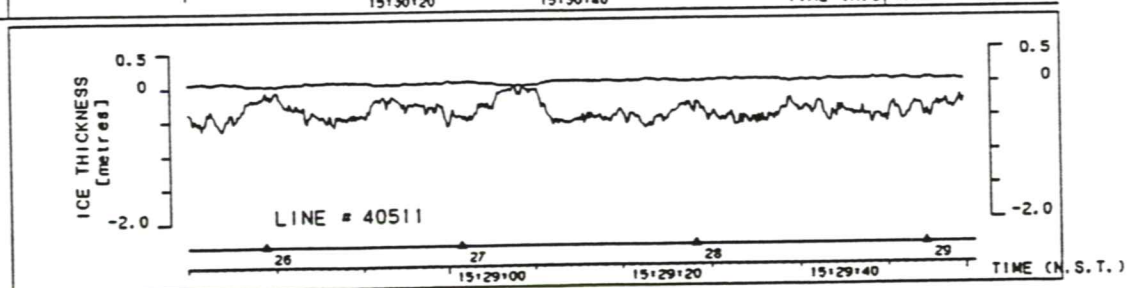
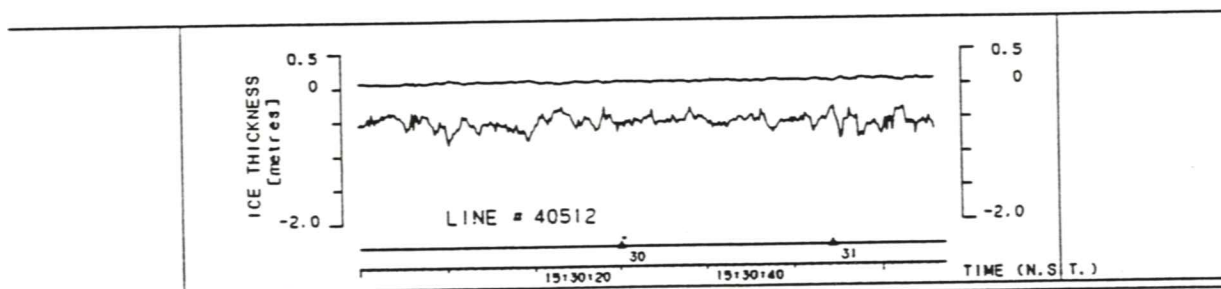
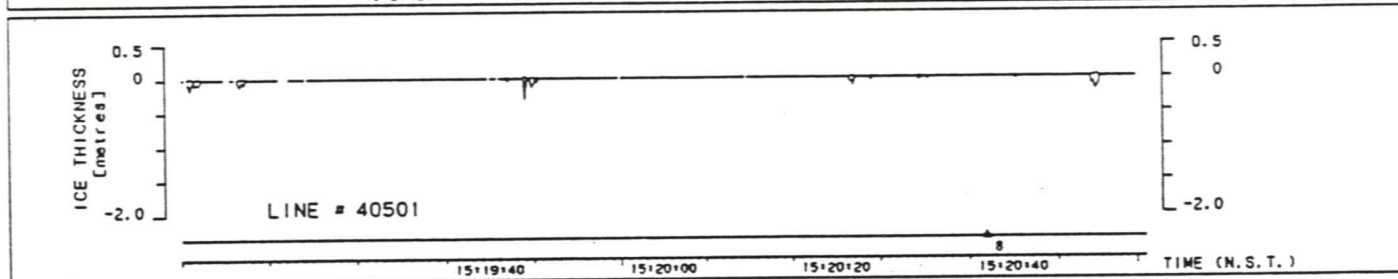
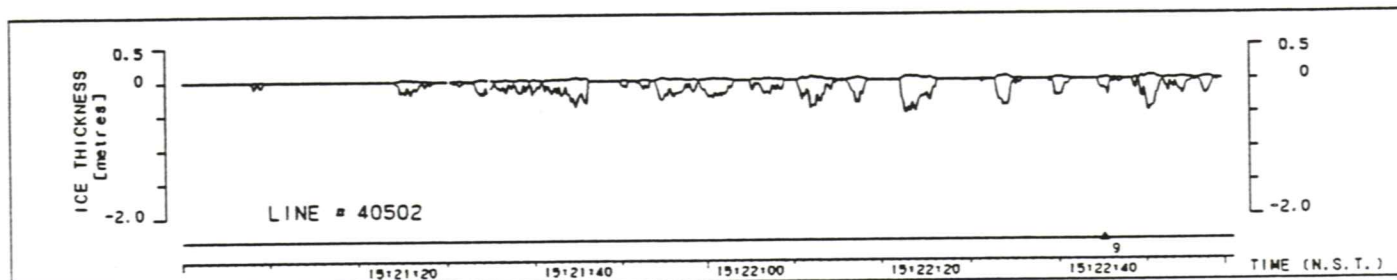
Time stamp (local)	Raw EM data		Drift-corrected EM		Calibrated EM		Ice		Laser altitude	
	I-P	Q	I-P	Q	I-P	Q	thickness	conduct.	raw	de-spiked
	(bits)		(arbitrary)		(ppm)		(m)	(S/m)	(m)	(m)
14:47:20.0	-1782.0	-144.0	130.5	5.5	1136.0	74.7	1.00	0.053	36.78	36.78
14:47:21.0	-1871.0	-148.0	141.3	6.0	1230.0	81.3	0.53	0.000	36.18	36.18
14:47:22.0	-1958.0	-156.0	151.9	7.0	1322.0	92.2	0.59	0.000	35.18	35.18
14:47:23.0	-2074.0	-174.0	166.1	9.2	1446.0	114.3	0.65	0.000	34.02	34.02
14:47:24.0	-2238.0	-179.0	186.1	9.8	1620.0	123.6	0.63	0.000	32.69	32.69
14:47:25.0	-2446.0	-195.0	211.5	11.7	1841.0	145.4	0.66	0.000	31.21	31.21
14:47:26.0	-2635.0	-212.0	234.5	13.8	2041.0	168.4	0.63	0.000	30.12	30.12
14:47:27.0	-2829.0	-228.0	258.2	15.8	2247.0	190.7	0.71	0.000	29.01	29.01
14:47:28.0	-2972.0	-245.0	275.6	17.8	2398.0	211.7	0.54	0.000	28.53	28.53
14:47:29.0	-3142.0	-261.0	296.4	19.8	2579.0	233.4	0.46	0.000	27.85	27.85
14:47:30.0	-3402.0	-292.0	328.1	23.6	2855.0	273.0	0.32	0.057	26.99	26.99
14:47:31.0	-3668.0	-315.0	360.5	26.4	3136.0	304.1	0.47	0.057	25.97	25.97
14:47:32.0	-3866.0	-340.0	384.6	29.4	3346.0	335.2	0.43	0.058	25.44	25.44
14:47:33.0	-4043.0	-356.0	406.2	31.4	3534.0	357.1	0.51	0.058	24.83	24.83
14:47:34.0	-4270.0	-380.0	433.9	34.3	3775.0	388.0	0.64	0.060	24.15	24.15
14:47:35.0	-4436.0	-402.0	454.1	37.0	3950.0	415.7	0.67	0.062	23.73	23.73
14:47:36.0	-4566.0	-416.0	470.0	38.7	4088.0	433.8	0.63	0.061	23.48	23.48
14:47:37.0	-4775.0	-442.0	495.5	41.9	4310.0	466.9	0.76	0.064	22.91	22.91
14:47:38.0	-4991.0	-468.0	521.9	45.0	4539.0	499.4	0.80	0.065	22.42	22.42
14:47:39.0	-5194.0	-495.0	546.6	48.3	4754.0	533.2	0.59	0.061	22.23	22.23
14:47:40.0	-5459.0	-526.0	578.9	52.1	5035.0	573.0	0.50	0.060	21.88	21.88
14:47:41.0	-5653.0	-554.0	602.6	55.5	5241.0	607.5	0.54	0.061	21.48	21.48
14:47:42.0	-5834.0	-574.0	624.7	58.0	5433.0	633.8	0.51	0.060	21.24	21.24
14:47:43.0	-6062.0	-604.0	652.5	61.6	5674.0	670.9	0.57	0.060	20.88	20.88
14:47:44.0	-6244.0	-634.0	674.7	65.3	5867.0	707.7	0.59	0.063	20.56	20.56
14:47:45.0	-6498.0	-672.0	705.7	69.9	6136.0	754.1	0.56	0.063	0.10	20.25
14:47:46.0	-6703.0	-700.0	730.7	73.4	6353.0	789.8	0.57	0.062	19.97	19.97
14:47:47.0	-6931.0	-725.0	758.4	76.4	6594.0	821.6	0.54	0.061	19.73	19.73
14:47:48.0	-7194.0	-762.0	790.5	80.9	6873.0	867.4	0.66	0.065	19.31	19.31
14:47:49.0	-7631.0	-823.0	843.8	88.4	7336.0	943.7	0.78	0.068	18.75	18.75
14:47:50.0	-7948.0	-871.0	882.5	94.2	7672.0	1002.2	0.59	0.063	18.60	18.60
14:47:51.0	-8341.0	-923.0	930.5	100.6	8089.0	1067.9	0.40	0.059	18.38	18.38
14:47:52.0	-9124.0	-1046.0	1026.0	115.6	8918.0	1218.2	0.46	0.061	17.69	17.69
14:47:53.0	-9815.0	-1154.0	1110.3	128.7	9650.0	1349.7	0.51	0.061	17.07	17.07
14:47:54.0	-10242.0	-1235.0	1162.4	138.6	10102.0	1446.7	0.31	0.058	16.82	17.02
14:47:55.0	-9682.0	-1141.0	1094.1	127.2	9509.0	1333.3	0.31	0.058	17.32	17.32
14:47:56.0	-9315.0	-1083.0	1049.3	120.1	9120.0	1262.2	0.21	0.056	17.79	17.79
14:47:57.0	-8888.0	-1014.0	997.2	111.7	8668.0	1178.3	0.37	0.058	17.95	17.95
14:47:58.0	-8444.0	-938.0	943.0	102.4	8198.0	1086.1	0.38	0.059	18.36	18.36
14:47:59.0	-7965.0	-875.0	884.6	94.7	7690.0	1007.0	0.31	0.058	18.86	18.86
14:48: 0.0	-7686.0	-838.0	850.5	90.2	7394.0	960.8	0.45	0.060	19.05	19.02
14:48: 1.0	-7488.0	-814.0	826.3	87.3	7184.0	930.6	0.62	0.064	19.06	19.06
14:48: 2.0	-7030.0	-752.0	770.4	79.7	6698.0	852.8	0.44	0.061	19.77	19.77
14:48: 3.0	-6274.0	-647.0	678.2	66.9	5897.0	722.3	0.32	0.058	20.77	20.77
14:48: 4.0	-5984.0	-608.0	642.8	62.1	5590.0	673.2	0.55	0.064	21.12	20.96
14:48: 5.0	-5964.0	-608.0	640.4	62.1	5569.0	672.7	0.71	0.069	20.90	20.90
14:48: 6.0	-5886.0	-596.0	630.8	60.7	5485.0	658.6	0.52	0.063	21.15	21.15
14:48: 7.0	-5794.0	-593.0	619.6	60.3	5388.0	652.8	0.59	0.067	21.23	21.23
14:48: 8.0	-5879.0	-610.0	630.0	62.4	5478.0	673.2	0.85	0.079	20.61	20.87
14:48: 9.0	-6075.0	-656.0	653.9	68.0	5685.0	726.9	0.85	0.090	20.33	20.55
14:48:10.0	-6227.0	-650.0	672.4	67.3	5846.0	724.6	0.64	0.069	20.45	20.56
14:48:11.0	-6119.0	-633.0	659.3	65.2	5733.0	703.6	0.52	0.064	20.82	20.82
14:48:12.0	-5930.0	-599.0	636.2	61.0	5532.0	662.3	0.47	0.060	21.10	21.10
14:48:13.0	-5710.0	-566.0	609.4	57.0	5299.0	621.9	0.59	0.063	21.35	21.35
14:48:14.0	-5568.0	-551.0	592.0	55.2	5148.0	602.7	0.50	0.061	21.46	21.62
14:48:15.0	-5566.0	-548.0	591.8	54.8	5147.0	599.1	0.53	0.061	21.74	21.66
14:48:16.0	-5555.0	-547.0	590.4	54.7	5134.0	598.0	0.53	0.062	21.65	21.65
14:48:17.0	-5551.0	-544.0	589.9	54.3	5130.0	594.4	0.65	0.064	21.57	21.57
14:48:18.0	-5476.0	-530.0	580.7	52.6	5050.0	577.7	0.76	0.065	21.58	21.58
14:48:19.0	-5420.0	-526.0	573.9	52.1	4991.0	571.9	0.61	0.063	21.78	21.78
14:48:20.0	-5539.0	-546.0	588.4	54.6	5117.0	596.7	0.75	0.068	21.48	21.48
14:48:21.0	-5674.0	-562.0	604.9	56.5	5260.0	616.6	0.74	0.067	21.24	21.24
14:48:22.0	-5684.0	-562.0	606.1	56.5	5271.0	616.9	0.43	0.060	21.54	21.54
14:48:23.0	-5504.0	-539.0	584.1	53.7	5080.0	588.0	0.40	0.059	21.83	21.83
14:48:24.0	-5387.0	-528.0	569.9	52.4	4956.0	573.7	0.38	0.058	22.07	22.07
14:48:25.0	-5229.0	-511.0	550.6	50.3	4788.0	551.5	0.52	0.063	22.23	22.23

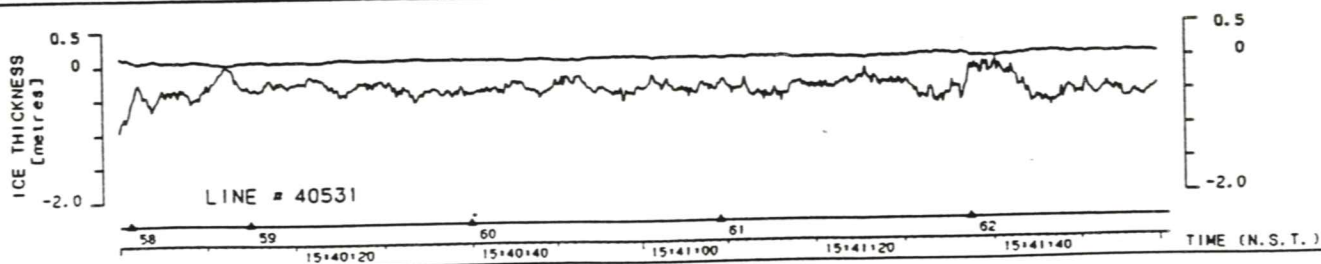
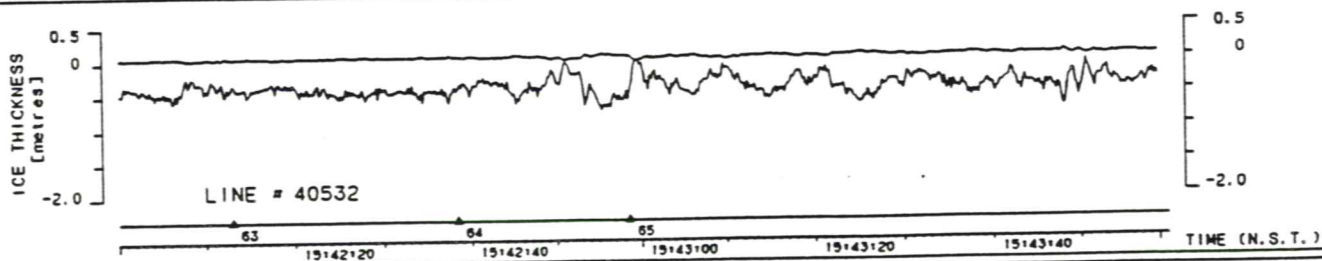
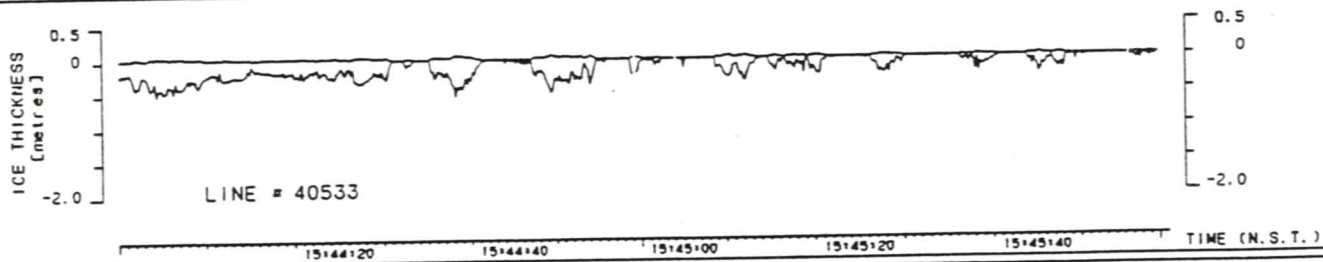
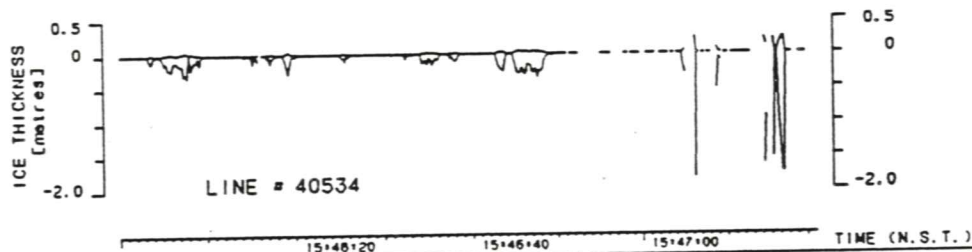
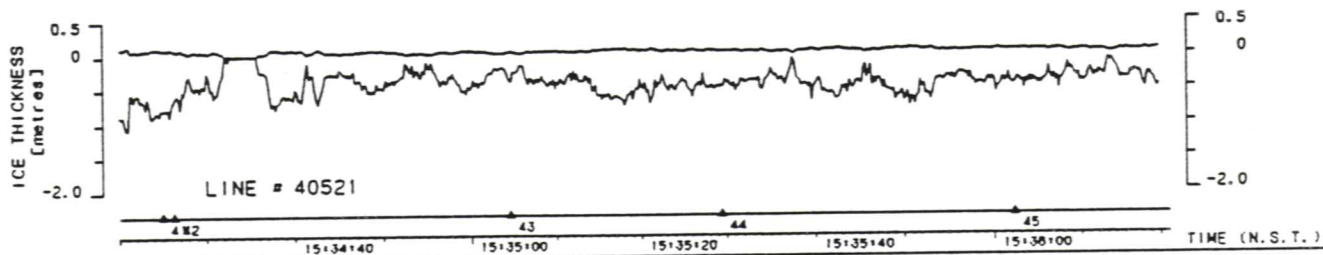
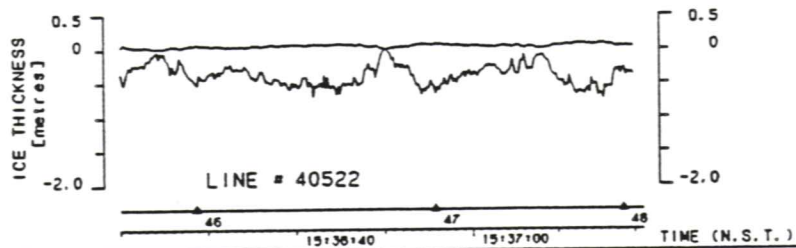
14:48:26.0	-4991.0	-478.0	521.6	46.3	4536.0	510.6	0.54	0.062	22.66	22.66
14:48:27.0	-4746.0	-447.0	491.7	42.5	4277.0	471.4	0.62	0.064	23.08	23.08
14:48:28.0	-4662.0	-431.0	481.4	40.5	4187.0	451.8	0.63	0.062	23.25	23.25
14:48:29.0	-4627.0	-426.0	477.1	39.9	4150.0	445.7	0.62	0.062	23.27	23.35
14:48:30.0	-4563.0	-423.0	469.2	39.6	4081.0	441.5	0.74	0.066	23.22	23.41
14:48:31.0	-4412.0	-414.0	450.8	38.5	3921.0	428.1	0.61	0.065	23.83	23.83
14:48:32.0	-4344.0	-412.0	442.5	38.2	3849.0	423.8	0.68	0.070	23.82	23.95
14:48:33.0	-4301.0	-404.0	437.3	37.2	3804.0	414.0	0.79	0.072	23.93	23.93
14:48:34.0	-4206.0	-396.0	425.7	36.3	3703.0	403.8	0.64	0.068	24.30	24.30
14:48:35.0	-4138.0	-377.0	417.4	33.9	3631.0	381.2	0.46	0.060	24.66	24.66
14:48:36.0	-4059.0	-361.0	407.7	32.0	3547.0	362.6	0.60	0.061	24.81	24.76
14:48:37.0	-3901.0	-338.0	388.5	29.2	3380.0	334.3	0.57	0.058	25.21	25.21
14:48:38.0	-3703.0	-317.0	364.3	26.6	3170.0	306.6	0.40	0.056	25.98	25.98
14:48:39.0	-3505.0	-308.0	340.2	25.5	2960.0	292.1	0.53	0.061	26.50	26.50
14:48:40.0	-3344.0	-296.0	320.5	24.1	2788.0	275.8	0.86	0.072	26.43	26.76
14:48:41.0	-3160.0	-282.0	298.1	22.4	2593.0	256.4	0.56	0.066	27.70	27.70
14:48:42.0	-3135.0	-266.0	295.0	20.4	2567.0	238.4	0.49	0.059	28.00	27.92
14:48:43.0	-3059.0	-257.0	285.7	19.3	2486.0	226.9	0.68	0.000	28.05	28.05
14:48:44.0	-2912.0	-240.0	267.8	17.2	2330.0	204.9	0.65	0.000	28.73	28.73
14:48:45.0	-2839.0	-235.0	258.8	16.6	2252.0	197.8	0.65	0.000	29.08	29.08
14:48:46.0	-2827.0	-231.0	257.3	16.1	2239.0	193.1	0.74	0.000	29.06	29.06
14:48:47.0	-2821.0	-231.0	256.6	16.1	2233.0	193.0	0.62	0.000	29.29	29.20
14:48:48.0	-2832.0	-232.0	258.0	16.3	2245.0	195.0	0.56	0.000	29.27	29.22
14:48:49.0	-2863.0	-237.0	261.7	16.9	2277.0	201.0	0.51	0.000	29.09	29.09
14:48:50.0	-2918.0	-239.0	268.4	17.1	2336.0	204.1	0.57	0.000	28.79	28.79
14:48:51.0	-2962.0	-242.0	273.8	17.5	2383.0	208.7	0.50	0.000	28.56	28.63
14:48:52.0	-2974.0	-243.0	275.3	17.6	2396.0	209.9	0.43	0.000	28.65	28.65
14:48:53.0	-2960.0	-245.0	273.6	17.8	2381.0	211.3	0.47	0.000	28.67	28.67
14:48:54.0	-2944.0	-241.0	271.6	17.4	2364.0	207.4	0.54	0.000	28.70	28.70
14:48:55.0	-2896.0	-237.0	265.8	16.9	2313.0	201.8	0.45	0.000	29.00	29.00
14:48:56.0	-2859.0	-234.0	261.2	16.5	2273.0	197.4	0.50	0.000	29.17	29.17
14:48:57.0	-2821.0	-232.0	256.6	16.3	2233.0	194.7	0.51	0.000	29.36	29.36
14:48:58.0	-2746.0	-223.0	247.5	15.2	2154.0	183.3	0.53	0.000	29.69	29.69
14:48:59.0	-2683.0	-218.0	239.7	14.5	2086.0	175.6	0.52	0.000	30.04	30.04
14:49: 0.0	-2663.0	-220.0	237.2	14.8	2064.0	177.7	0.49	0.000	30.25	30.20

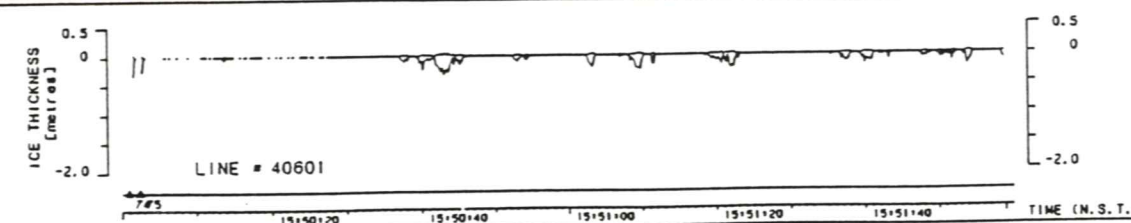
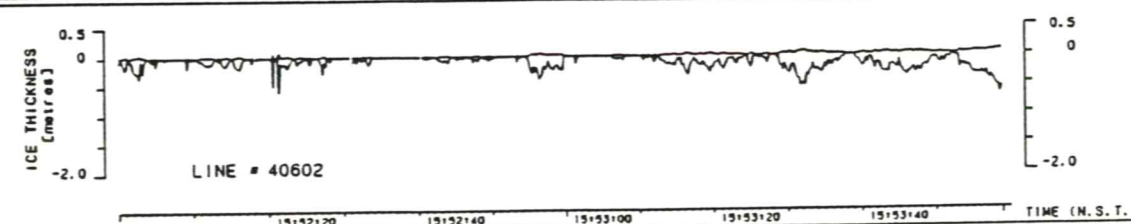
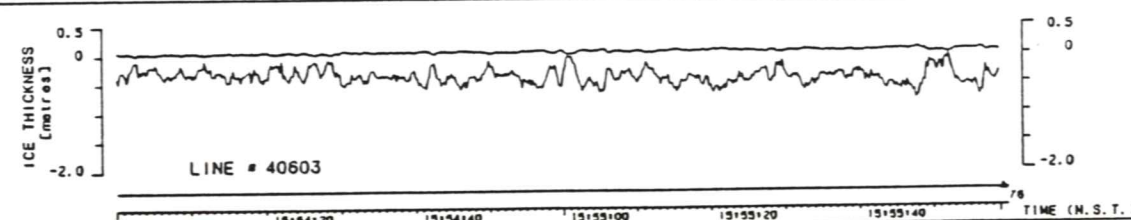
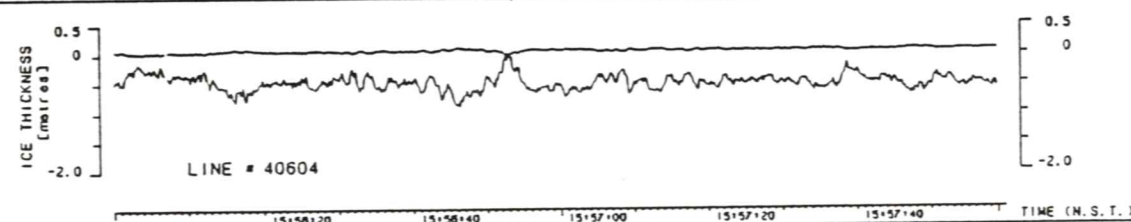
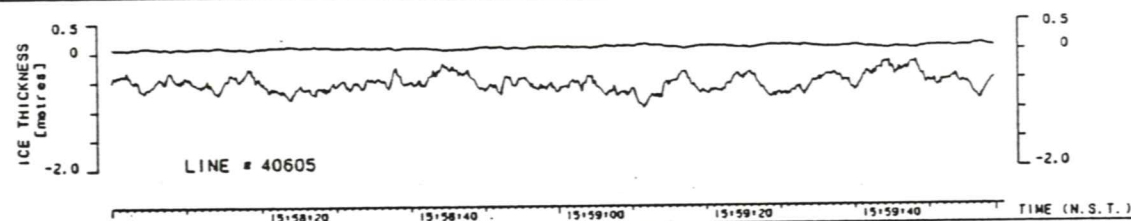
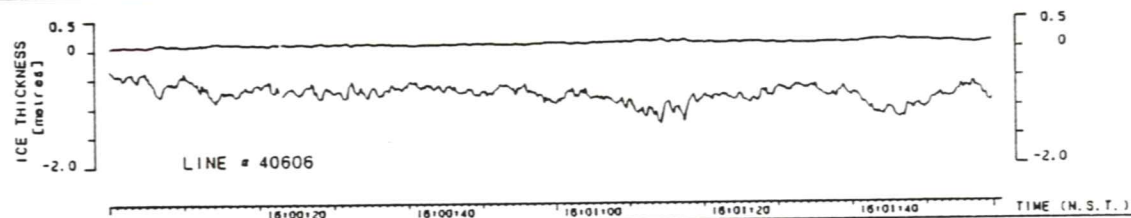
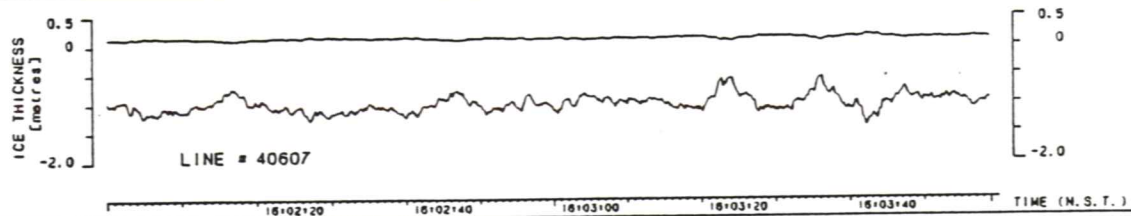
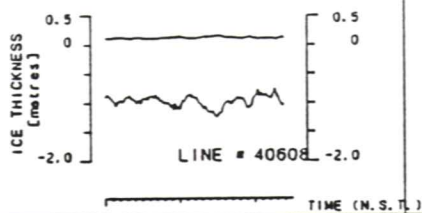


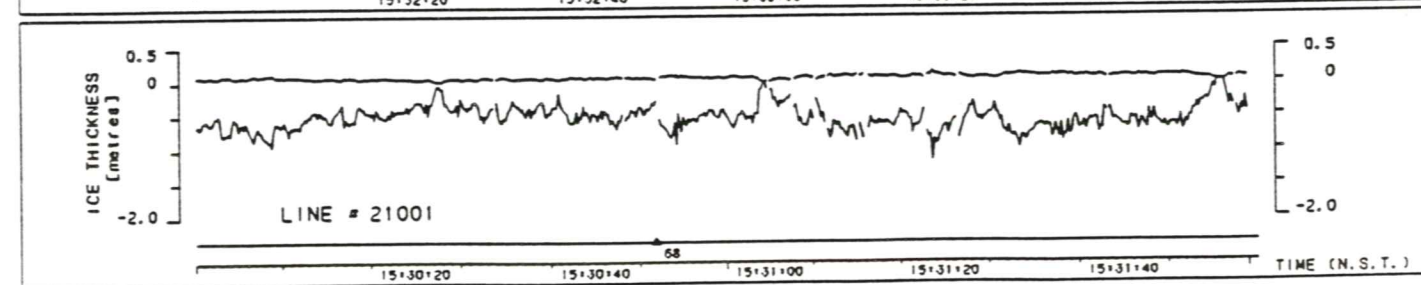
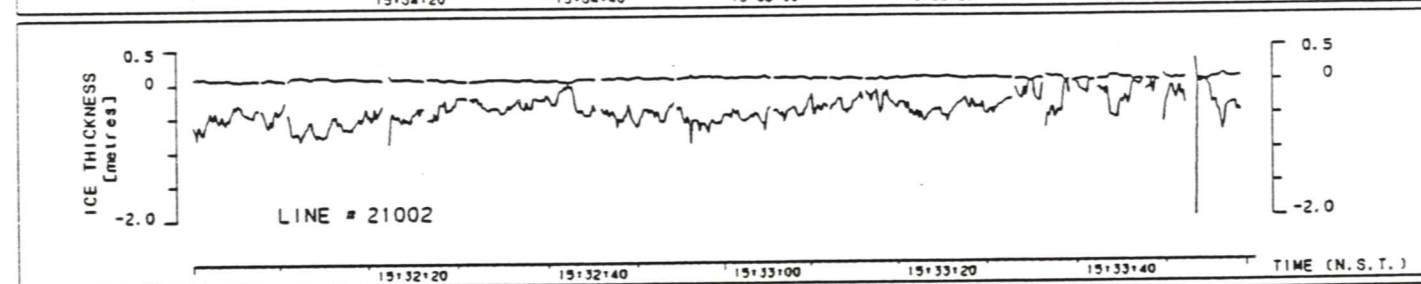
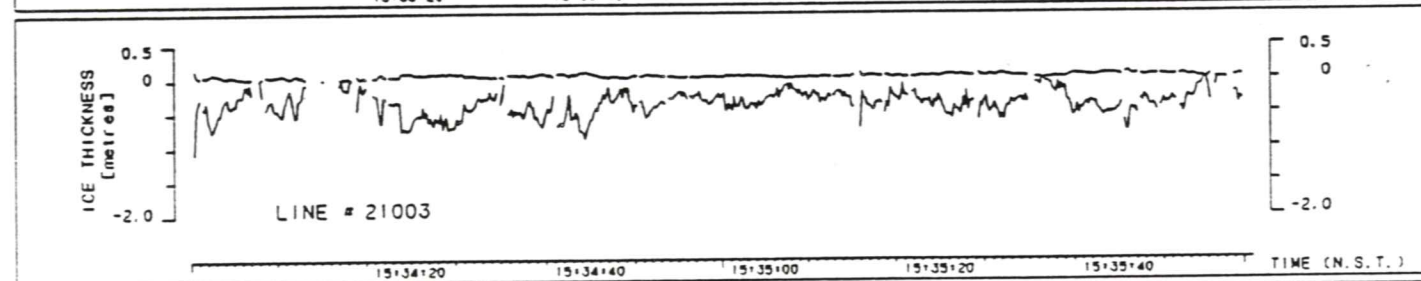
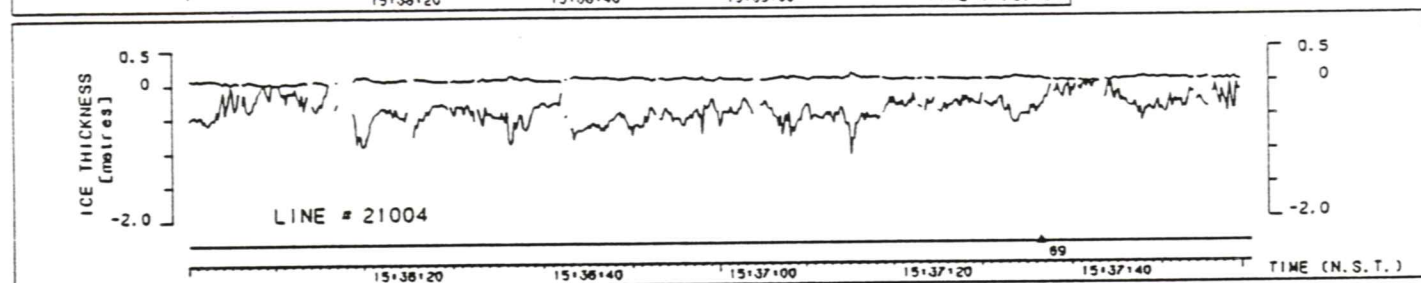
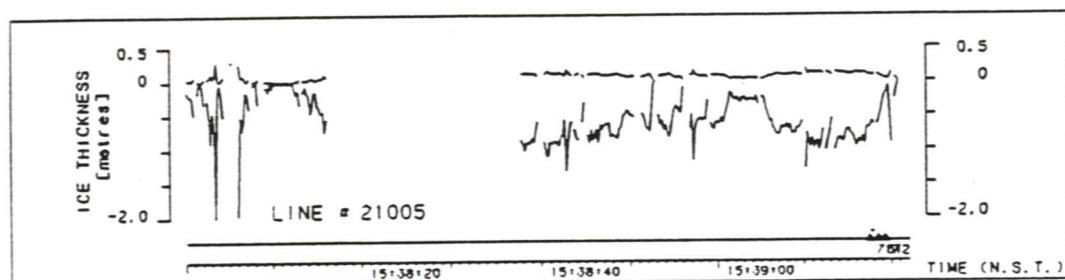


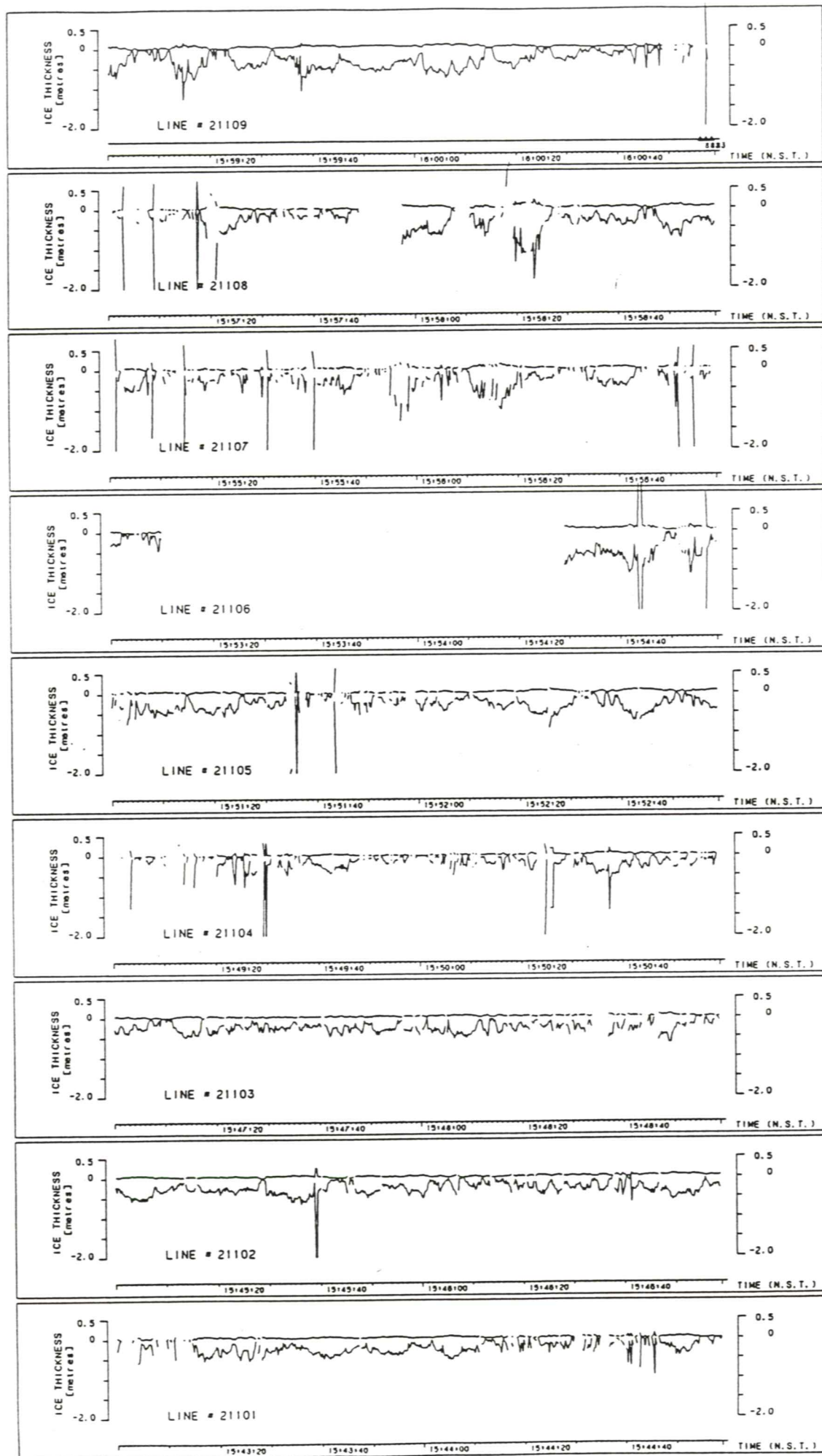














MEMORIAL UNIVERSITY OF NEWFOUNDLAND

St. John's, Newfoundland, Canada A1C 5S7

Department of Mathematics & Statistics

Tel.: (709) 737-8783/84
Fax: (709) 737-4569
Telex: 016-4101
Email: MATHSTAT@MUN

March 9th, 1990

Dear Scott,

I know that I should have written earlier about your ice thickness problem, but the matter is hardly trivial: I could not write down a simple answer and have lacked the time to answer it with the detail it deserves. However I have not been entirely idle; the questions you had seemed similar to a problem in estimating fish stock abundances on the Grand Banks that I was looking at and I got a bit carried away thinking about it. But to get back to your original queries I think that the difficulty stems from the questions themselves, which are insufficiently precise.

1) You wanted to compare histograms. Now there is a general test, the Kolmogorov-Smirnov test for comparing two sample distribution functions (better than the histogram and similar). I can send you the details. It is an old test, but effective. Unfortunately it can be rather too effective, since the distributions you would be comparing, produced from the aerial and the ground data, are estimating different things, have different sources of bias and would hence show up to be different.

2) In fact, the real question here is how to estimate the histogram, or better yet, the distribution of ice thickness using the different sources of data. Roughly speaking, there are two sorts of estimates to consider: parametric and non-parametric. If you are prepared to assume that the ice thickness follows some well-known distribution, such as the normal or the gamma, then all you need do is estimate the relevant parameters of these distributions (not more than two in number) and their estimators. With the volume of data at your disposal, these variances will be very small. They may also be meaningless, since it is likely that the distribution is changing with distance. This is undoubtedly the case when you pass over open stretches of water covered with patches of ice.

3) When you know nothing about the shape of the distribution you can estimate the distribution non-parametrically. A standard reference to this problem is Richard A. Tapia and James R. Thompson's "Nonparametric Probability Density Estimation". I have to think some more about how you would apply those methods to the smoothed and "staggered" measurements that you have, but I think that should be straightforward. Even more straightforward should be the problem of estimating the spectrum under those circumstances. I will let you know about that when I figure it out myself. By the way, the histogram is a non-parametric estimate of the density.

Appendix B. Statistics of Ice Thickness Distribution

During this project Dr. Catherine Dalzell of the Department of Mathematics and Statistics, Memorial University of Newfoundland, was approached to obtain her view on comparisons of ice thickness distributions by auger and by airborne methods. She was not able to quantitatively address this question during the current project, but had a number of salient points on this topic which are outlined in the attached letter.

4) What really concerns me here is the lack of stationarity and independence in the data, since the usual methods for estimating densities, distributions et al. assume independent and identically distributed data. When the underlying structure changes (For instance, you pass from solid ice to ice patches on the sea) you lack stationarity; when adjacent measurements are related, as they must be in the case of a continuous surface measured sequentially, then you lack independence. My own feeling is that the best way to display the aerial data, which in the final analysis is what you want to be able to do, is to estimate densities or spectra as you go, allowing them to change as a function of distance. One could then test if the distribution of thickness remains the same. This is the problem that interested me in connection with the fish stock data, where it was required to estimate the distribution of fish stocks in different locations. However I think that your data is much better suited to that kind of thing since you have so much of it. The fish stock people were trying to get too many densities from too little data, and I don't think it make sense to attack their problem in that way.

5) But at the end of the day we must always return to first questions. What really do you want to know? Don't say that you want to estimate the variance of a histogram unless you really want the variance of a histogram. You want a histogram because you want the distribution of ice thickness, and the histogram is one of many estimators of that distribution, although not the best. Why, then, do you want the distribution of ice thickness? Is it enough to estimate the mean thickness, or the mean and the variance of the thickness? You only need the entire distribution if you are interested in higher moments, just as you only want to estimate a spectrum if you are interested in periodic effects of many frequencies. Don't make the problem more complicated than it is.

6) Questions statisticians cannot answer: if your method differs from "ground truth" because of peculiar features, such as mistaking snow for ice, then estimating the distribution cannot help. Statistical methods assume that the data are clean. There are ways of adjusting for certain difficulties in the data but additional information is required. For instance if there is some characteristic of snow as opposed to ice one might be able to detect numerically those parts of the data sets in which snow had been mistaken for ice. Generally speaking, an effect that is operating everywhere is easier, such as the moving average effect of the measuring device. Also: do not use statistics as a substitute for your own eyes. Numerical methods are not required for knowing if you are flying over open water since that is obvious to anyone present.

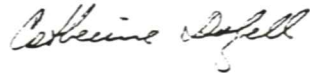
7) I would like to work on the problem of estimating a density or spectrum that is changing slowly with distance. I have already begun thinking about that problem, and I was hoping that I might use some of your data at some point to test out what I am planning. As a start, I will look up how to estimate a spectrum from moving average data. The density is a bit more tricky since these estimates usually assume independent data, which you do not have. It is less obvious why one is interested in a density for dependent data, as a matter of fact. I am beginning to realize that when a problem is not in the literature it is often because it makes no sense to

solve it.

8) Let me repeat, as a final shot, that I don't think I can go much further with your question without a sharper definition of the problem to be solved. The best statistical analyses are geared to answering very specific questions. You may think that the question "what is the variance of the histogram?" is such a question, but it is not. To answer it I have to posit a theoretical density for the data, although if I knew what the density was, I would not need to estimate it. If you want the density as a means to something else, then it may be easier to estimate that other thing directly.

I hope these remarks are of some help. Please keep in touch about the problem, which sounds interesting. There is no charge for this advice since I do not feel that I have come up with any genuine answers.

Yours sincerely,

A handwritten signature in cursive script, appearing to read "Catherine Dalzell".

Catherine Dalzell.

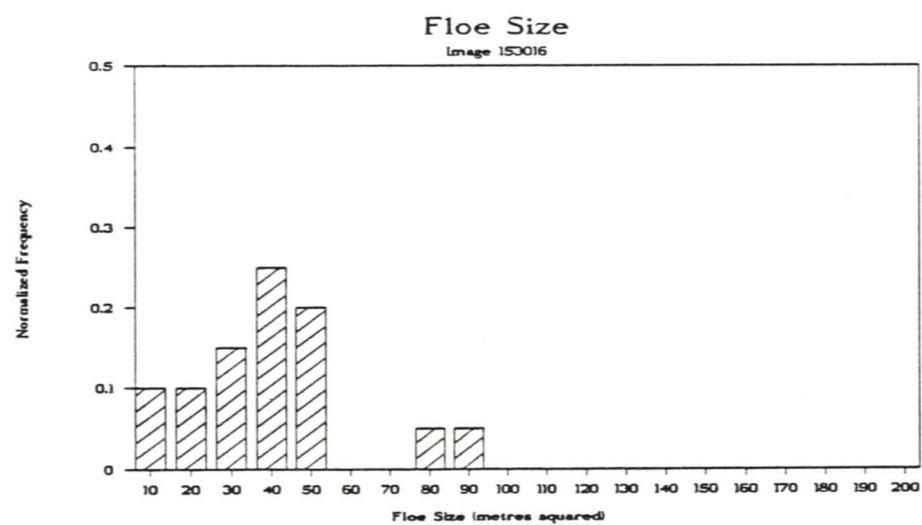
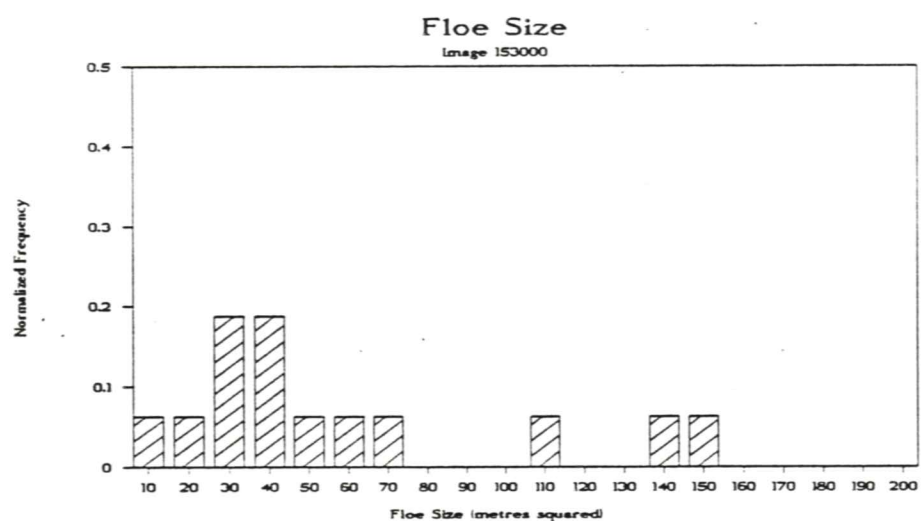
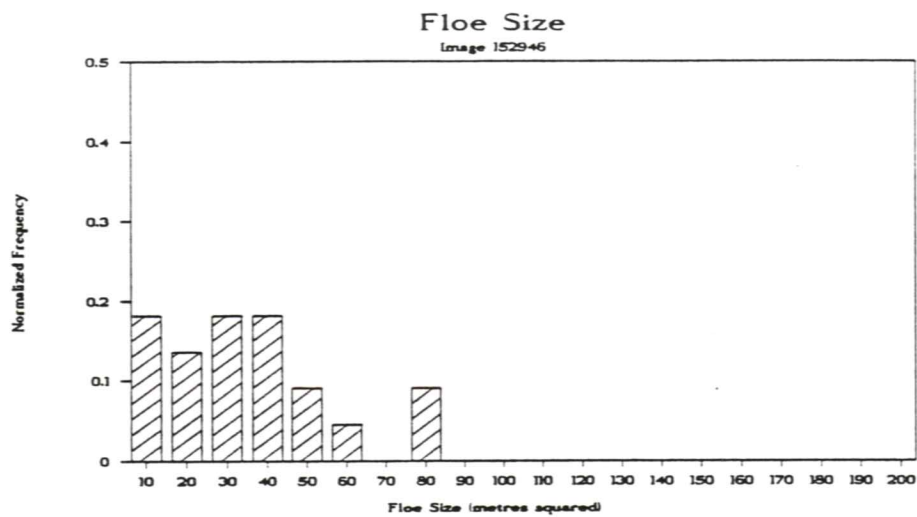
Appendix C. Histograms of Floe Size

The plots in this appendix contain histograms of floe sizes in thirty-nine of the forty images for which ice concentrations were computed. The fortieth image, at the time 15:34:16, was excluded because the helicopter was passing over a region of open water.

The floe sizes were calculated from a digitized image of the videotape record of the flight, as described in the main body of the report. The perimeter of the ice floe was traced out using a mouse. The area of the floe was then calculated as the number of pixels lying within or on the perimeter. Using the altitude recorded by the laser altimeter, a scaling factor was calculated for each image in order to convert the area units to metres squared.

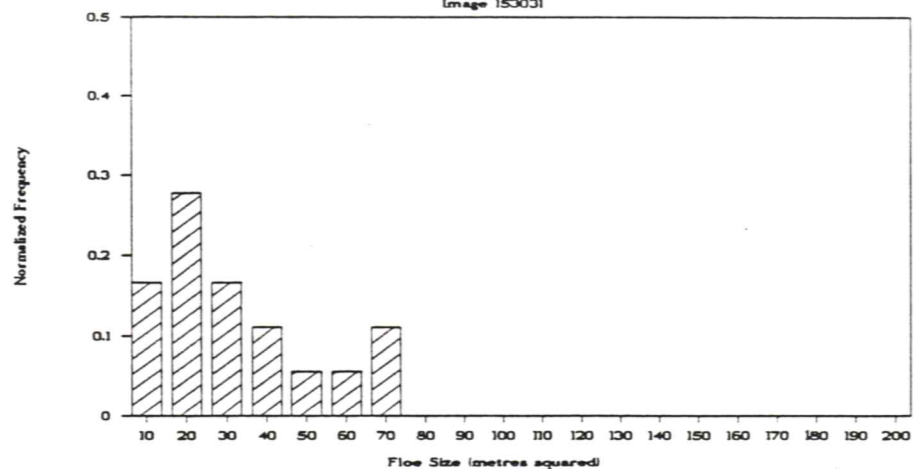
In the following figures, the floe sizes have been binned in intervals of 10 m^2 , and have been tagged according to the central value in the data bin; thus, for example, the bin labelled as " 10 m^2 " contains the fraction of floes whose areas are between 5 and 15 m^2 . The height of the bar represents the normalized frequency, the fraction of the ice floes which fall within that bin. Floes smaller than 5 m^2 or larger than 205 m^2 in area are not plotted, but are counted when calculating the number of floes for normalization.

The number of floes for each frame is given in Table 3 of the report. Some of the differences between the shape of different histograms are probably due to a larger number of small floes being counted for some histograms than for others.



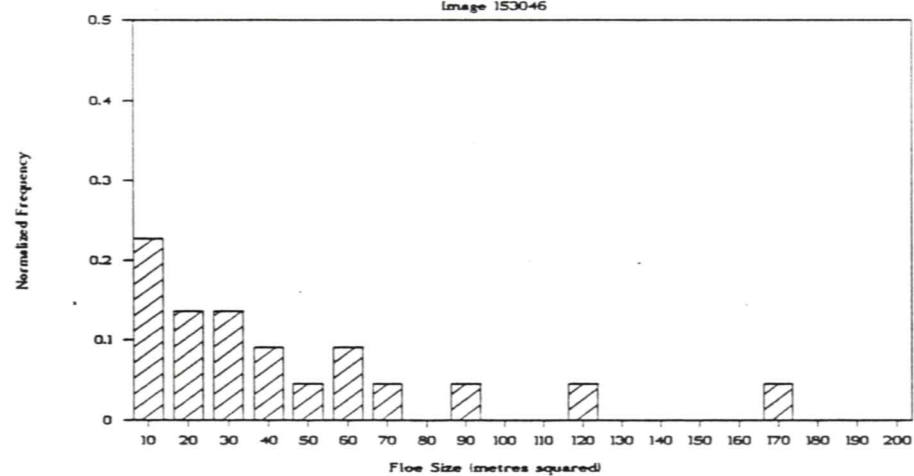
Floe Size

Image 153031



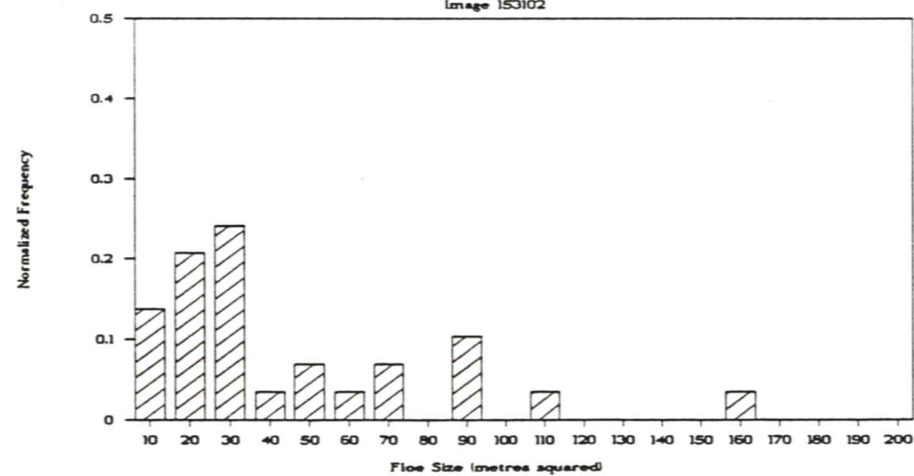
Floe Size

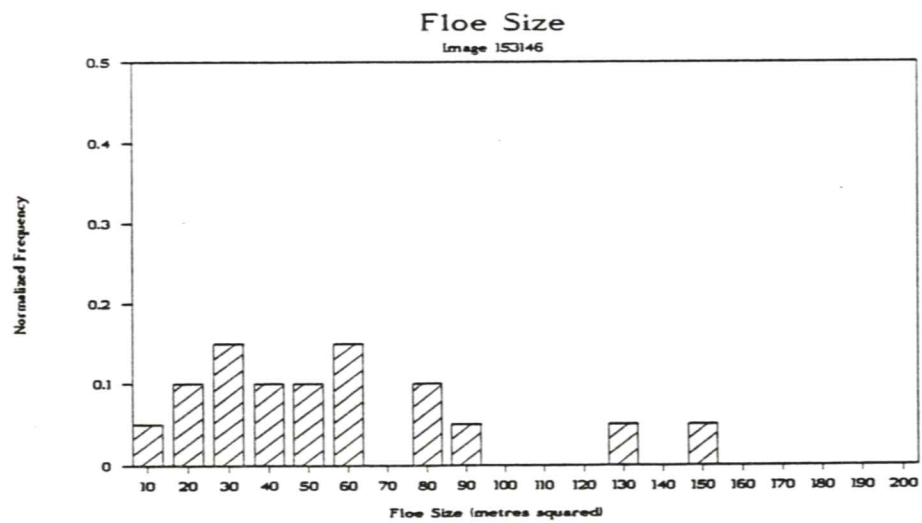
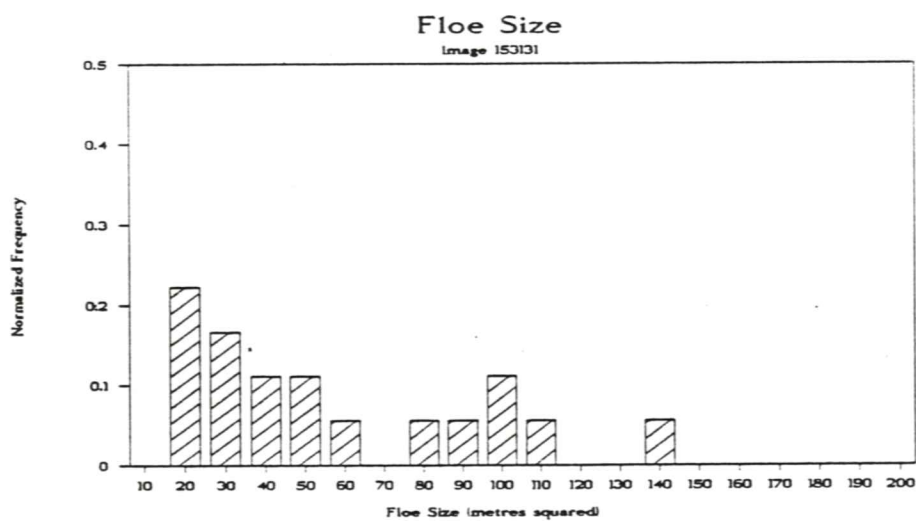
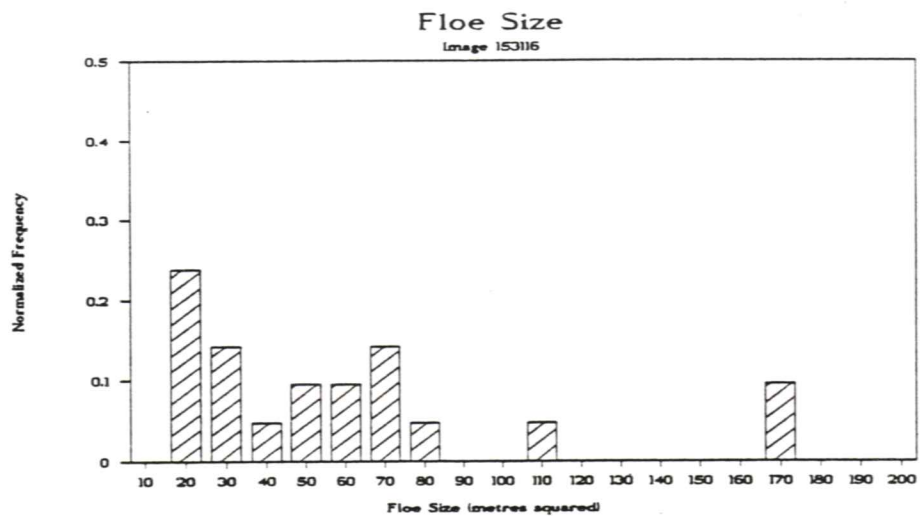
Image 153046

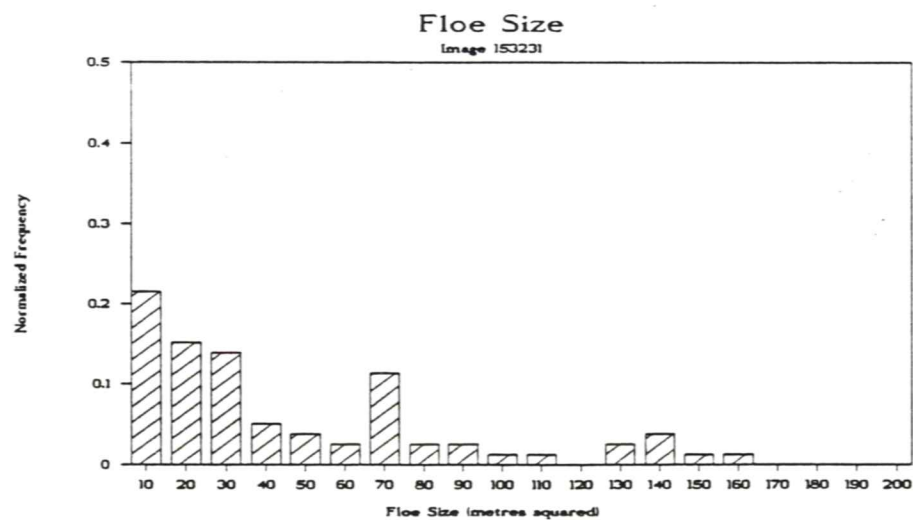
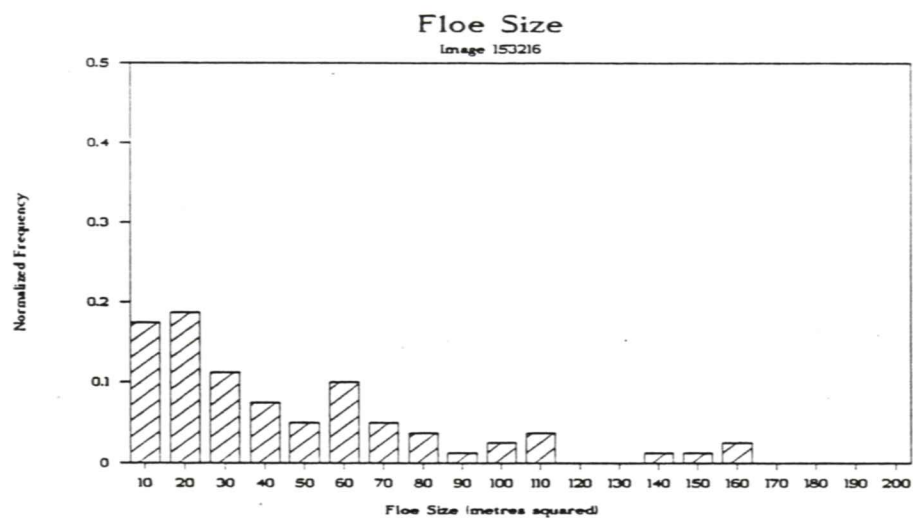
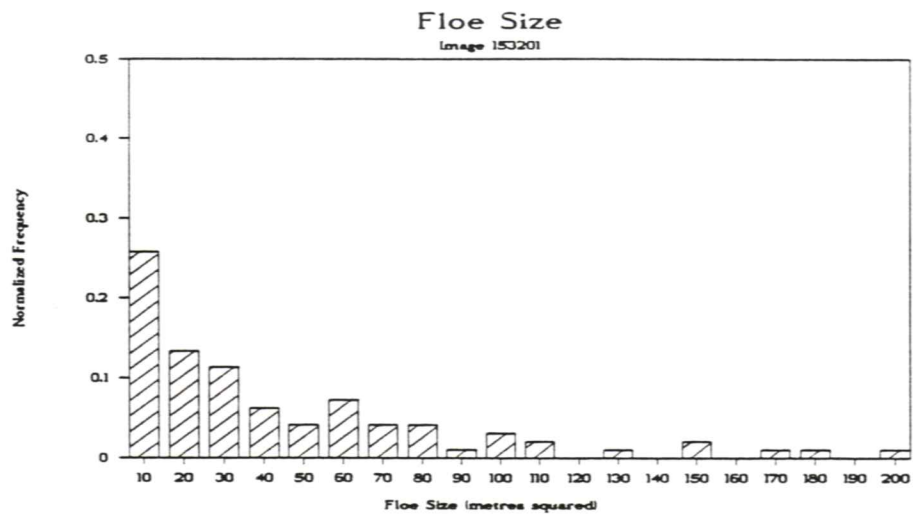


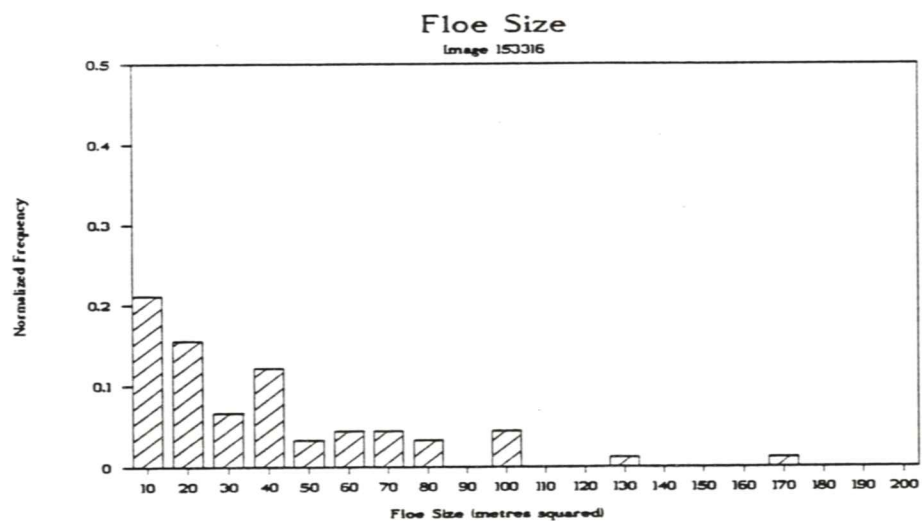
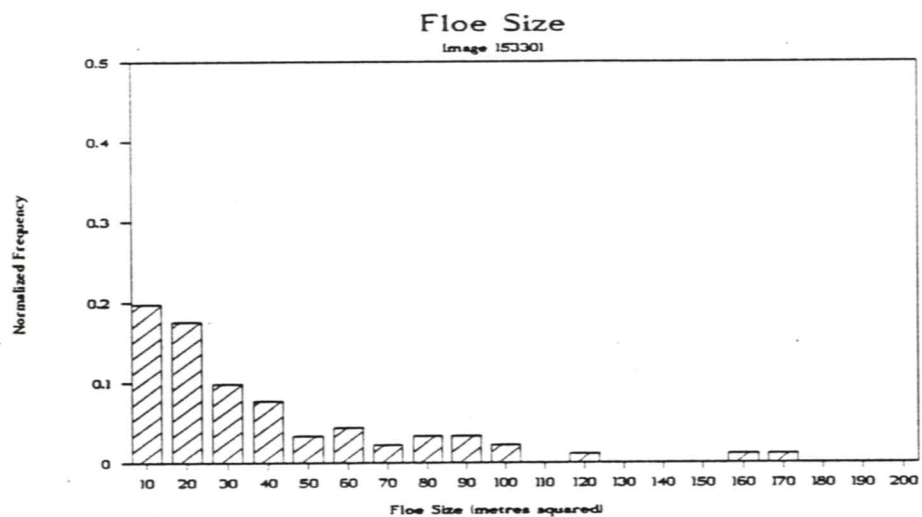
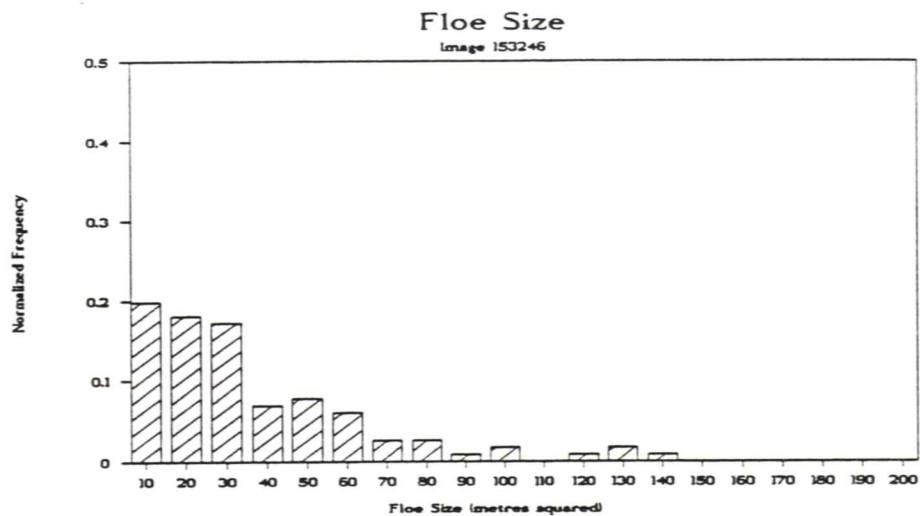
Floe Size

Image 153102



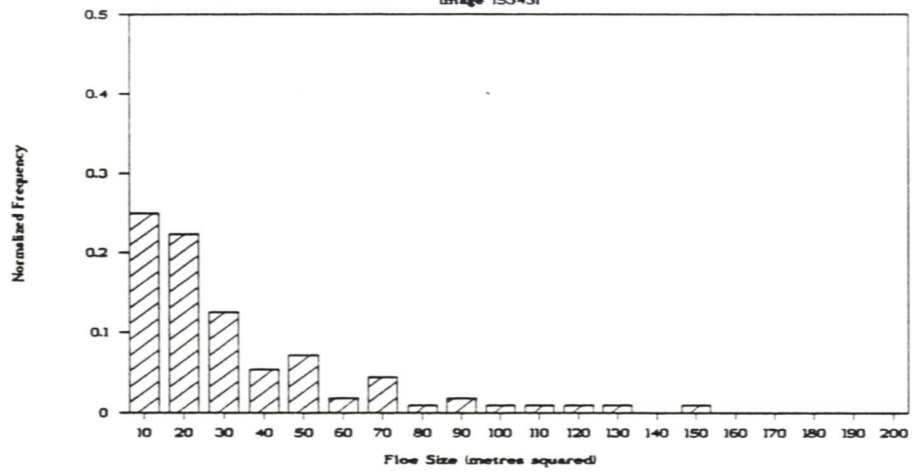






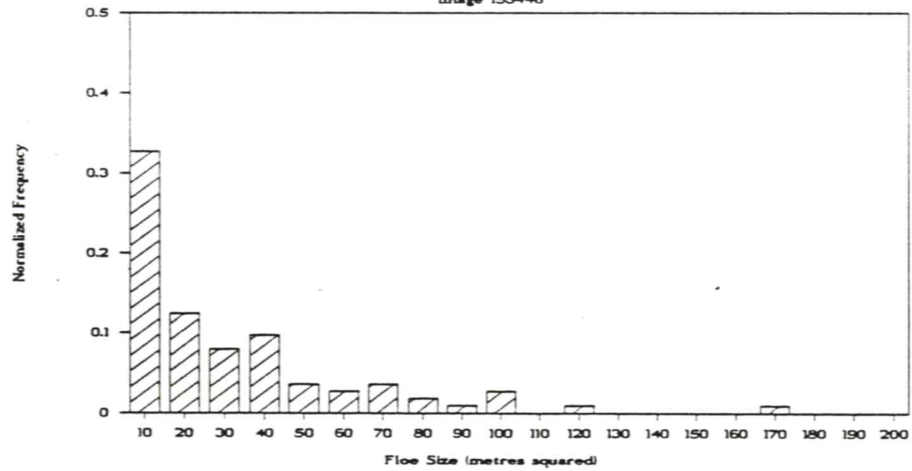
Floe Size

Image 153431



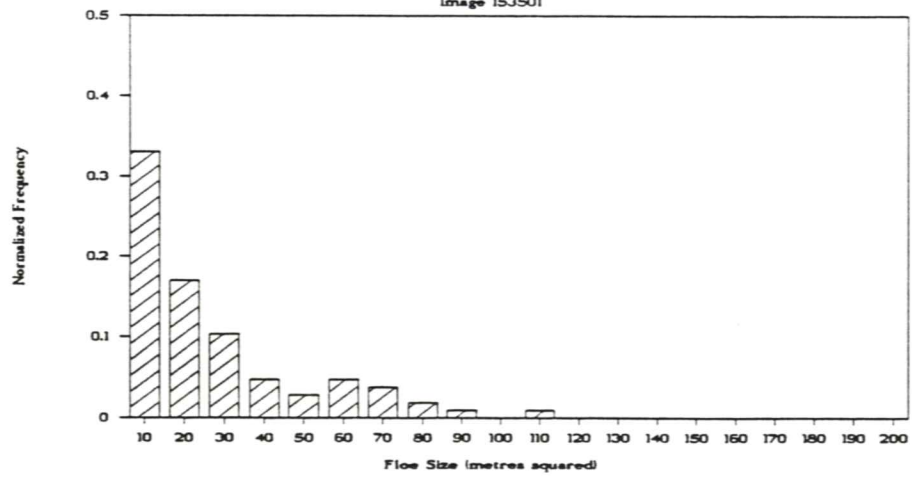
Floe Size

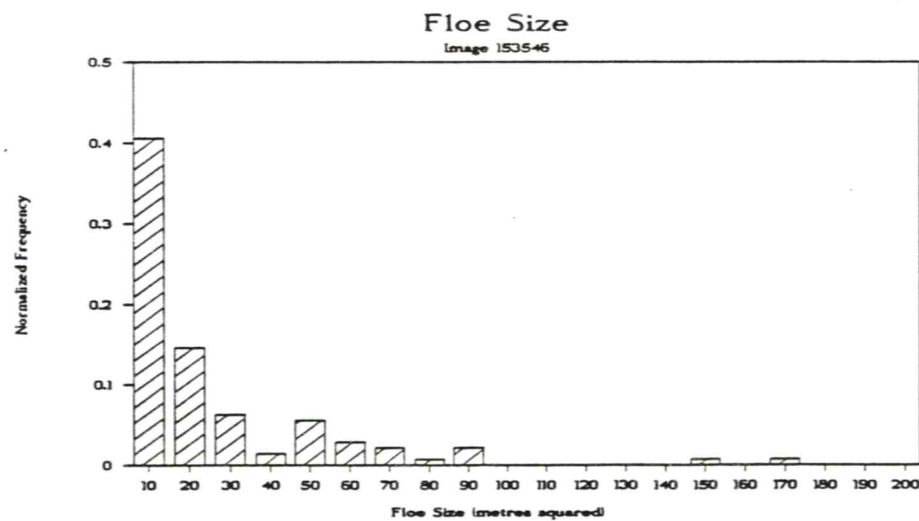
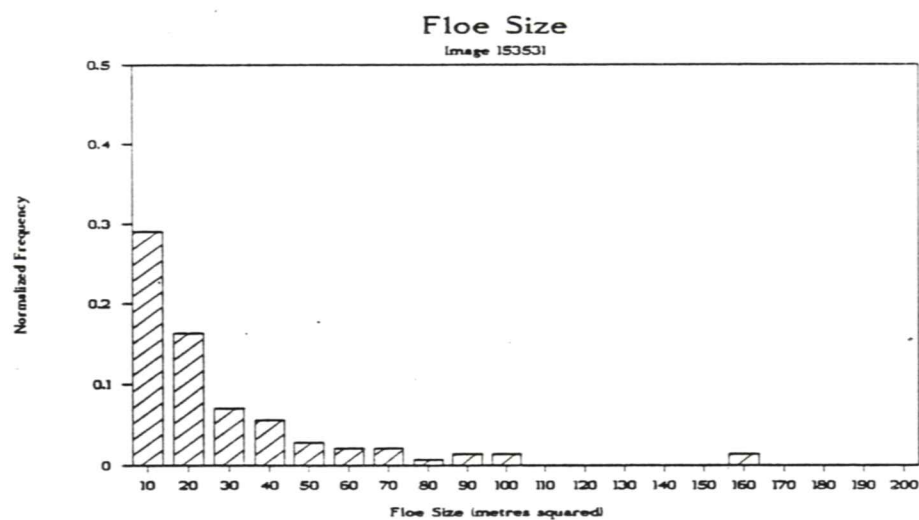
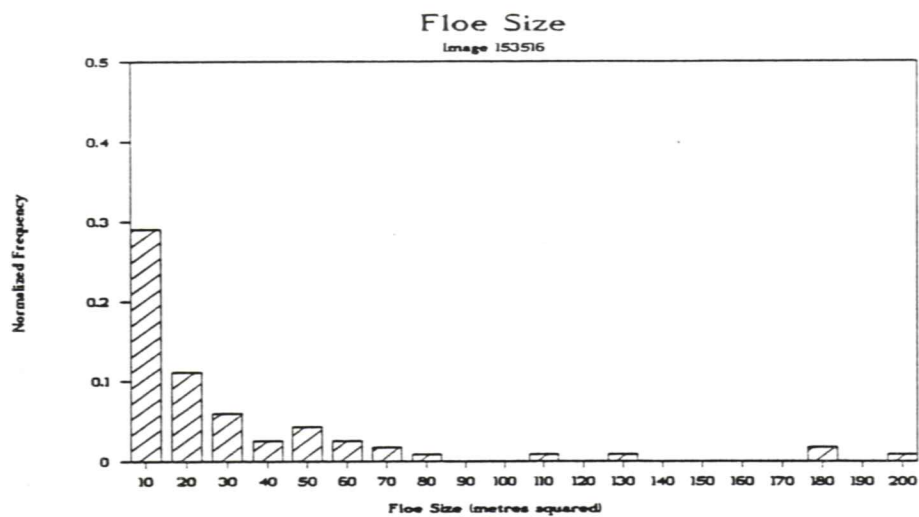
Image 153446



Floe Size

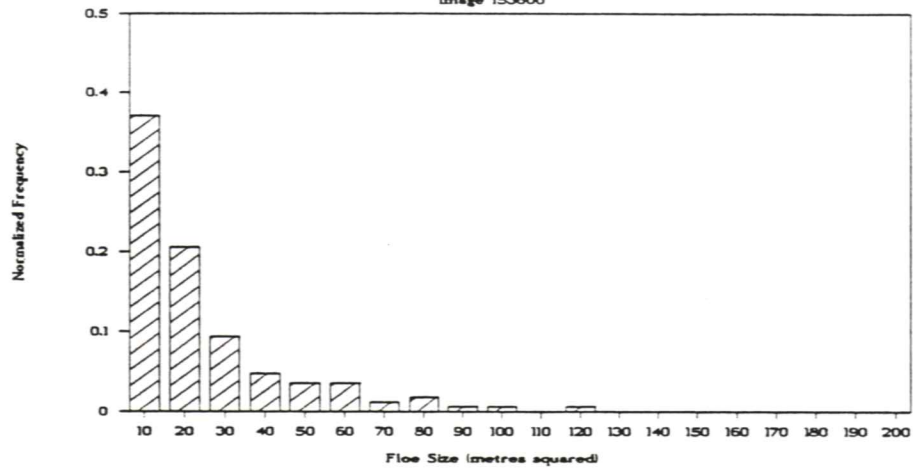
Image 153501





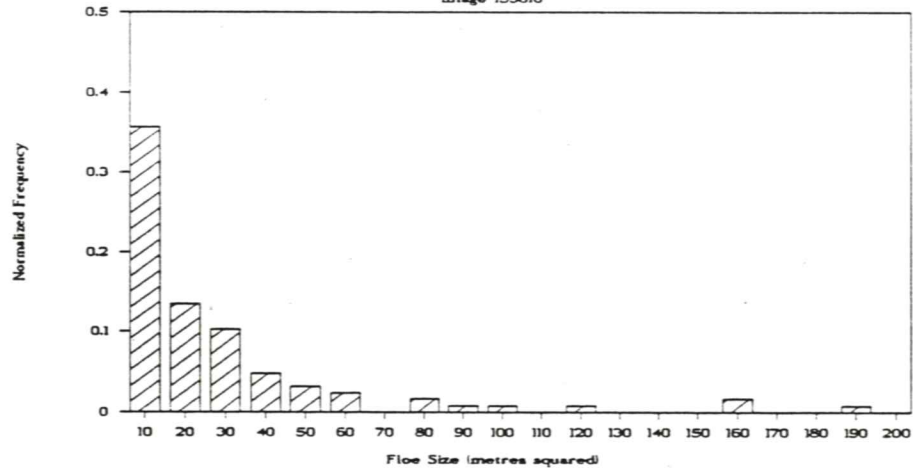
Floe Size

Image 153600



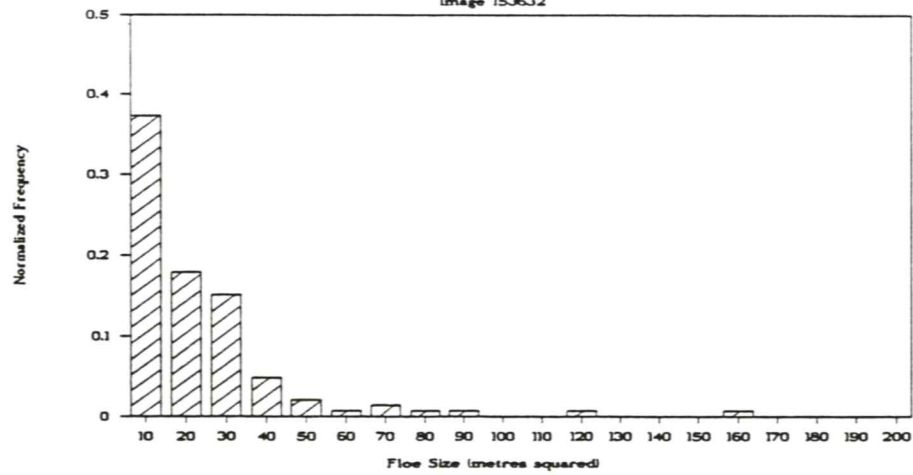
Floe Size

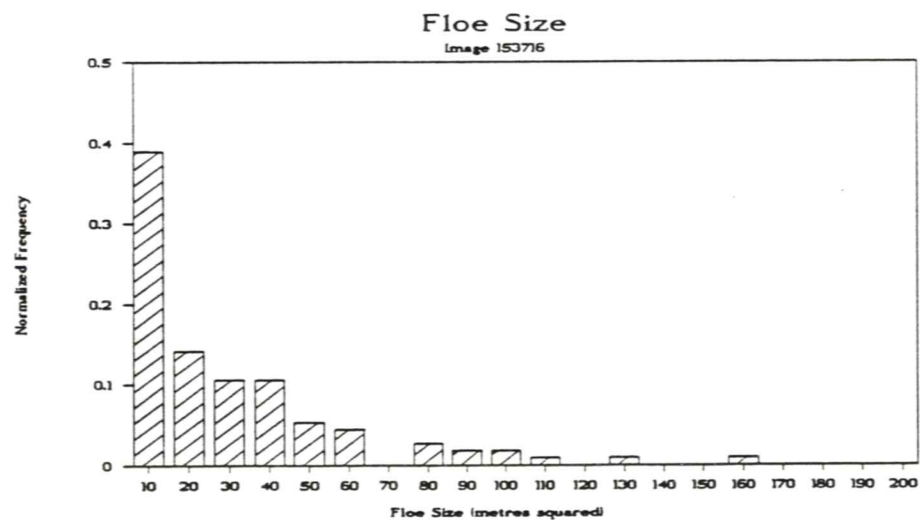
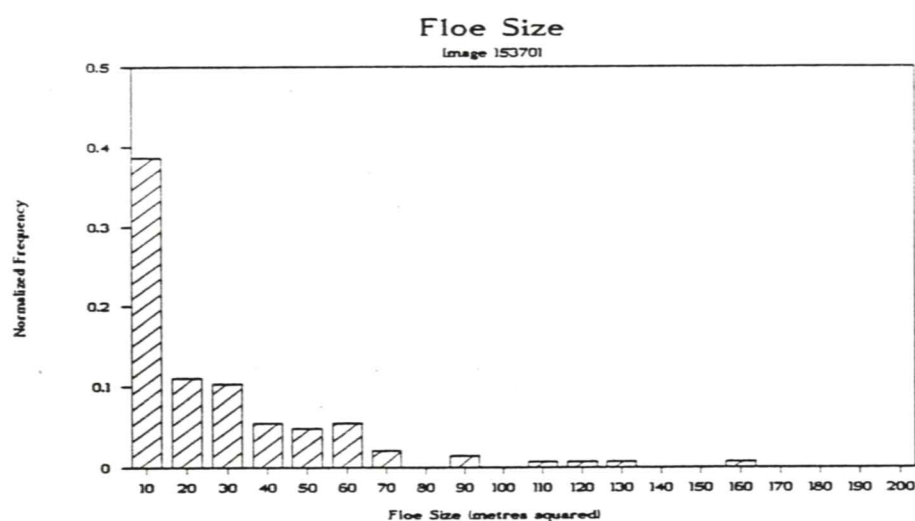
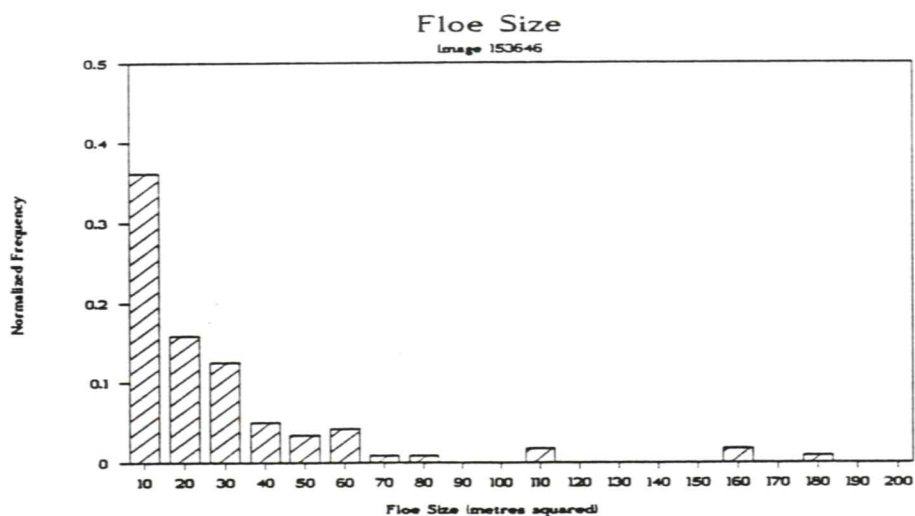
Image 153616

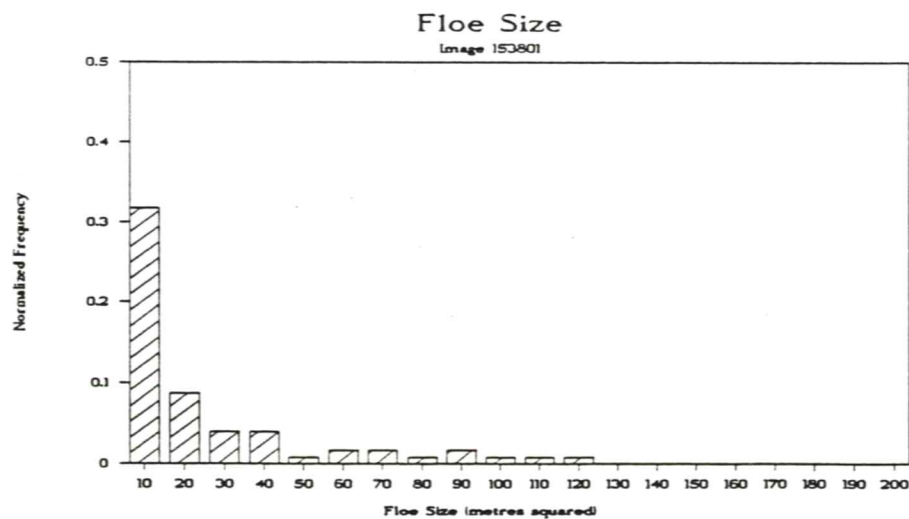
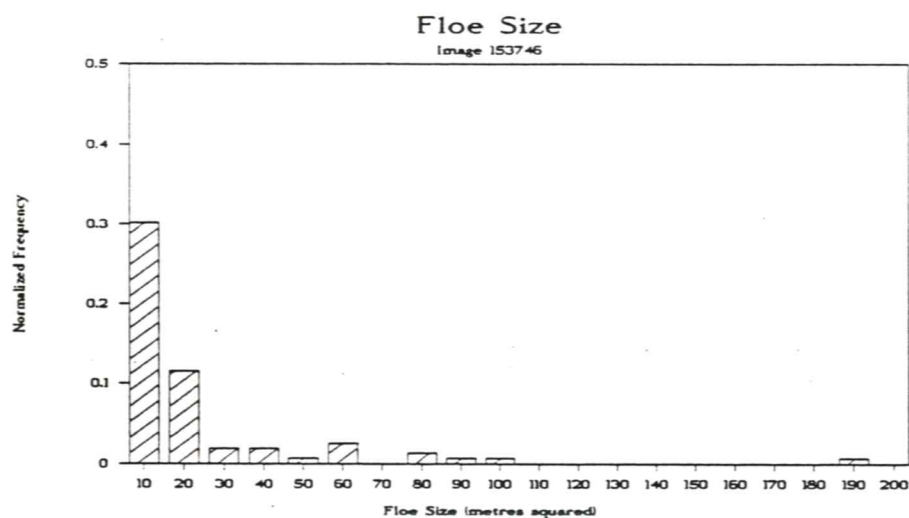
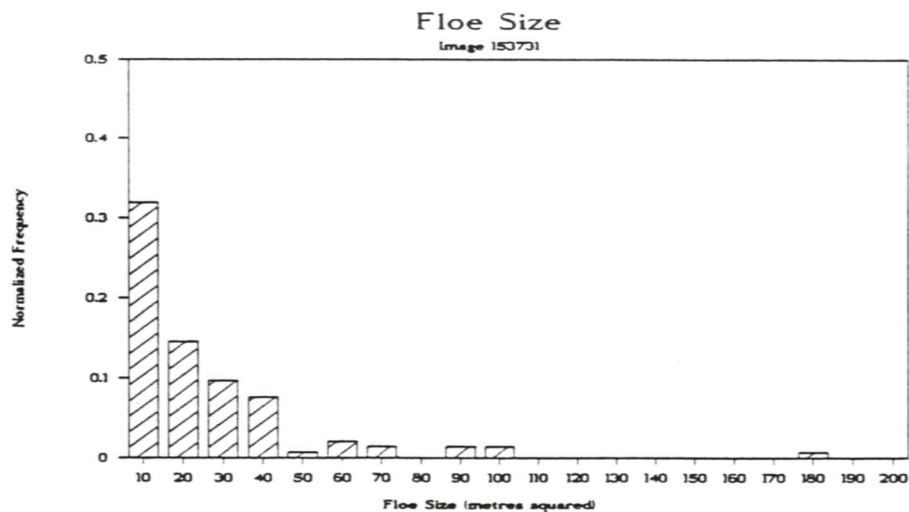


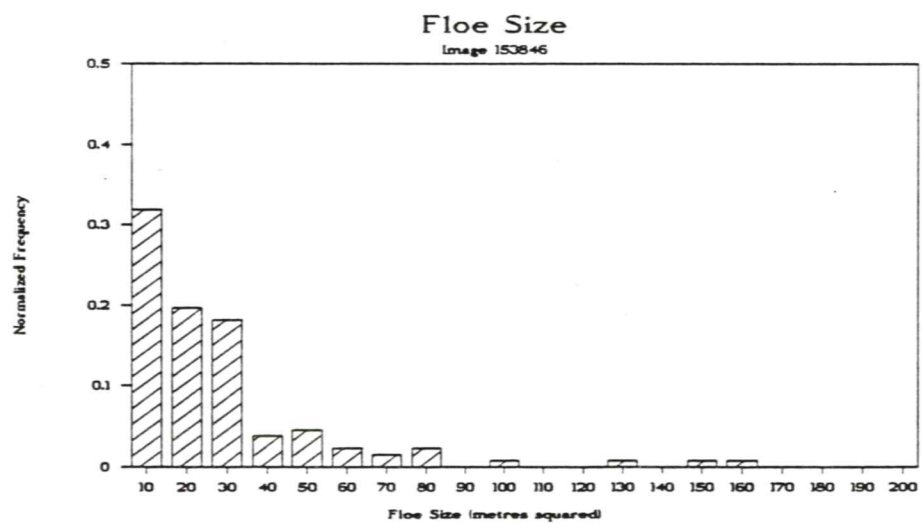
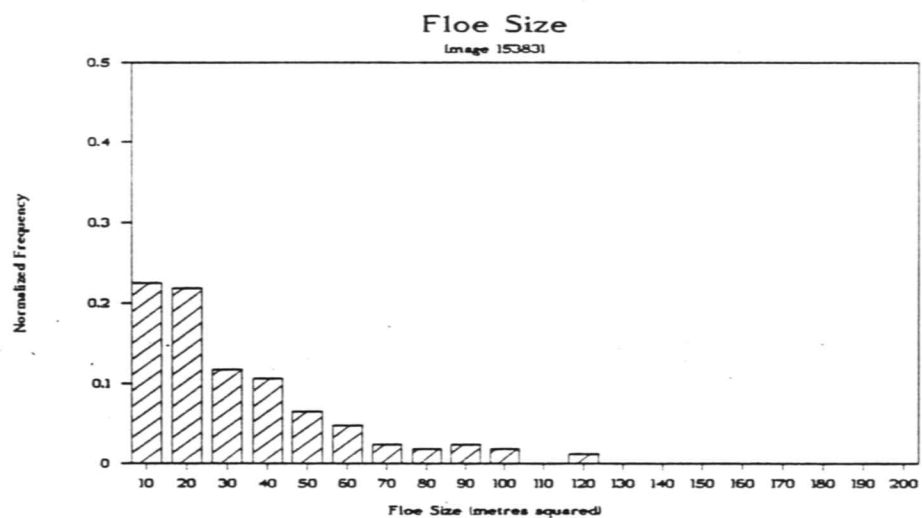
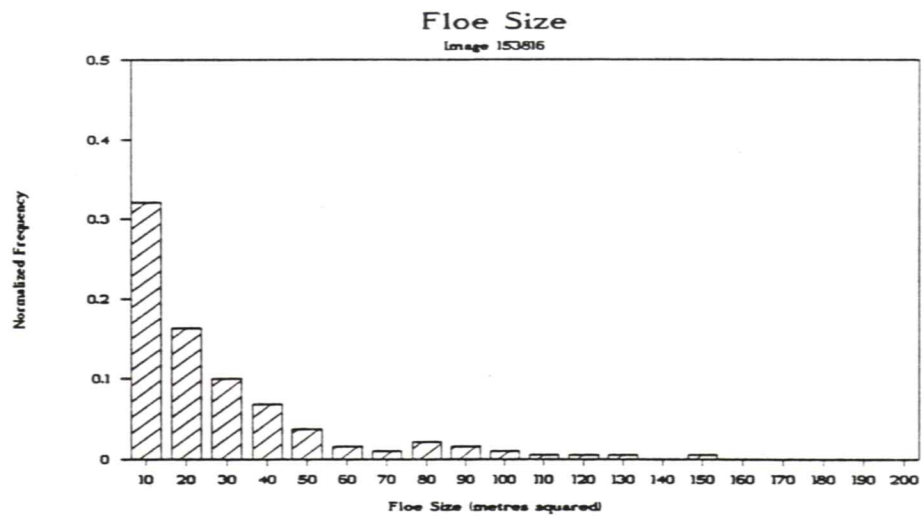
Floe Size

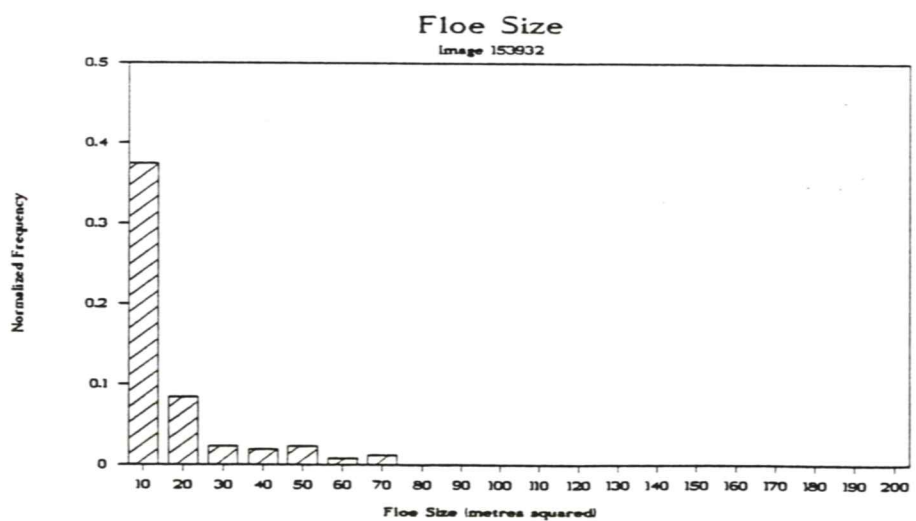
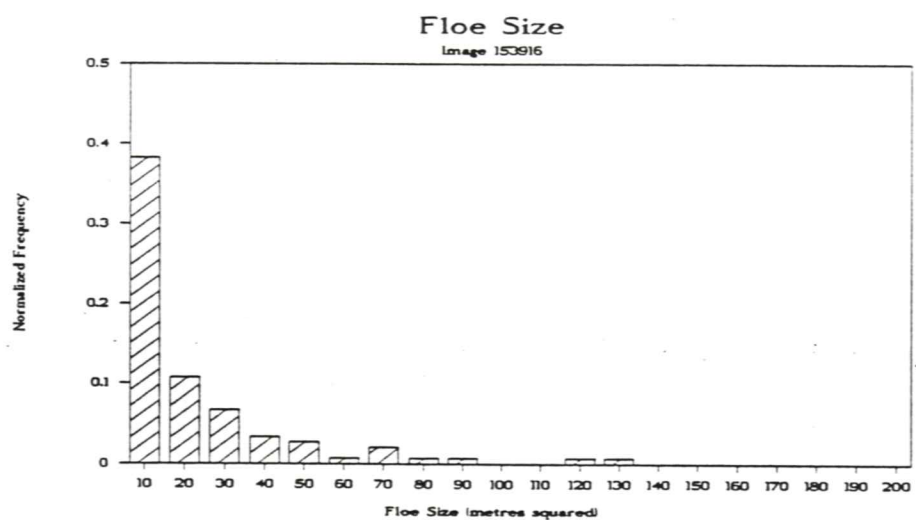
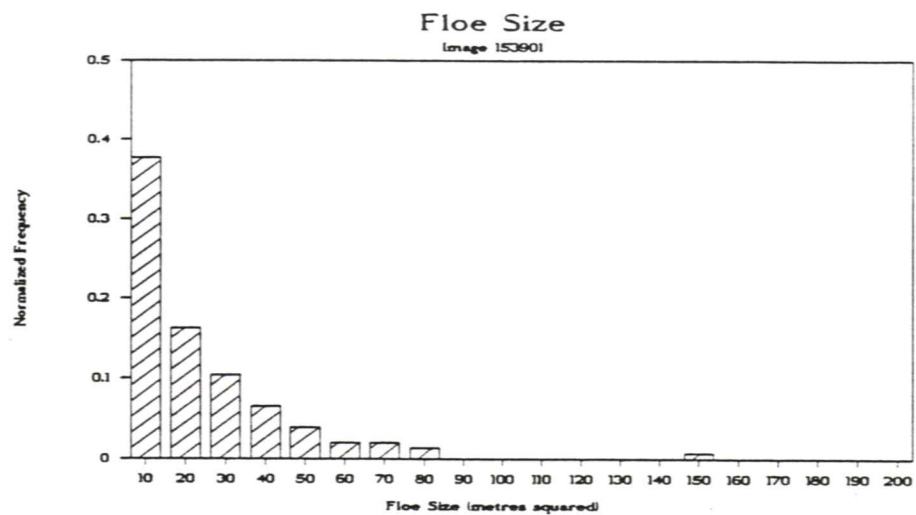
Image 153632











Appendix D. OMAE Conference Paper

The attached paper was presented by Dr. Scott Holladay at the 9th International Conference on Offshore Mechanics and Arctic Engineering, Houston, Texas, 18-23 February, 1990, and will be included in the conference proceedings.

The paper summarizes much of the work reported here and some results from prior experiments.

AIRBORNE MEASUREMENT OF SEA ICE THICKNESS USING ELECTROMAGNETIC INDUCTION

J. Scott Holladay, Aerodat Limited, Canada;

James R. Rossiter, Canpolar Inc., Canada;

Austin Kovacs, U.S. Army Cold Regions Research and Engineering Laboratory, U.S.A.

SUMMARY

Remote measurement of ice thickness is important both for practical operations and for a variety of scientific applications. Over the past few years electromagnetic (EM) induction sounding has indicated that this method is a promising one for measuring sea ice thickness from a low-flying helicopter. In this paper the background of the method is described, and extracts of measurements made in Prudhoe Bay, Alaska and off the coast of Newfoundland as part of the LIMEX'89 project in March 1989 are presented. The latter survey work was conducted to aid in the assessment of ice cover in the Labrador Sea as part of a climatological investigation. Measurements were made both over shorefast first year ice and over first year pack ice. The ice was near the freezing point. Agreement with auger thickness measurements is within ± 0.1 m over relatively level ice. These results suggest that EM induction can be used to collect ice thickness data reliably. Work is underway to design systems for operational use.

INTRODUCTION

There are a variety of reasons for requiring knowledge of ice thickness, including route selection for ships, scientific ice dynamics and climatology studies, design of offshore structures, and defence applications. To date ice thickness has been measured directly at specific locations, inferred from other observations, or estimated using impulse radar. All these approaches have strong limitations, particularly for warm and deformed ice (Canpolar Consultants Ltd., 1985).

A practical technique for the measurement of sea ice thickness from an airborne platform, based on electromagnetic (EM) induction, is now reaching the end of its validation stage (although the more difficult problem of detailing the thickness of ice ridges is still the subject of research). The basic method has been demonstrated in the Arctic (Kovacs *et al.*, 1987a; 1987b; Kovacs and Valleeau, 1987; Rossiter and Lalumiere, 1988; Kovacs and Holladay, 1989 a,b) and off Cape Breton Island, N.S., during Spring 1988 (MacLaren Plansearch, 1988).

In this paper, the scientific basis of the EM sounding method and the current state of the art will be described. Results from a May, 1987 field evaluation study near Prudhoe Bay, Alaska and from the March, 1989 LIMEX'89 field program off Newfoundland, Canada (Raney and Argus, 1988) work will then be presented, followed by a discussion of system accuracy. The paper will conclude with a brief description of present research directions.

Scientific basis

The EM induction method typically uses frequencies in the 50 Hz to 50,000 Hz range. A set of transmitter and receiver coils are towed in a bird about 15 to 30 m above the ice, as shown in Figure 1. The transmitted primary field induces eddy currents in nearby conductors which in turn generate secondary EM fields. These secondary fields are detected at the receiver.

For ice thickness measurement, the sea water is the dominant conductor, since it is typically several orders of magnitude more conductive than the ice. By measuring the amplitude and phase of the secondary field (in parts per million of the primary field) at the receiver coil location, the distance of the bird to the water can be estimated. A laser profilometer is used to measure the distance from the bird to the top of the snow and/or ice. The difference between the two measurements gives the thickness of the snow plus ice layer. Areas of open water provide calibration points for the system. The approximate "footprint" of the EM system is about the same as the bird height (the laser spot size is much smaller). When lateral changes in ice thickness are rapid compared to the flying height, such as are observed near ridges, the peak ice thickness tends to be underestimated.

Present State of the Art

Prototype birds designed primarily for ice measurement have been described by Kovacs *et al.*, 1987b, Kovacs and Holladay (1989 a,b) and by Rossiter and Lalumiere (1988). The sensor packages used during the Prudhoe Bay and LIMEX'89 work included three principal elements: a multifrequency helicopter-towed EM sounding system; a laser profilometer mounted in

the towed bird; and a video camera mounted in the helicopter. The EM system included an electromagnetic signal processor unit and a data acquisition/logging unit mounted inside the helicopter. A set of bird attitude sensors measuring pitch and roll were inside the bird. All data were sampled at 0.1 second intervals before digital recording on magnetic tape. The video imaging system mounted on the helicopter monitored ice conditions below the bird, and the image was annotated with time, flight and survey line identifiers before being recorded on video tape using a video cassette recorder. A single-engine helicopter was used for surveying over shorefast ice. Safety and range considerations mandated the use of a much larger twin-engine helicopter for offshore work during LIMEX'89. Differences between the CRREL and Aerodat systems lay in the bird size, weight and number of frequencies: the CRREL bird is about 3.5 m long, weighs about 100 kg and operates at 800, 4,500 and 50,000 Hz, while the Aerodat system is about 7 metres long, weighs about 250 kg and operates at frequencies of 930, 4,175, 4600 and 33,000 Hz.

The CRREL bird was a prototype, and a variety of problems were encountered in its operation during the Prudhoe Bay survey. For the most part, these problems were related to excessive noise and drift in the system. Despite these difficulties, data quality was quite adequate to permit ice thickness measurement along a series of relatively short survey lines flown over several sites at which exhaustive ground truth had been obtained. Results from one of these areas will be presented in a later section. The performance of the Aerodat EM hardware on the LIMEX'89 survey flights was, for the most part, highly satisfactory. The EM noise levels were typically less than 1 ppm, while small amounts of drift were observed during the early portions of the Bay of Exploits flights, but did not affect the profiles over the main lines. A slightly longer warmup period (about 1 hour) would probably have prevented most of this drift. Drift was essentially insignificant for the offshore lines. The laser profilometer performed well over snow and ice, but provided erratic altitudes above open water. The unit has since been modified to eliminate this problem, and is now undergoing airborne testing.

EM DATA REDUCTION

Calibration and drift removal

There are three stages in the data reduction: transcription of the field data tape to a computer disk (data volumes range up to 4 Mbytes per hour at present); removal of baseline drift; and calibration of the data. The data transcription operation is relatively straightforward, and leaves the data in a format in which it can be manipulated easily in later stages of reduction.

Correction for instrument drift presently requires that the sensor package be flown to high altitude (above about 500 metres) approximately every 30 minutes during the flight to remove the sensor package from the vicinity of the highly conductive seawater. Variations in these high-altitude measurements provide a reliable way to correct for small amounts of drift in the system, based on the assumption of linear drift between these baseline measurements. As EM system drift becomes smaller and more predictable with improved equipment, the permissible baseline interval will become progressively longer, increasing survey efficiency.

Once the data have been drift-corrected, they can be calibrated. At present, the most reliable way to estimate the

sensitivity of the system is to fly over deep, open water having a known conductivity-depth profile to at least 30 metres: an accurate prediction of the response is then compared with the measured response, and correction factors can be calculated which are applied to bring the measured response into line with the expected response of the known situation. This technique has become known as "ground-truth calibration", and has proven quite satisfactory under a variety of conditions. Instrumentation advances are expected to provide a stable, accurate internal calibration method during the next year, at which point ground-truth calibration will become a verification tool rather than a calibration tool.

Another operation which is sometimes performed on EM data is called spheric removal, and involves the removal of noise pulses in the EM data caused by distant lightning strokes. The algorithm used for this operation is useful for removing spikes from other relatively smooth data as well; the laser profilometer data was filtered in this way to remove errors caused by inconsistent performance of the profilometer over open water.

Inversion of Survey Data for Ice Thickness

The drift-corrected, calibrated data, which consist of the secondary field response in phase with and out-of-phase with the transmitted or primary field, vary according to the altitude of the bird (and, to a small extent, upon its attitude) above the surface of the seawater underlying the ice. The response is not a particularly simple function of altitude, and is also affected by the conductivity of the seawater (at low frequencies) and of the ice (at high frequencies), but forward computer models which can predict the EM response over a given ice/water model have been written (Kovacs et al, 1987a). Inverse models which directly calculate bird height from measured data do not yet exist.

For this reason, a number of relatively complex methods have been developed to approximately invert the data. The most robust of these methods, in the sense of providing good results even in the presence of data error, is the Generalized Inverse method, which uses a forward model to generate model responses and a matrix of derivatives of those responses with respect to the desired parameters, such as ice thickness and seawater conductivity. An initial forward model response is compared to the observed response, and the differences between them used, along with the generalized inverse of the derivative matrix, to estimate the changes in the model parameters required to make the model response more closely resemble the measured response.

A few iterations of this algorithm usually provides estimates of the ice thickness that are accurate to within the range of accuracy of the laser altimeter, at least for relatively level ice. Ice that has large thickness variations over short horizontal distances tends to have its thickness underestimated by this method: more suitable approaches are being developed to deal with these situations (Becker et al, 1987; Liu and Becker, 1988).

MEASUREMENTS

The CRREL survey was intended primarily as a detailed assessment of the sensor and the method, and consisted mainly of repeated passes over a set of clearly marked ground-truth sites on shorefast ice near Prudhoe Bay. These sites were drilled on a 5 metre grid pattern to obtain an extremely detailed set of snow, ice and freeboard measurements. The

snow and ice thicknesses were added and averaged over swaths down the middle of the grids to generate an average snow plus ice thickness for comparison to the airborne results.

The LIMEX'89 survey actually consisted of two distinct efforts (see Figures 3, 5 and 6 for location maps). The first was concentrated on shorefast ice in the Bay of Exploits southwest of Twillingate, and provided a check on system performance and further validation of the method using surface truth measurements conducted by Canpolar and Aerodat personnel. A total of 16 augered holes were measured, along with ice, water, and CDT profiles to 2.25 m depth (see Figure 4). Ice varied from 38 to 59 cm in thickness; snow cover, from 0 to 21 cm in thickness; the water under the ice had a conductivity of about 0.5 S/m, increasing sharply to 2.5 S/m at a depth of about 1.0 m. The second consisted of a 500 km run from St. John's out to the Terra Nordica (the LIMEX'89 project ship) and back. Measurements were made over most of the flight, i.e. about 300 km. Ice encountered varied from strips and patches of brash ice, to small cakes of first year ice, to small floes of first year ice around the ship. Although most of the ice was not rafted, there were some rafted pieces visible on the video flight record and reported by surface teams working on the ice. At the time of the flight, the C-CORE Ice Motion Sensor and a MacLaren Plansearch ARGOS beacon (see Figure 6) had been set up for other purposes. These sites were clearly visible from the air, and estimates of ice thickness were available there. A number of other sites were also augered, but were either not marked and could not therefore be located using the video record, or were too close to the ship.

RESULTS

The Prudhoe Bay survey was conducted in early May, 1987. Data over marked grids on 3 multi-year ice floes, a first-year pressure ridge and a variety of extended survey lines were obtained with the EM system. An example from Multi-Year Floe 1 is presented in Figure 2: this figure includes the averaged snow plus ice thickness and 4 EM ice thickness profiles, as indicated in the legend on the figure. It is apparent that the EM-derived profiles follow the long-period thickness trends but not the short-period undulations. This was expected due to the effective footprint of the EM system, which is on the order of 30-50 metres. The average EM-derived floe thickness and the average borehole snow plus ice thickness differ by less than 10%.

Interpretation of the Bay of Exploits EM data was based on a two-layer model for the water, used to account for the brackish water layer under the ice. Results of the inversion are given in Figure 7. The agreement with auger measurements (circled points) is well within ± 0.1 m. The EM results suggest a gradual thinning of ice from 0.5 m to 0 m as the line progresses offshore. Water depth was typically greater than 75 m so that bias in the ice thickness measurement due to finite water depths should be negligible.

A selected portion of data near the ship is given in Figure 8. The first year pack ice was made up of many pans, typically 10 m in diameter and, varying from 0.3 to over 1.6 m in thickness. Ice salinity was typically 5 ppt and temperature around -2°C . Although there were few comparative points, data from two auger holes are shown (bars indicate range of auger measurements). The EM results agree with the surface data within 0.05 m at one site (the Ice Motion Sensor) and within 0.2 m at another (the ARGOS beacon).

A histogram of ice thickness based on 125 "random" auger hole measurements made by investigators in the same area is shown in Figure 9, along with the histogram computed from Line 2100 of the airborne survey (see Figures. 5 and 8). The differences point out the effects of apparent local variability in the ice. However, they also underline two difficulties in comparing airborne and auger results: a) the surface measurements are only taken at specific points whereas the EM system averages over an area of approximately $10^2 - 10^3 \text{ m}^2$; and b) surface measurements are inevitably biased against thin ice (too thin to stand on) and/or thick ice (beyond the auger stem). These differences represent one of the important advantages of remote ice thickness measurement for scientific applications.

Comparison of the surface measurements obtained along the main survey line in the Bay of Exploits and at the marked sites on offshore ice with the EM results indicates that the typical accuracy of the method was within ± 0.05 metres in ice that was typically 0.5 metres thick. It should be noted that the 0.05 metre accuracy was probably the result of laser profilometer errors, which would be constant for uniform ice of any thickness. There was one significant exception to this observed accuracy: in the one survey line that passed over the ARGOS beacon, the EM-measured ice thickness was 0.2 m less than the smallest of the three auger measurements. The two most likely reasons for this disparity are local rafting in the floe (three auger holes all encountered water-filled zones, the first at 0.5 metres depth) and the effects of lateral thickness variation (the floe was less than one system footprint wide and about one footprint long, and was largely surrounded by slush and seawater).

CONCLUSIONS

Even more than on previous studies, the LIMEX'89 survey results indicate that airborne EM sounding appears to be capable of being used for routine ice thickness measurement. In the 1987 CRREL study, cold first-year and multi-year ice was profiled, with accuracies of about 10% being typical for relatively flat ice. In particular, representative average ice thicknesses were obtained. In the LIMEX'89 work relatively warm ice was sounded successfully. Although the EM induction technology is relatively mature in terms of geophysical measurements, there is still room for optimization in ice sounding applications. In particular, the use of higher frequencies to facilitate estimation of ice conductivity would be particularly useful, since this parameter is closely coupled to ice strength (Kovacs et al., 1987). The technique appears to be suitable for routine operational use as a data collection tool when used by specialists. It could be used for long traverses of ice thickness data collection which would be exceedingly difficult to collect manually, especially over the short time windows required when mobile ice is being studied.

ONGOING WORK

1. Further validation, particularly over ridges, is required. The techniques under development at the University of California at Berkeley (Liu and Becker, 1988) are being investigated.
2. The development of operational prototypes using two distinct approaches for the EM hardware is underway. These projects include:
 - a. reduction of the size and weight of the bird;

- b. design of a system that can be used by non-specialist personnel;
- c. provision of real-time ice thickness output;
- d. processing capability for two and three-dimensional structures;
- e. provision for measurement of ice conductivity.

3. The statistics of ice measurement by conventional and airborne means are being studied to clarify their relationship.

ACKNOWLEDGEMENTS

The LIMEX'89 work was funded under the DSS Unsolicited Proposal Program through DSS Contract No. FP953-8-0848/01-OSC; Simon Prinsenbergh, of the Bedford Institute of Oceanography, Dartmouth, N.S. was the Scientific Authority. We express our thanks to other LIMEX'89 investigators who provided surface information and other assistance, including C. Mason of the Bedford Institute of Oceanography, W. Winsor and G. Crocker of C-CORE; B. Eid and S. Melrose of MacLaren Plansearch; L. McNutt and S. Argus from the Radarsat Office; and K. Asmus of AES. Field work was conducted with the able assistance of C. Bassani and B. Simon from Aerodat.

The CRREL study was funded by the U.S. Department of Navy, Naval Ocean Research and Development Activity, under contract N6845286-MP60003. Surface measurements were provided by a team organized by W. B. Tucker III which included J.W. Govoni, Dr. A.J. Gow, Dr. D.A. Meese and R.J. Roberts of CRREL. EM hardware and data processing assistance were provided by W.Y.L. Chan, J.L.C. Lee and G.C.E. Luus, formerly of Geotech, Ltd. Data processing was also provided by G.E. Fellers and J.B. Bement of CRREL.

REFERENCES

Becker, A., Liu, G., and Morrison, H.F., 1987, "Airborne Electromagnetic Sensing of Sea Ice Thickness," Final Report prepared for CRREL under U.C.B. contract DACA89-85-K-0008, U.C. Berkeley.

Canpolar Consultants Ltd., 1985, "Review of Floating Ice Thickness Measurement Capability, Technologies and Opportunities," report to Department of Fisheries and Oceans, Contract No. 01SE.FP921-3-0624.

Holladay, J.S., Valleau, N.C., and Morrison, E., 1986, "Application of Multi-frequency Helicopter Electromagnetic Surveys to Mapping of Sea-ice Thickness and Shallow-water Bathymetry," in Airborne Resistivity Mapping, ed., G.J. Palacky, Geological Survey of Canada Paper 86-22, pp. 91-98.

Kovacs, A., Valleau, N.C., and Holladay, J.S., 1987a, "Airborne Electromagnetic Sounding of Sea Ice Thickness and Sub-ice Bathymetry," Cold Regions Science and Technology, vol. 14, pp. 289-311.

Kovacs, A., Valleau, N.C., and Holladay, J.S., 1987b, "Airborne Measurement of Sea Ice Thickness and Subice Bathymetry," in Proc. Developments and Applications of Modern Airborne Electromagnetic Surveys, U.S.G.S., Denver, CO, Oct. 7-9, 1987.

Kovacs, A., R.M. Morey and C.F.N. Cox, 1987, "Modelling the Electromagnetic Property Trends in Sea Ice, Part I", Cold Regions Science and Technology vol 1, No. 14.

Kovacs, A. and Valleau, N.C., 1987, "Airborne Measurement of Sea Ice Thickness and Subice Bathymetry," Proc. 9th International Conference on Port and Ocean Engineering under Arctic Conditions, University of Alaska-Fairbanks, 17-21 August 1987.

Kovacs, A. and Holladay, J.S., 1989a, "Airborne Sea Ice Thickness Sounding," Proc. 10th International Conference on Port and Ocean Engineering under Arctic Conditions, Lulea University of Technology, 12-16 June 1989, pp. 1042-1052.

Kovacs, A. and Holladay, J.S., 1989b, "Airborne Sea Ice Measurement System Development and Field Test Results", CRREL Report, in press.

Liu, G. and Becker, A., 1988, "Inversion of Airborne Electromagnetic Data For Sea Ice Keel Geometry," report to Naval Ocean Research & Development Activity (NORDA) under contract no. N00014-87-K-6005, University of California, Berkeley.

MacLaren Plansearch Ltd., 1988, "Study the Sea Ice Climate of the Northumberland Strait," Report to Fisheries and Oceans, Bedford Institute of Oceanography, Contract No. FP950-7-0058/01-OSC.

Morey, R. M., Kovacs, A., and Cox, G.F.N., 1984, "Electromagnetic Properties of Sea Ice," CRREL Report 84-2.

Raney, R.K., and Argus, S., 1988, "Science Plan for LIMEX'89," RADARSAT Program Office, Ottawa.

Rossiter, J.R. and Lalumiere, L.A., 1988, "Evaluation of Sea Ice Thickness Sensors," report to Transportation Development Centre, Report No. TP9169E.

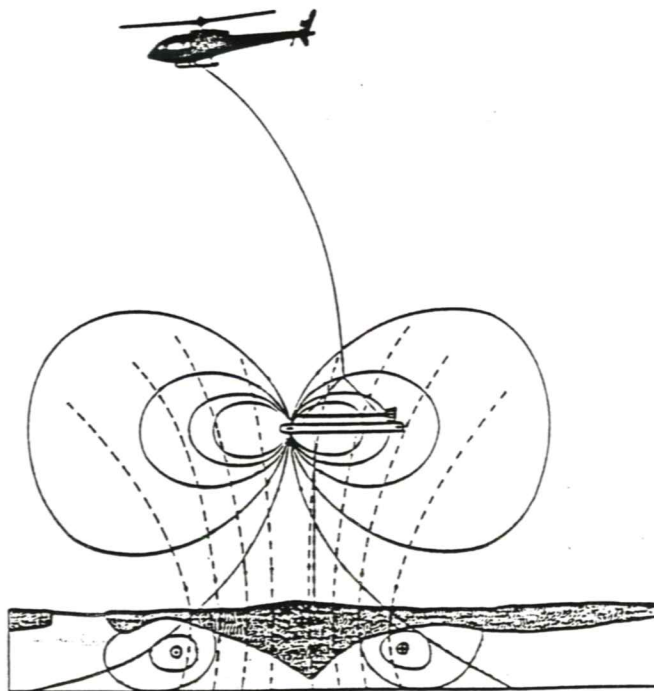


Figure 1. Sketch of EM system and ice sounding concept.

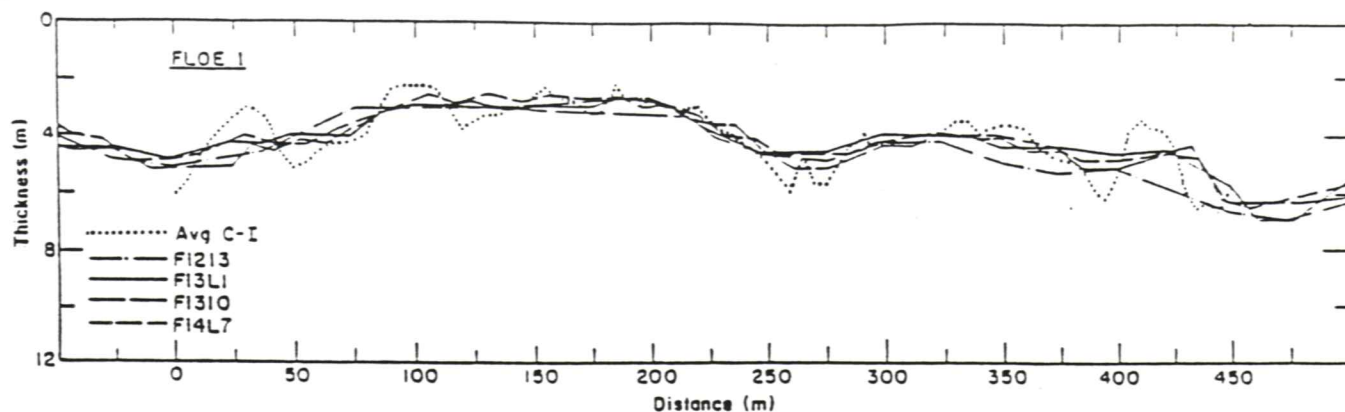


Figure 2. Results from the 1987 CRREL Prudhoe Bay survey: average snow plus ice thickness for 30-m-wide swath C-I down center of grid on Multi-Year Floe 1 vs. AEM-derived snow plus ice thickness for four sounding flight lines (F...).



Figure 3. Location sketch map for LIMEX'89 ice thickness measurements.

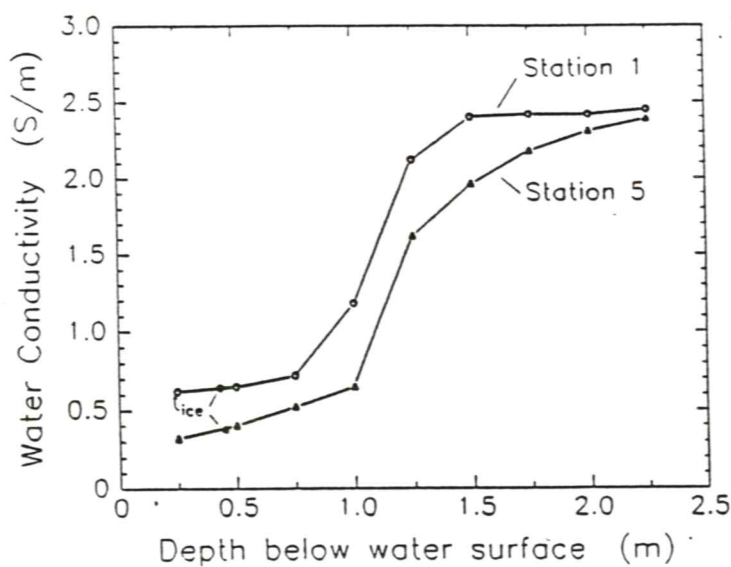


Figure 4. Typical water conductivity vs. depth curves in Bay of Exploits.

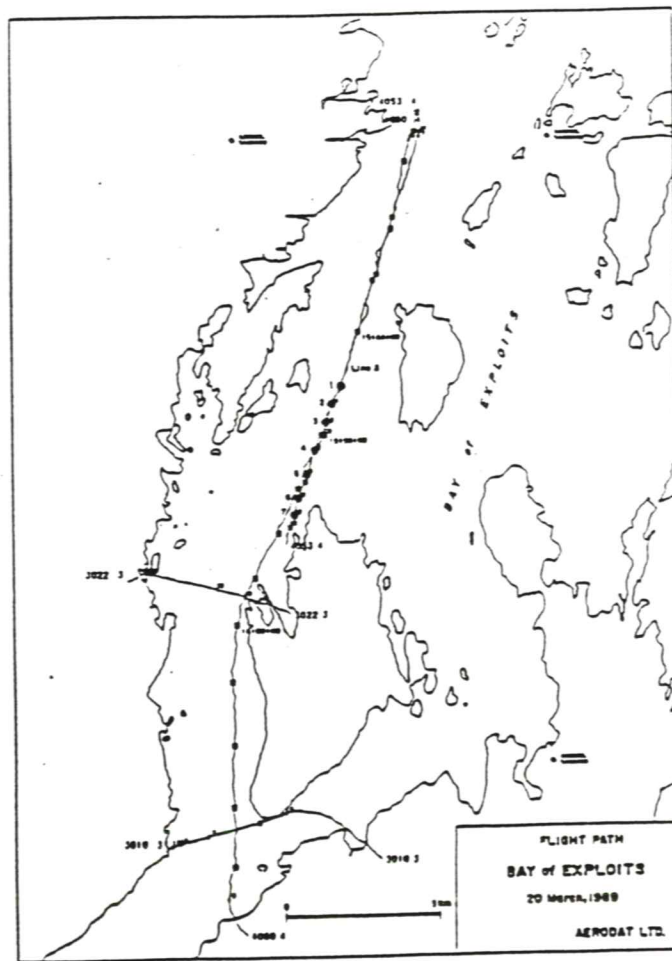


Figure 5. Flight path and survey points in Bay of Exploits.

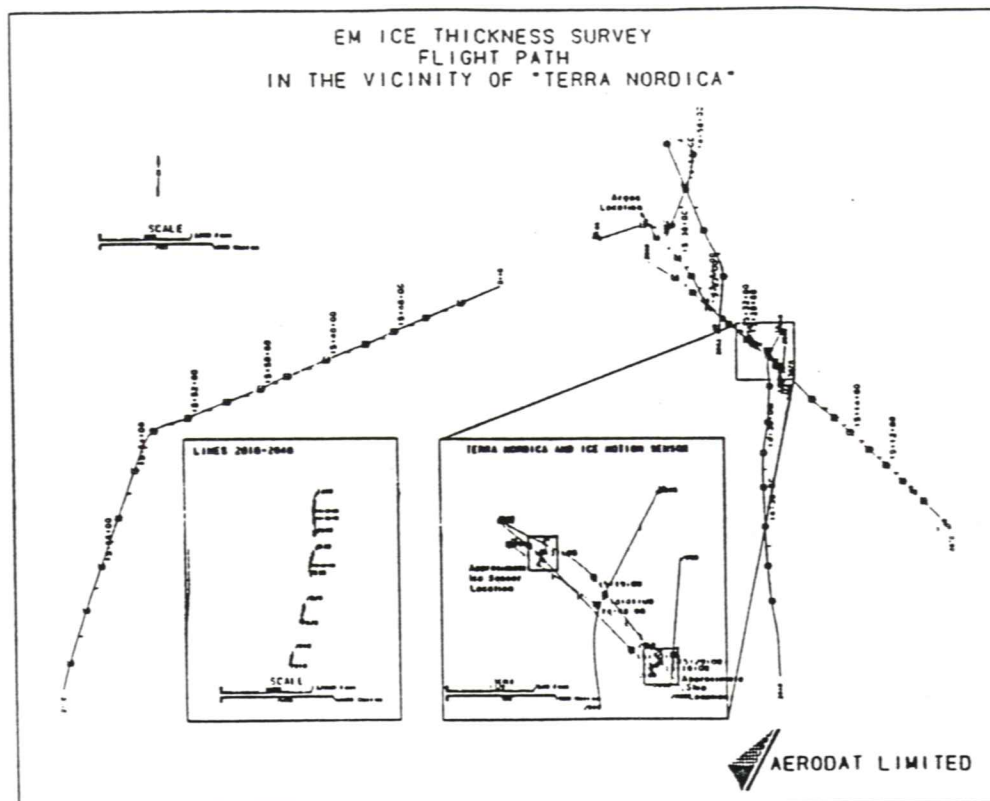


Figure 6. Flight path in the vicinity of the Terra Nordica.

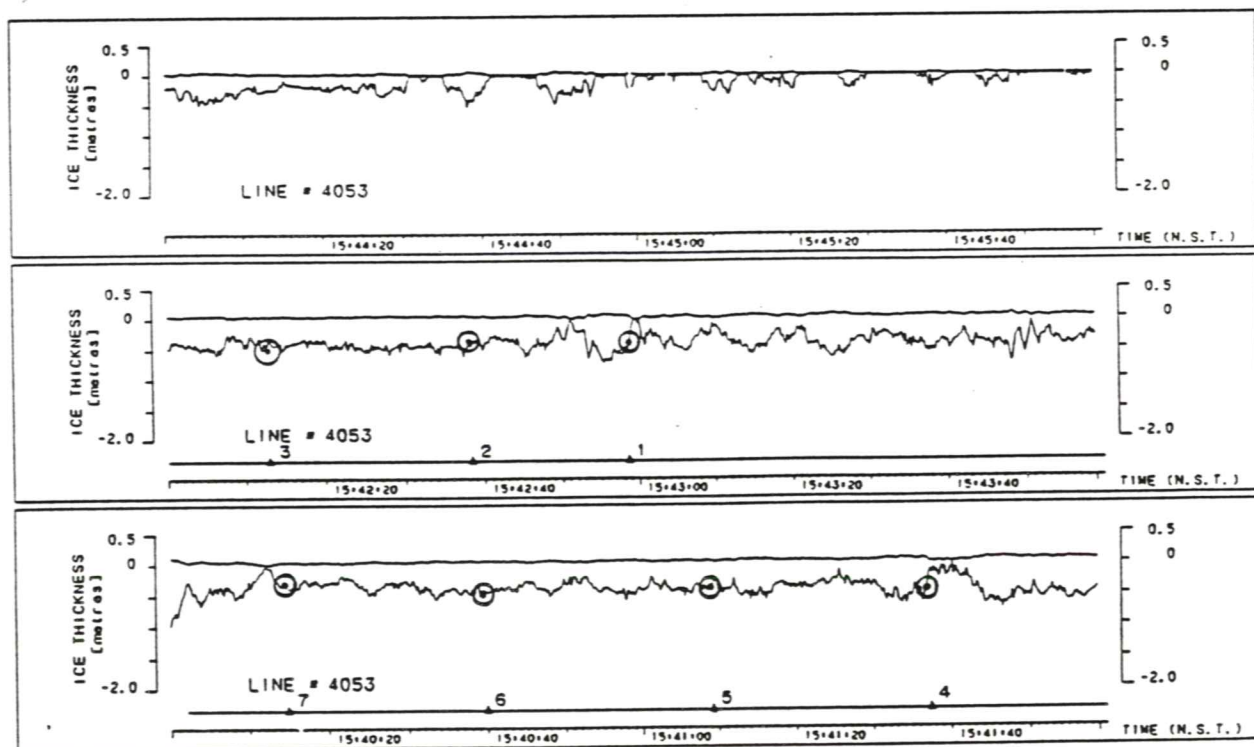


Figure 7. EM sounding and auger ice thickness measurements (circled points) for shorefast ice in the Bay of Exploits.

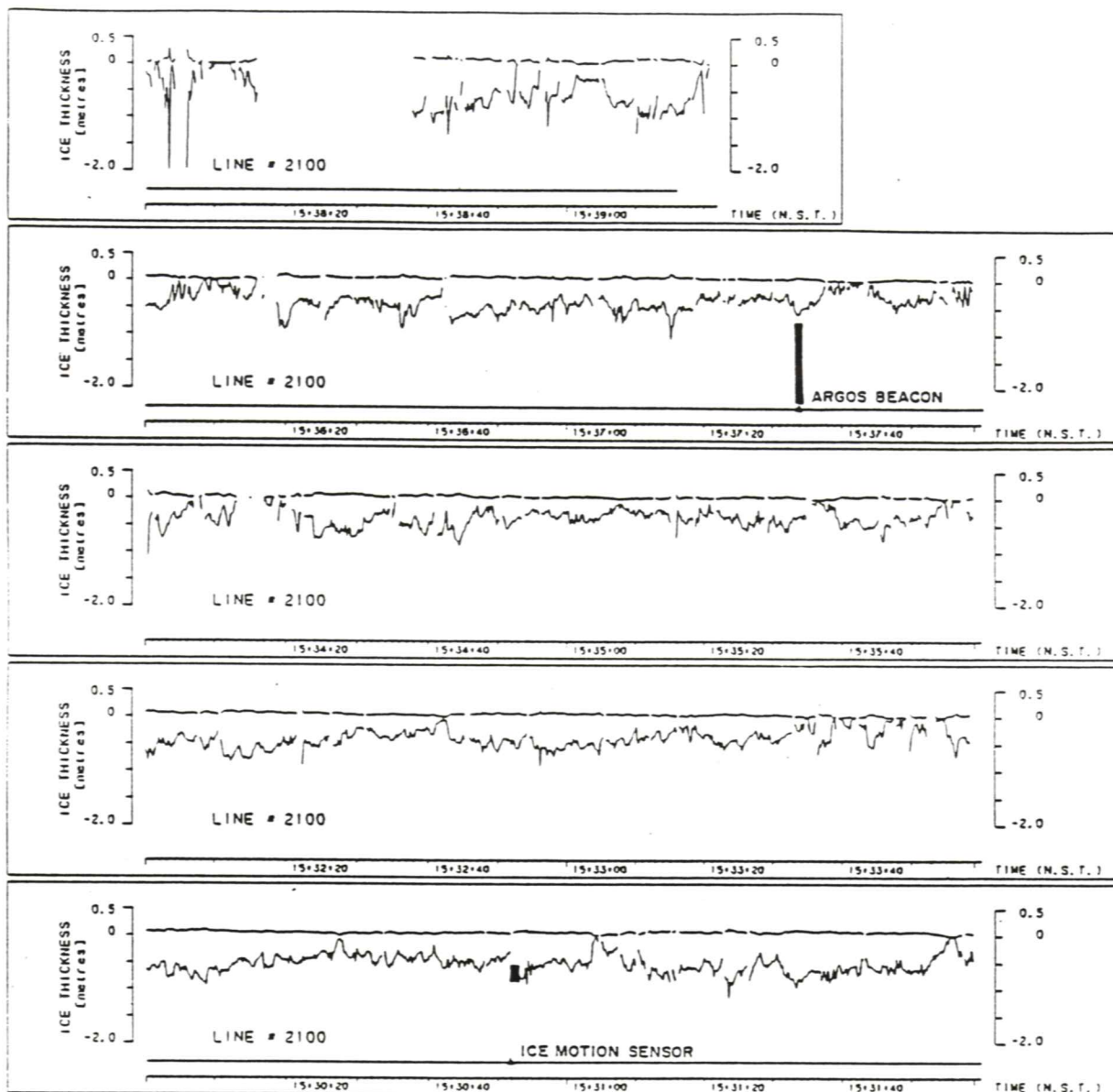


Figure 8. EM and auger ice thickness measurements (range of auger estimates shown as bar) near the Terra Nordica.

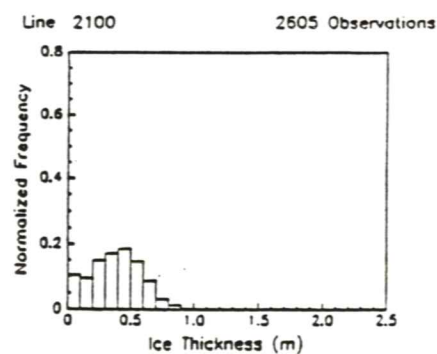
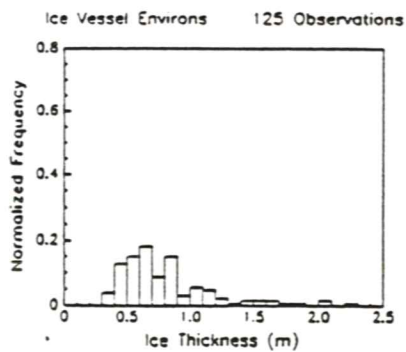


Figure 9. Histograms of ice thickness measured in the vicinity of the Terra Nordica by auger and for the segment of the airborne EM survey shown in Figure 8.